THE ROLE OF RELIABILITY IN CHARACTERIZING GREEN STORMWATER INFRASTRUCTURE IN URBAN AREAS

BY

RESHMINA WILLIAM

DISSERTATION

Submitted in partial fulfillment of the requirements
for the degree of Doctor of Philosophy in Civil Engineering
in the Graduate College of the
University of Illinois at Urbana-Champaign, 2019

Urbana, Illinois

Doctoral Committee:

Assistant Professor Ashlynn S. Stillwell, Chair
Professor Praveen Kumar
Professor Paolo Gardoni
Professor Bryan Endres
Research Assistant Professor Arthur R. Schmidt

ABSTRACT

As cities continue to expand, the issues of flood control and urban water quality have risen to the forefront of modern sustainability challenges. Green infrastructure— the use of nature-based solutions to target, treat, and store stormwater at its source— has emerged as a possible solution. While green infrastructure does offer multiple benefits for urban users, its performance is also highly variable. This dissertation addresses a key gap in the literature by explicitly addressing how uncertainty in environmental and anthropogenic factors affects green infrastructure performance at modular, systemic, and policy levels.

Three primary contributions are made by this research, using an underlying fragility function methodology. Firstly, an analysis of the impact of temporal and spatial variability on modular rain garden performance offers insights into challenges commonly faced by green infrastructure: clogging and maintenance, back-to-back rainfall, and variable urban soils. Building on these findings, the second contribution is the use of fragility functions to characterize green infrastructure performance within the context of an existing separated storm sewer network. A case study approach is used to analyze the effect of green infrastructure implementation at multiple spatial scales and configurations. Finally, an in-depth policy analysis incorporating game theory, environmental psychology, and environmental law evaluates how and why green infrastructure should be integrated into the existing urban policy landscape.

This research fills an important gap in the literature by offering a new perspective on green infrastructure performance, using an interdisciplinary, risk-based approach to analyze how green infrastructure can be better integrated into the urban landscape.

ACKNOWLEDGMENTS

I would like to thank my advisor, Ashlynn Stillwell, for her guidance and help throughout the course of my degree program. I would also like to thank my committee members — Art Schmidt, Paolo Gardoni, Praveen Kumar, and Bryan Endres — for encouraging me, challenging me, and allowing me to broaden my intellectual horizons.

Many thanks to Mark Shen, Mary Pat McGuire, Andrew Phillips, David Grimley, and the rest of the team working on the Calumet Corridor project for their hard work and assistance with data processing and soil mapping.

A heart-felt thanks to all the members of the Stillwell Research Group — past and present. You have been wonderfully supportive of all my efforts, and have always encouraged me to do my best work.

Last, but certainly not least, thank you to my wonderful family, including my parents and my husband Kevin for helping me to remember why I love what I do.

This work was supported by a CEE Distinguished Fellowship from the Department of Civil and Environmental Engineering, a Mavis Future Faculty Fellowship from the College of Engineering, and a PEO Scholars Fellowship. This work was also supported in part by the Illinois-Indiana Sea Grant College Program, grant number NA18OAR4170082, and the Illinois Water Resources Center. DHI provided additional support through free access to their MIKE URBAN modeling software. The Baltimore City Department of Public Works provided GIS data for the Baltimore sewer network.

TABLE OF CONTENTS

LIST OF ABBREVIATIONS

AMC	Antecedent moisture content
BAU	Business as usual
CDF	Cumulative Density Function
CWA	Clean Water Act
EPA/USEPA	U.S. Environmental Protection Agency
GSI	Green stormwater infrastructure
LA	Load Allocation
LID	Low impact development
MS4	Municipal separated stormsewer system
NPDES	National Pollutant Discharge Elimination System
NRCS	Natural Resources Conservation Services
NSQD	National Stormwater Quality Database
PDF	Probability Density Function
POTW	Publicly owned treatment works
SCM	Stormwater control measure
SDT	Self Determination Theory
SLCA	Stochastic life cycle analysis
SSURGO	Soil Survey Geographic Database
SWIP	State Watershed Implementation Plan
TMDL	Total Maximum Daily Load

TSS	Total suspended sediments
USGS	U.S. Geological Survey
WLA	Waste Load Allocation

CHAPTER 1

INTRODUCTION

More than half of the global population lives in cites; consequently, the management of urban areas has been heralded as one of the most important development challenges of the 21st century [1]. As the size and density of urban areas increase, the growth of paved areas has led to a sharp rise in issues of degraded water quality and localized flooding. The U.S. Environmental Protection Agency (EPA) reports that urban runoff is a leading source of pollutants causing water quality impairment related to human activities in ocean shoreline waters. Overall, the impairment of U.S. waters by urban runoff constitutes nearly 5,000 square miles of estuaries, 1.4 million acres of lakes, and 30,000 miles of rivers across the country [2]. In some watersheds, the impact of urban runoff can be even more concentrated. For example, urban runoff constitutes nearly 15% of the nitrogen entering the Chesapeake Bay watershed, and is the only source that is still increasing [3].

To address some of these challenges, many urban areas are turning to green infrastructure, a low-cost, distributed, flexible alternative to traditional (grey) infrastructure. Green stormwater infrastructure (GSI) is the use of natural processes to filter, capture, treat, and store storm runoff at its source [4]. However, many green infrastructure benefits are also highly variable. For example, Jennings [5] points out that the effectiveness of comparable rain gardens varies from 51 to 100% across the contiguous United States. The efficiency of green infrastructure in reducing runoff is contingent on a variety of different factors. Green infrastructure typically shows the greatest mitigating ability for smaller storms with shorter return periods [6–9]. However, green infrastructure capabilities are greatly reduced during high intensity events. Storm size continues to be a good predictor of GSI performance at the catchment scale [10]. Antecedent soil moisture conditions and interstorm duration also play an important role in green infrastructure runoff reduction [11, 12]. Other factors that af-

fect green infrastructure efficiency include soil texture, media depth or pavement thickness, drought stress, and vegetation type [13–18]. Finally, infrastructure age and maintenance play a crucial role in determining GSI efficiency [19, 20].

Because of this inherent uncertainty, reliability analysis is a useful tool to analyze GSI performance. This dissertation approaches the modeling of GSI implementation through the lens of reliability analysis to answer the following motivating question: *How does incorporating uncertainty into the impacts of green infrastructure implementation affect the performance of an existing system, from engineering and policy perspectives?* The explicit incorporation of uncertainty and system reliability into the modeling of catchment-scale GSI implementation has little precedent, and provides a unique perspective as to when and where the implementation of green infrastructure is effective. This overarching goal is addressed using three research objectives. Figure 1.1 diagrammatically presents an overview of this research.

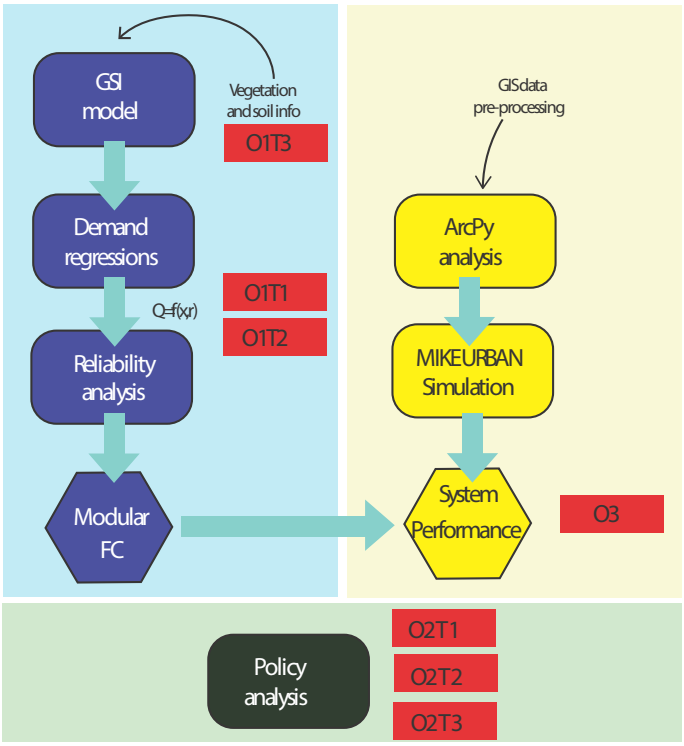

Figure 1.1: The overarching research question can be further divided into three objectives.

Objective 1: Characterize GSI modular variability

In order to understand how green infrastructure implementation affects network-scale system

reliability, a determination of how a single green infrastructure installation performs under varying weather, maintenance, and soil regimes is needed. In this objective, an EPA-SWMM model of a test rain garden is calibrated and validated using data collected from a USGS site in Madison, WI, to understand how green infrastructure fragility functions are affected by common challenges to their performance. Perturbing the rain garden in this fashion allows the evaluation of how it responds to variability in both time and space. Objective 1 is subdivided into the following three tasks:

Task 1 (O1T1): Evaluate performance changes due to clogging

A stochastic life-cycle analysis (SLCA) approach is adopted to evaluate how rain garden performance changes over time when exposed to different levels of clogging fine sediments. This approach is used to make recommendations for appropriate maintenance 'windows' to avoid rain garden failure.

Task 2 (O1T2): Evaluate the impact of back-to-back rainfall events

A similar SLCA approach is used to evaluate how rain gardens respond to antecedent moisture conditions in both the short and the long terms.

Task 3 (O1T3): Evaluate performance changes due to spatial location

Finally, rain garden performance is evaluated under different loading ratios and native soil conditions typically found in two cities within the Calumet River Corridor in Northern Illinois.

Objective 2: Simulate GSI network performance at the catchment scale

In Objective 2, the fragility curves developed in Objective 1 are used to analyze the impact of green infrastructure placement on network performance. A combination of software tools is used to develop a network model of a separated stormwater sewer system in the Gwynn's Run watershed located in west Baltimore, MD, as a representative case study. The effects of clustered and randomized distributions of green infrastructure are compared for varying levels of spatial coverage at the block and watershed scales.

Objective 3: Evaluate the policy implications of GSI implementation

The success of green infrastructure implementation at a city scale is contingent on a well-thought-out approach to public-private partnerships. Objective 3 evaluates how green infrastructure can be integrated into the built environment from a policy perspective. This

over-arching objective can be divided into three sub-tasks:

Task 1 (O3T1): Evaluate current municipal incentives policies for green infrastructure implementation

A collaborative game theory framework is used to study four policies commonly used by municipalities to incentivize private green infrastructure installation. The findings are used to evaluate implications for environmental justice with regards to green infrastructure implementation.

Task 2 (O3T2): Consider green infrastructure integration through an environmental psychology lens

Although game theory provides a useful framework to understand user behavior, it is limited by its assumption that all agents are rational and selfish. This section explores the implications of literature from environmental psychology on green infrastructure implementation, and uses them to make recommendations for practical next steps.

Task 3 (O3T3): Understand the implications of green infrastructure implementation within the framework of current U.S. law

Lastly, the framework of the U.S. Clean Water Act is used to better understand green infrastructure policy. The implications of using a point source framework for a non-point source problem, as well as the current deterministic framing of green infrastructure solutions, are studied. Potential paths forward are proposed, including new paradigms for municipal separated stormsewer (MS4) monitoring and maintenance, as well as a potential legal regime that offers a more holistic perspective on green infrastructure, and on watershed-scale challenges as a whole.

CHAPTER 2

BACKGROUND

2.1 GSI Benefits

Many types of green infrastructure incur multiple benefits. Green infrastructure helps to mitigate urban runoff by both attenuating stormwater volume and by reducing and delaying peak flows [15, 21, 22]. A combination of different types of GSI at the catchment scale can lead to substantial reductions in runoff volume in dense, highly built-up environments [23, 24]. In many instances, green infrastructure presents a viable alternative to traditional grey infrastructure. Lucas and Sample [25] showed that during years with high rainfall, green infrastructure with outlet controls is equivalent to or exceeds grey infrastructure performance. Green infrastructure and green-grey hybrid infrastructure has also been shown to be cost-effective [26]. The relative cost of green infrastructure compared to grey infrastructure has decreased substantially as population density continues to increase [27].

Multiple studies have shown that green infrastructure can be used to remove heavy metals, sediment, nutrients, and other contaminants of interest from urban runoff [28–34]. In particular, infiltration-based, vegetated GSI has multiple mechanisms for pollutant mitigation. For example, Leroy et al. [34] showed that vegetated swales with deep plant root systems help to physically slow down water, allowing greater retention of total suspended sediments. At the same time, Roy-Poirier et al. [35] showcased multiple chemical and biological mechanisms that bioretention systems use to influence phosphorus, pH, and heavy metal uptake.

In addition to its water quality and flood mitigation benefits, urban green infrastructure has multiple other co-benefits, including mitigation of the urban heat island effect and associated improved air quality [36, 37]. Studies have shown that green roof or green wall implementation can substantially decrease ambient air temperature around buildings, lead-

ing to reduced energy loads for building cooling and improved overall quality of life [38, 39]. A recent modeling study by Kong et al. [40] showed that increasing urban green space could reduce maximum air temperatures by over 3°C. Field experiments corroborate this finding, showing that the implementation of a green wall can reduce maximum air temperatures by around 6°C [41].

Other green infrastructure benefits are less tangible. Urban green space has been associated with multiple benefits for mental and physical health, including decreased stress and a decrease in sympathetic nervous activity, which can promote healing [42]. Similarly, studies have found that the effect of green space on the attention spans of children with ADHD is comparable to those achieved with recent formulations of methylphenidate drugs [43]. Green spaces have also been shown to reduce aggression and enhance pro-social behavior, thus leading to significant reductions in violent crime [44, 45]. As a result, access to green space is implicitly tied to issues of social and environmental equity [46].

2.2 GSI Challenges

Despite these benefits, green infrastructure continues to be viewed as a "risky" investment [47]. Part of this perception of risk stems from the high variability in green infrastructure performance [48]. In general, there is a lack of data regarding environmental factors that can be used to quantify variability in green infrastructure performance [49]. However, previous research has shown that soil type and condition, land use, vegetation type, and existing soil moisture and water table height can all affect the runoff reduction performance of green infrastructure [50]. At the network scale, the placement and configuration of green infrastructure makes a significant difference in its ability to reduce runoff from impervious areas [51]. Rainfall distribution also plays a significant role in runoff mitigation ability, with green infrastructure generally performing better for smaller storms than larger ones [6–8]. For example, rain gardens are least effective in the Atlantic and Gulf Coast states due to the prevalence of high intensity rainfall events; rain gardens in regions with more temporally dispersed rainfall tend to perform better overall [5]. The combination of these environmental uncertainties leads to significant variability in performance, especially at the watershed

scale [50].

A probabilistic approach to quantifying green infrastructure performance is both feasible and necessary. Policy has begun to shift towards a framing of infrastructure benefits in terms of urban resilience, reliability, and risk [52]. The non-stationarity created as a result of land use changes and climate change necessitates a risk-based evaluation of flood and water quality infrastructure [53]. Multiple studies highlight that effectively communicating uncertainty is a useful tool in communicating with the general public [54, 55]. This paradigm shift is particularly relevant for green infrastructure implementation and uptake [56]. As Livesley et al. [57] state, with a growing awareness of the multiple benefits of urban green infrastructure comes a need "to answer the questions of 'how beneficial' and 'under what circumstance'." Because of the high variability in performance between green infrastructure installations across both space and time, optimal performance cannot be assumed, making the use of green infrastructure to address regulatory challenges much more difficult [48].

The research presented in this dissertation provides a framework that quantifies green infrastructure performance uncertainty, and uses that framework to answer questions about how performance varies under different spatial and temporal configurations. In doing so, this work provides helpful tools that can allow green infrastructure users to better understand when and where green infrastructure can be most effective in the urban environment. The background and methodology behind the creation of these tools is explored in the next section.

2.3 Reliability Analysis and Fragility Functions

Reliability is defined as the probability that capacity is greater than demand for a given component or system, to determine whether or not they are in failure [58]. One approach to quantifying performance reliability is through the use of fragility functions. Fragility is defined as the conditional probability of attaining or exceeding a specified standard of performance conditioned on different demand variables (i.e., loading intensity measures). Originally developed in the field of earthquake engineering [59, 60], fragility functions have been used in multiple other applications [61, 62]. A similar framework has been adopted by

water resources engineers in modeling flood risks in urban environments [63]. In particular, Sayers et al. [64] highlighted the importance of using a reliability-based approach to characterize an adaptive decision-making process, and presented metrics for calculating risk based on different failure modes.

Failure for GSI can be defined in terms of different hydrologic or environmental standards and targets. In this paper, failure is defined as the inability of the green infrastructure to reduce runoff volume below a specified percentage of the effluent from a similarly-sized paved area. Following the conventional notation in reliability analysis [61, 65], Equation 2.1 mathematically defines the conditional probability of failure F for a given rainfall magnitude r:

$$F = P([\alpha V_{paved}(\mathbf{x}, r) - V_{GSI}(\mathbf{x}, r)] \leq 0 | R = r) \tag{2.1}$$

where α is a specified fractional "reduction standard", $\mathbf{x}$ is a vector of state variables that define the state of the paved area and the GSI, r is the rainfall magnitude, V_{paved} is the runoff volume from the paved area, and V_{GSI} is the runoff volume from the GSI. In the context of reliability analysis, $\alpha V_{paved}(\mathbf{x}, r)$ represents the capacity of the GSI and $V_{GSI}(\mathbf{x}, r)$ represents the demand the GSI is subject to for a given rainfall of magnitude r.

The general methodology for creating fragility functions for as-built green infrastructure performance is discussed in detail in William and Stillwell [15]. In brief, fragility functions are generated in a three-step process:

1. **Hydrologic model of GSI.** Design storms are passed through a calibrated green infrastructure model (executed in the EPA stormwater management model (EPA-SWMM), MIKE SHE, or another model with GSI capabilities), generating output hydrographs for different randomized scenarios created by varying selected model parameters.

2. **Regression analysis to represent demand.** The output hydrographs are then used to generate regressions relating runoff peak, volume, and peak delay to the different variables under consideration for each storm. These relationships define the demand

for the purposes of the reliability analysis.

3. **Reliability analysis.** The demand function, capacity, and random variable distributions are input to the MATLAB-based reliability analysis program Finite Element Reliability Using MATLAB (FERUM) [66] to calculate the probability of failure using Monte Carlo simulation.

This dissertation builds on previous studies of reliability analysis to create tools that can be used to evaluate how green infrastructure evolves in time and space, and how it can be effectively incorporated into the urban environment.

2.4 Stochastic Life-Cycle Analysis (SLCA)

In contrast to traditional, deterministic life-cycle analysis, stochastic life-cycle analysis (SLCA) [58, 67, 68] evaluates costs and benefits over the lifetime of a project from a probabilistic perspective. SLCA uses fragility functions and probability distributions of different deterioration and recovery mechanisms to account for the effects of degradation on systems over time. SLCA describes the deterioration and restoration of a system as either gradual over a span of time, or as a series of instantaneous shocks. The SLCA model makes use of two components in calculating the change in system fragility over time: 1) the distribution of the intensity of the shocks and recovery over time; and 2) an understanding of how the disruption to the system affects the state variables. Figure 2.1 shows a diagram of how deterioration and recovery can be modeled within the context of existing fragility functions. SLCA has been applied in modeling the cost of structural damage caused by hazards such as earthquakes over a project's lifetime [69]. Other potential applications include flood mitigation [64], and market and inventory analysis [70].

To quantify the effects of shock deterioration on future infrastructure performance, Jia et al. [58] used a metric called "instantaneous reliability". Instantaneous reliability (Q) (given in Equation 2.2) is defined as:

$$Q = 1 - P_f(t) = 1 - \int F[r(t)]f[r(t)]dr \tag{2.2}$$

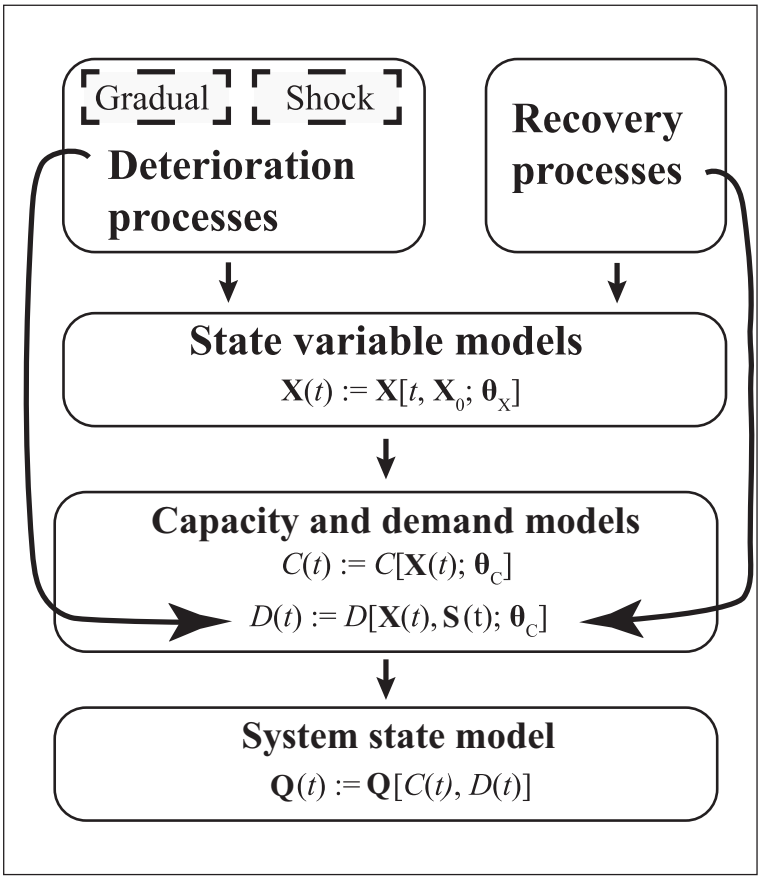

Figure 2.1: SLCA is based on a modeling of deterioration and recovery processes over time.

where P_f is the probability of failure at a future time t defined as the integral of F (defined in Equation 2.1) at time t multiplied by the probability density function (PDF) of $r(t)$ also at time t, $f[r(t)]$. Instantaneous reliability is a metric for system functionality, since it allows the quantification of future performance over the entire fragility curve based on current deterioration. While the SLCA framework is used extensively in both Section 4.2 and Section 4.3, instantaneous reliability primarily plays a role in the study of green infrastructure clogging, a shock deterioration process.

CHAPTER 3

MODEL DEVELOPMENT

3.1 SWMM Rain Garden Model

Rain gardens, planted areas designed to collect and infiltrate stormwater runoff, are a form of GSI commonly used in urban areas [16]. A model "test" rain garden is developed using the EPA Stormwater Management Model (EPA-SWMM), and calibrated and validated using data provided by the U.S. Geological Survey (USGS) for a rain garden field site in Madison, WI (William Selbig, personal communication, July 13th 2016). The Madison rain garden was constructed in 2003, and is around 9.3 m^2 (100 ft^2) in area, draining a 46-m^2 (500-ft^2) asphalt shingle roof. The native surrounding soil is a clay loam; the rain garden itself is filled with a sandy loam mixed with screened compost. Hydrological and climate measurements (including rainfall, relative humidity (RH), net radiation, wind speed, temperature, soil moisture, ponding depth, and runoff volume) were taken over the course of five years. In this analysis, data from summer 2006 are used in calibration and validation as an example of a particularly wet season with multiple different-sized rainfall events.

EPA-SWMM has been used in multiple studies modeling urban flooding and drainage networks [71]. SWMM's low impact development (LID) management modules have been used to model the catchment-wide impacts of implementing a wide variety of types of green infrastructure in urban environments [9, 17, 18, 72]. While SWMM is a lumped model rather than a distributed model, fine-scale spatial resolution SWMM models with adequate land use data can reach high predictive performances [71]. The SWMM test rain garden is modeled as two subcatchments: one representing the roof, and the other the rain garden. The second subcatchment (representing the rain garden) contains a 'bioretention cell' LID module to better capture the differences between the sandy soil in the rain garden and the clayey native

soil. Because the model is designed to represent a rain garden with no underdrain or extra storage, the thickness of the storage layer module is decreased while retaining the seepage rate functionality. The drain functionality is removed from the model. Figure 2 shows a schematic diagram of the setup of the rain garden in SWMM.

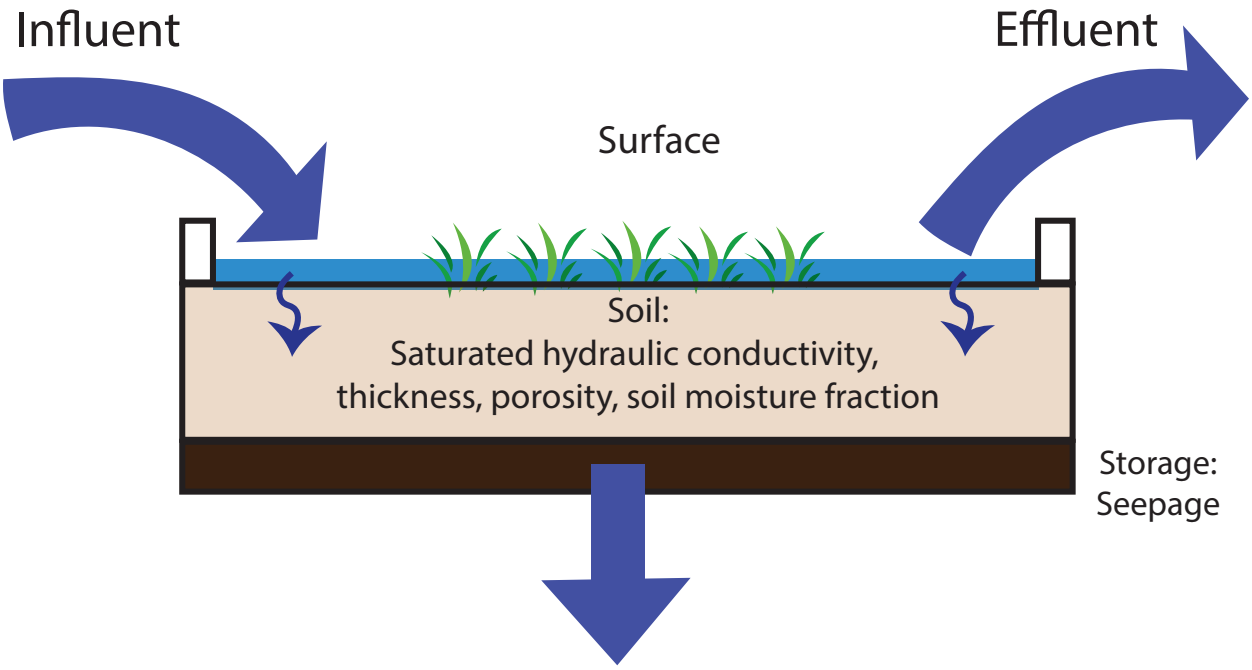

Figure 3.1: The bioretention cell module within EPA-SWMM was used to model a test rain garden. Five variables were modified to represent variability under different soil and climate conditions.

To test the ability of the model to respond accurately to multiple storm events, the model calibration encompasses a 16-day period from July 12 to July 28. A warm-up time of one month of rainfall data is used. Calibration parameters are mainly chosen from the soil layer of the model, although the seepage rate is also a significant calibration parameter. Using the calibrated parameters shown in Table 3.1, the calculated Nash-Sutcliffe Efficiency (NSE) for this time period is 0.76, within the bounds of effectiveness set by Moriasi et al. [73]. The chosen parameter values are reasonable based upon literature values taken from the SWMM User Manual. A shorter validation period was chosen on August 24 to test the ability of the model to respond to single, larger storm events. The NSE calculated for this event is 0.71. The SWMM model was thus considered an appropriate representation of the hydrologic responses of the system under real conditions.

Table 3.1: Calibrated model parameters

Parameter	**Calibrated value**
Thickness	483 mm
Porosity	0.44
Conductivity	115 mm/hr
Seepage rate	8 mm/hr
Void Ratio	0.1

Five random variables outside of precipitation magnitude were identified as impacting runoff volume: saturated hydraulic conductivity, thickness, porosity, initial soil moisture fraction, and seepage. The probability distributions of each of these variables were based on the calibration or on literature, as listed in Table 3.2. Note that the standard deviation for the $sat.frac$ was based on the sensitivity of a standard soil moisture probe that would be used to take the measurement, rather than the overall range of initial saturated fraction over the course of the summer. Thirty-five scenarios randomly sampled from the distributions of the five variables were batch processed in SWMM.

Table 3.2: Random variable distribution type, mean, and standard deviation

Random variable	**Distribution type**	**Mean**	**Standard deviation**	**Citation**
$ksat$	Lognormal	11.7 cm/hr	7.6 cm/hr	[74, 75]
$seepage$	Lognormal	0.76 cm/hr	0.08 cm/hr	[74, 75]
$porosity$	Lognormal	0.44	0.047	[76, 77]
$thickness$	Lognormal	48.3 cm	7.6 cm	[15]
$sat.frac$	Lognormal	50	1.33	[78]

3.2 Regression Analysis

A combination of logistic and linear regressions was used to determine how the rain garden responded hydrologically to different storm conditions. These regressions comprise the demand ($V_{GSI}(x, r)$) used in later reliability calculations. Regressions are divided into three sections based on the quantity of runoff generated for storms within that section. Section 1 contains storms that produce no effluent in most random variable permutations, and thus

have very low probabilities of failure. Section 2 contains storms that produce a combination of effluent and no effluent, depending on the values of the input variables. The regressions for Section 2 storms follow a two-stage process: a logistic regression to separate outputs into storms producing effluent versus those not producing effluent, followed by a linear regression. Section 3 contains storms that always produce effluent, regardless of the combination of input variables used.

Rosner tests are used as appropriate to remove outlier points, while backwards stepwise regression is used to reduce the number of variables and simplify the model. All of the model coefficients are statistically significant ($p < 0.05$). Table 3.3 includes model form, coefficient values, and R-squared for 2-hour duration design storms (used in Section 4.2), while Table 3.4 presents these values for the 24-hour duration design storms (used in 4.3). Regression best-fit curves are presented in Appendix A.

Table 3.3: Model form, coefficient values and R-squared for the 2-hour duration storm.

Section	**Model form**	**Coefficient values**		**Model Fit**
Section 1 ($r \leq 30$ mm)	$V = 0$	N/A		N/A
Section 2 (30 mm $< r \leq$48 mm)	$h = \frac{1}{1+e^{25.1-0.43ksat+19.8porosity-1.05r}}$ $V = \theta_0 + \theta_1 porosity + \theta_2 ksat + \theta_3 r, h > 0.5$	θ_0	-19.3	Accuracy = 0.96 R^2=0.83
		θ_1	-7.02	
		θ_2	-5.62	
		θ_3	0.46	
($r >$ 48 mm)	$V = \theta_0 + \theta_1 seepage + \theta_2 porosity + \theta_3 ksat + \theta_4 r$	θ_0	-133	R^2=0.97
		θ_1	2.45	
		θ_2	-5.23	
		θ_3	-1.90	
		θ_4	5.19	

Table 3.4: Model form, coefficient values and R-squared for the 24-hour duration storm.

Section	**Model form**	**Coefficient values**	**Model Fit**
Section 1 ($r \leq 5.3$ cm)	$V = 0$	N/A	N/A
Section 2 ($5.3cm < r \leq 7.1$ cm)	$h = \frac{1}{1+e^{51.3-0.21sat.frac+34.0seepage-9.95r}}$ $V = \theta_0 + \theta_1 sat.frac + \theta_2 seepage + \theta_3 r, h > 0.5$	θ_0 -22.7 θ_1 0.088 θ_2 -16.1 θ_3 4.65	Accuracy = 0.96 R^2=0.94
($r > 7.1$ cm)	$V = \theta_0 + \theta_1 sat.frac + \theta_2 seepage + \theta_3 porosity + \theta_4 r$	θ_0 -20.7 θ_1 0.11 θ_2 -19.26 θ_3 -11.6 θ_4 5.10	R^2=0.98

To calculate the capacity ($\alpha V_{Paved}(x, r)$), a new SWMM model was created by removing the bioretention LID module and increasing the impervious fraction of the subcatchment to 100%, effectively 'paving over' the rain garden surface. The relationship between precipitation (in mm) and effluent depth (mm) for a paved surface is linear, as shown in Equation 3.1.

$$V = (1 + 1/LR) \times (r - \text{initial abstractions}) \tag{3.1}$$

3.3 Probability Distribution of Storm Magnitude and Interstorm Duration

Many of the analyses in the following chapter are dependent on the temporal variability of both rainfall magnitude and interstorm duration. The distribution of storm events and magnitudes can be modeled as a homogenous spiked Poisson distribution. The distribution is assumed to be homogenous since there is no seasonality associated with the interstorm durations for the temperate, humid climate found in Urbana, IL. To determine the effect of a typical midwest climate on our test rain garden, storm magnitude is modeled based on 50 years of daily precipitation data (1977-2017) taken from the National Oceanic and Atmospheric Administration (NOAA) gage in northwest Urbana, IL. The best fit distribution of storm magnitude is defined by a gamma distribution with a shape parameter α =0.52 and rate parameter β =1.54. The length of the interstorm duration is modeled based on 5 years (2000-2005) of 15-minute increment precipitation data taken from the NOAA gage in west Champaign, IL. Data from this gage were used for the interstorm duration analysis because they were available at finer temporal resolution than the data at the Urbana, IL gage (Champaign, IL and Urbana, IL are adjacent). An interstorm period is defined as a period of at least 6 hours between measurable rainfall events, as per Wadzuk et al. [102]. The best fit distribution of interstorm duration is defined as an exponential distribution with a rate parameter λ =0.011. A Lilliefors-corrected Kolmogorov-Smirnov test was used to ascertain that an exponential distribution was a good fit for the data. Plots of the histogram and the best fit distributions can be found in Figure 3.2.

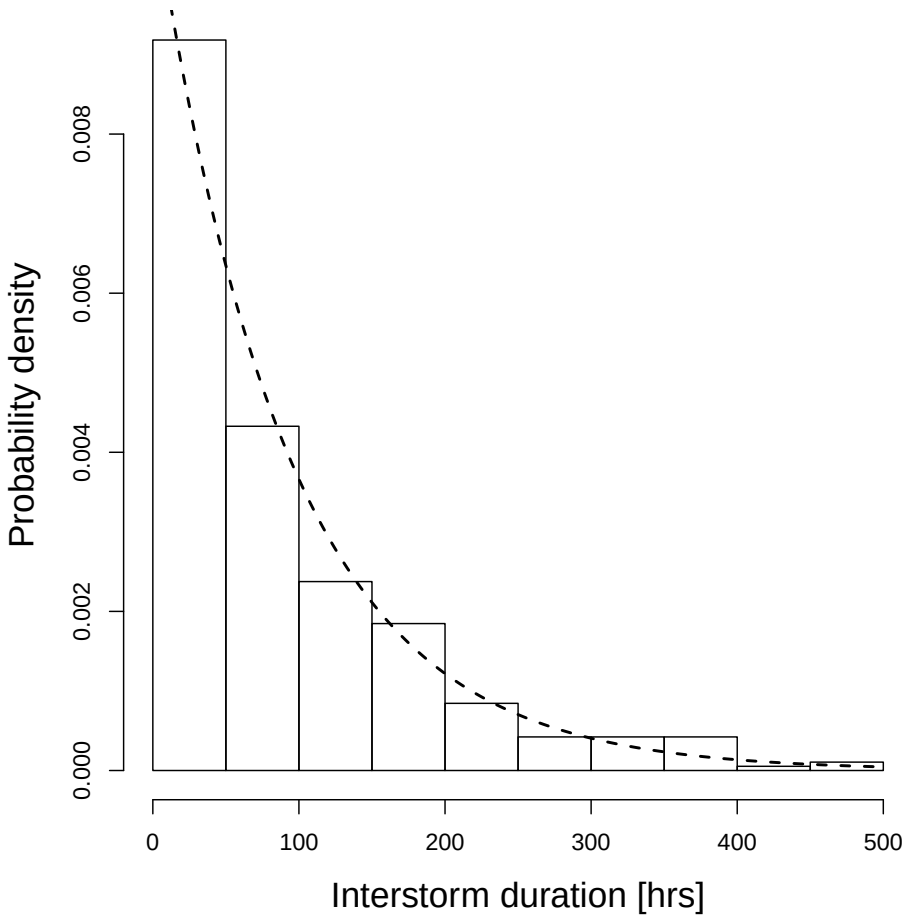

Figure 3.2: The best fit distribution of the interstorm duration is defined as an exponential distribution (shown as a dashed line plotted against a histogram of the interstorm duration).

CHAPTER 4

UNDERSTANDING MODULAR GREEN INFRASTRUCTURE PERFORMANCE UNDER SPATIAL AND TEMPORAL VARIABILITY

4.1 Overview

Modular "as-built" fragility curves from individual GSI installations can be used as a starting point to evaluate the variability of green infrastructure performance in time and space. They can also be 'scaled up' to determine the effectiveness of using GSI to reduce urban watershed pollution at the network scale. In this chapter, the test-case of a common form of residential green infrastructure, a rain garden, is used to evaluate the impact of three different phenomena on performance reliability. Firstly, the impact of long-term clogging on rain garden stormwater volumetric reduction is evaluated using the stochastic life-cycle analysis (SLCA) methodology developed by Jia et al. [58]. The clogging analysis assumes deterioration with no recovery, thus simplifying the modeling process, as described in Section 4.2. The second phenomenon involves modeling the impact of back-to-back rainfall events on rain garden performance. Again, the general framework from Jia et al. [58] is adopted, utilizing mechanisms to describe both deterioration and recovery (i.e., the processes of increasing soil moisture content during storms and decreasing soil moisture between storms, respectively). More detailed methodology for this second task can be found in Section 4.3. Finally, the impact of location on green infrastructure performance is simulated by changing the seepage rate within the model to simulate placing the rain garden in different surrounding soils. In this section, the effect of loading ratio on rain garden reliability is also investigated. This analysis provides the logical framework for the network-scale analysis conducted in Chapter 5.

4.2 A reliability-based approach to investigating long-term clogging in green stormwater infrastructure[1]

Multiple green infrastructure field studies highlight the issue of clogging [20, 79]. Clogging is often the result of the physical buildup of fines and other debris carried by influent water and deposited in the pores of the planting medium. A 1992 field study found that after four years of operation, many infiltration systems were found to be either not functioning as designed, or not meeting current design guidelines with respect to hydraulic conductivity [20]. In controlled column tests, Le Coustumer et al. [80] found that saturated hydraulic conductivity decreased substantially over time if the system was loaded with influent containing total suspended sediments (TSS) of mean concentration 120 mg/L. However, certain system characteristics can help mitigate or reduce the likelihood of clogging. The presence of plants, particularly those with coarser root systems, helps stabilize the saturated hydraulic conductivity [79–81]. In addition, the initial choice of soil greatly impacts clogging processes, since saturated hydraulic conductivity is primarily controlled by the top layer of soil [79]. Finally, lab studies indicate that an asymptotic value of saturated hydraulic conductivity is reached with increasing loading of pollutants, including TSS [80, 82].

In this section, a SLCA framework is used to assess the reliability of GSI considering the effects of clogging and different maintenance strategies. Specifically, a probabilistic method is developed to determine optimal maintenance timeframes to mitigate GSI performance degradation from clogging, demonstrated for a model rain garden. This work asks and answers the motivating question, "How often should infiltration-based green infrastructure be maintained to prevent clogging?", thereby filling an important gap in the literature.

4.2.1 General Modeling Setup

The methodology used to determine the time taken to clog a GSI follows two main steps, as shown in Figure 4.1. Step 1, shown in black boxes, involves changing the saturated hydraulic

[1]The content of this section is published as William, R., Gardoni, P.,and Stillwell, A.S. (2018). A reliability-based approach to investigating long-term clogging in green stormwater infrastructure. *Journal of Sustainable Water in the Built Environment, 5*(1), 04018015.

conductivity ($ksat$) to examine how it affects the resulting fragility curves; calculating the instantaneous reliability (Q) for each fragility curve; defining a relationship between Q and $ksat$; and using this relationship to find the acceptable value $ksat_{acc}$ corresponding to a given acceptable value of Q_{acc}. Step 2, shown in grey boxes, is an iterative while loop. Firstly, the distribution $f[r(t)]$ is used to determine whether a storm happens in a given month, and if so, how many storms occur, and how large they are. These results are used to determine the influent volume and the new $ksat$. Mathematical descriptions of these processes are detailed in the following sections. The results from Step 1 are then used to determine how the green infrastructure responds to a given storm, and to ascertain whether or not $ksat_{acc}$ has been reached. If it has, the value of the time step is output. If not, the cycle is repeated. This process is repeated 450 times to create a probability distribution of the time to clogging (t_{final}) for different influent TSS concentrations.

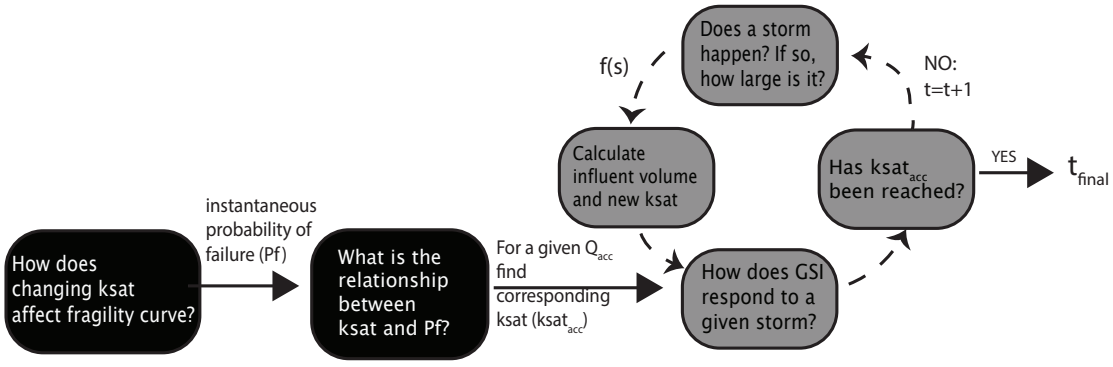

Figure 4.1: The general methodology for determining the probability distribution of the mean time to clogging is a two-stage process. In this diagram, Step 1 is colored black, and Step 2 (inside a while loop) is colored grey. The process is repeated 450 times to determine the probability distribution for the time to clogging.

4.2.2 Modeling the Clogging Process

Based on reporting from the SWMM User Manual as well as literature [82], saturated hydraulic conductivity ($ksat$) was identified as the primary random variable affected by progressive clogging. While clogging can be based on biochemical as well as physical processes [82], this study's modeling of clogging is based on sediment deposition, a physical process.

Total suspended sediments (TSS) are a major source of clogging impairment in bioretention cells and rain gardens, particularly for those without pre-treatment.

In modeling clogging, SWMM uses an empirical 'clogging factor' to decrease $ksat$ proportional to the volume of water influent into the bioretention cell. Rather than using this approach, this model follows the more precise logistic regression proposed by Viviani and Iovino [82]. The logistic regression model was chosen because of its mathematical simplicity, but also because it captures the $ksat$ asymptotic decay observed in many field studies of green infrastructure [7, 80, 83]. The relationship between $ksat$ and the TSS cumulative loading density L_{TSS} (the influent loading in terms of depth multiplied by the influent concentration) can be described as shown in Equation 4.1, where a and b are empirical parameters dependent on the type of soil in question, and $ksat(\tau_i)$ is the saturated hydraulic conductivity at time τ_i. In this analysis, a is 0.02 m^2/g and b is 0.513 based on Vivani and Iovino's [82] calculated values for a loam soil loaded with artificial wastewater (containing only suspended solids and no organic matter).

$$ksat(\tau_2) = \frac{ksat(\tau_1)}{1 + aL_{TSS}^b} \tag{4.1}$$

4.2.3 Results

The fragility curve of the as-built GSI, shown in Figure 4.2, highlights the three distinct regions used in the regression analysis. The $\pm\sigma$ uncertainty bounds are created using the methodology described in Gardoni et al. [59] to capture the epistemic uncertainty in the model parameters. Storms below 48 mm (1.9 in) of precipitation (Sections 1 and 2) have negligible probabilities of failure. These low values are unsurprising, given than many rain garden design standards specify a minimum volumetric retention depth on the order of 25 mm (1 in) of runoff. Storms above 48 mm show a rapid increase in the probability of failure.

Figure 4.3 plots the fragility curves for the rain garden after clogging (i.e., at reduced levels of $ksat$). The impact of $ksat$ on rain garden failure is significant, particularly for larger storms. As the garden becomes increasingly clogged, the curves shift up and to the left: smaller storms begin to generate effluent. The overall shape of the curve also changes,

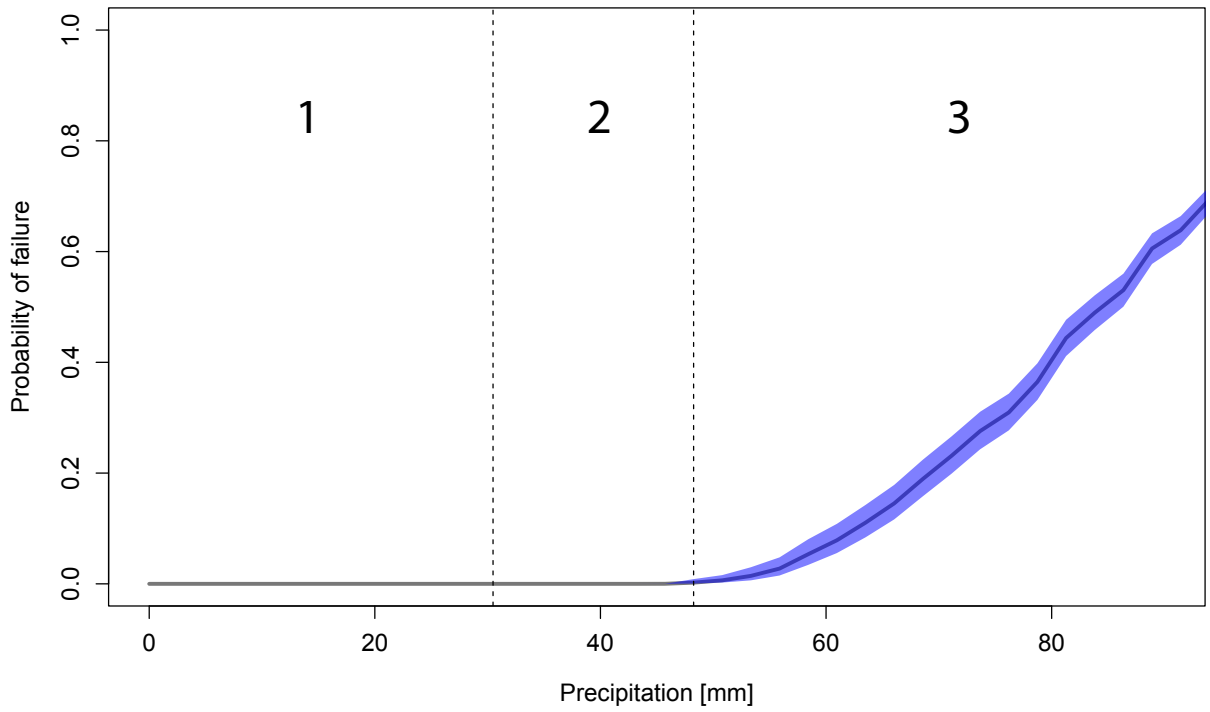

Figure 4.2: The as-built fragility curve for 80% volume reduction for a two-hour duration storm is divided into three distinct sections. The blue shaded area corresponds to the 1-sigma error bounds on the fragility curve.

with clogged curves showing steeper slopes in the early portion of the graph compared to the as-built curve. The graphs' curvatures also change as the system becomes more clogged. The unclogged, as-built system is concave, with a large increase in the conditional probability of failure for storms above a certain threshold. At lower $ksat$, the fragility curves tend towards a convex shape, reaching an asymptotic maximum failure at much smaller storm magnitudes.

The rapid increase in the conditional probability of failure as a result of decreasing $ksat$ leads to larger instantaneous probability of failure, and thus lower instantaneous reliability. As shown in Figure 4.4, instantaneous reliability decreases rapidly over time. Each "step" in the graph represents a storm or series of storms that has taken place in a given month. Months without a decrease in reliability indicate no precipitation. Importantly, because of the probability distribution of the rainfall magnitudes, a large jump in the graph is most likely due to several smaller storms rather than one large storm. As the simulation progresses, reliability asymptotically approaches the limit set by the chosen Q_{acc} (0.9, or a rain

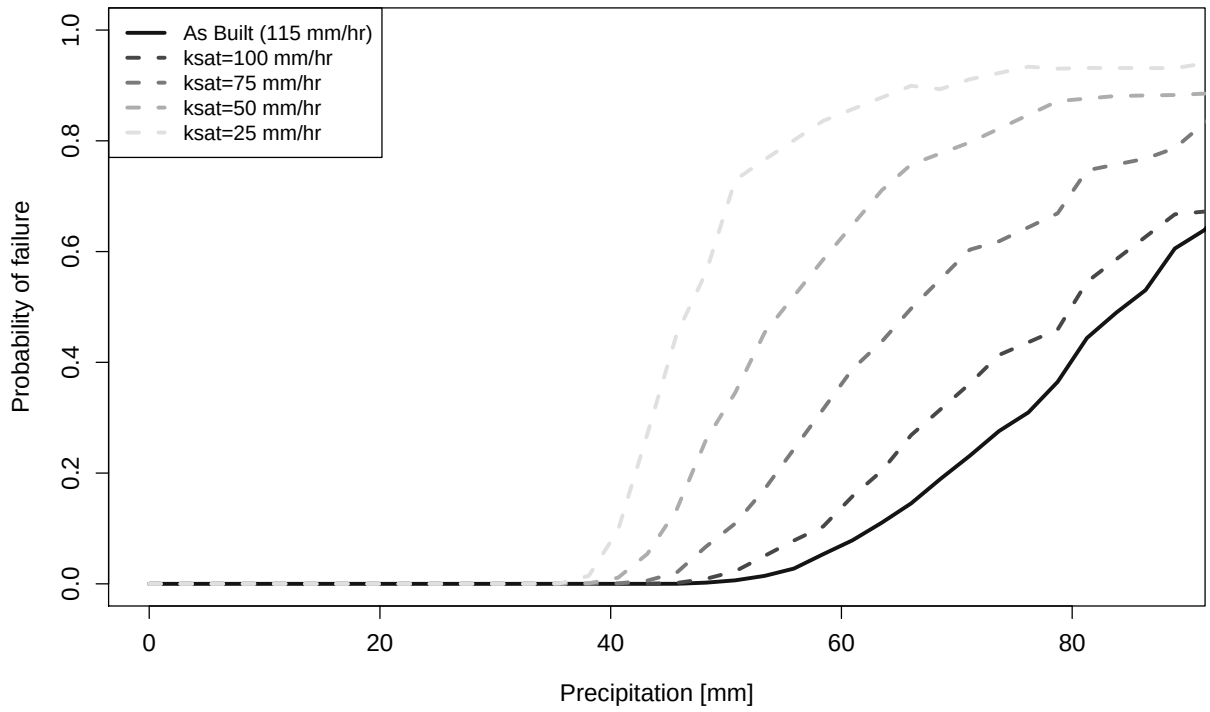

Figure 4.3: Changing the *ksat* via clogging significantly alters the shape of the fragility curve.

garden that performs as expected in nine storm events out of ten). This asymptotic decrease is reflective of the logistic regression used to recursively calculate the *ksat*. The asymptotic decrease in the instantaneous reliability also implies that the rain garden continues to function fairly well, even at low levels of *ksat*.

Finally, Figure 4.5 shows the change in the cumulative distribution function (CDF) of the time to clogged for different influent concentrations of TSS. The three influent concentrations are chosen as representative of runoff effluent from a roof gutter system (10 mg/L), runoff influent to a typical rain garden with some pre-treatment (40 mg/L), and runoff from a parking lot without pre-treatment (297 mg/L) [84, 85]. The 40 mg/L curve has a mean time to clogged of approximately 34 months, in contrast to approximately 66 months for 10 mg/L and approximately 15 months for 297 mg/L. Intuitively, these values make sense, since higher loadings of suspended sediments would tend to clog the system more quickly; many existing rain garden systems use pre-treatment for this reason. Interestingly, the general slope of the CDF decreases with decreasing TSS concentrations: the 10 mg/L CDF has an

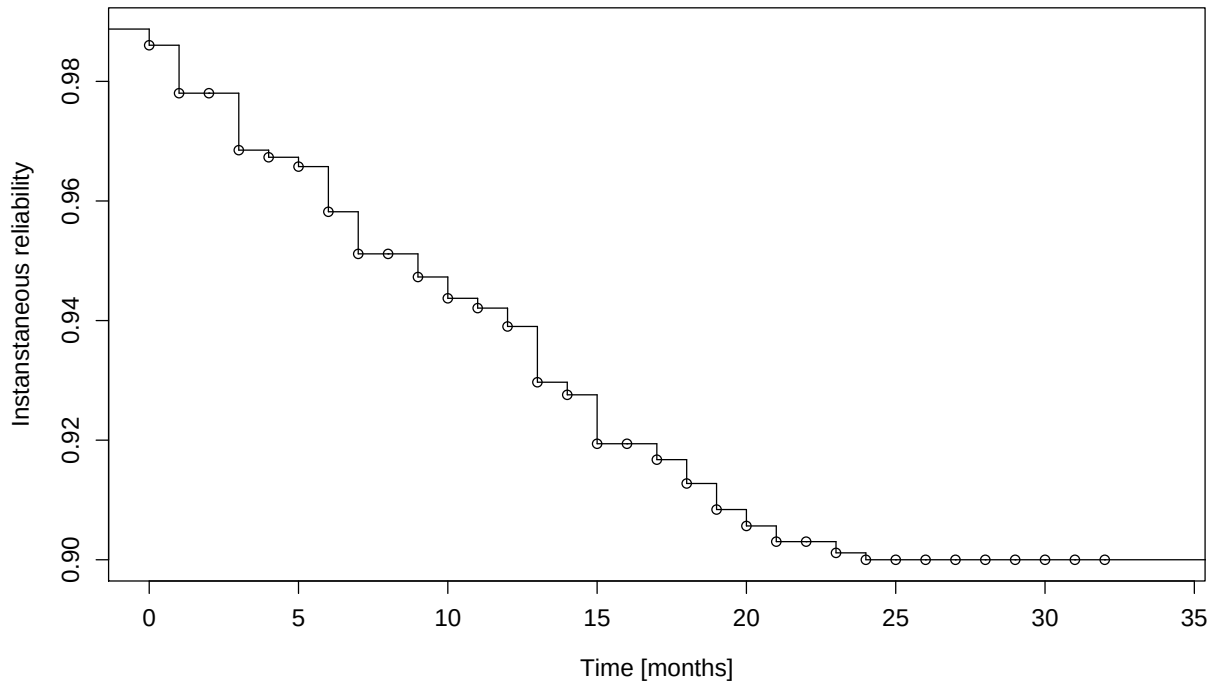

Figure 4.4: The instantaneous reliability (Q) shows an asymptotic decay towards the chosen threshold reliability (0.90) over time.

estimated standard deviation of 7 months, while the 40 mg/L CDF has a standard deviation of 5 months, and the 297 mg/L CDF has a standard deviation of 3 months. The reason for this trend is that the lower concentration CDF is more sensitive to the random distribution of rainfall events; a cluster of large storms tends to clog the system more quickly. In the case of the high concentration CDF, this effect is less pronounced, since every storm already carries a high sediment loading regardless of its size. The error bounds on the CDFs also increase with decreasing TSS concentration, illustrating that the effects of uncertainty in the model parameters are also more pronounced.

4.2.4 Discussion

The reliability analysis of rain garden clogging suggests that in a humid continental climate, monitoring and maintenance should ideally be conducted on average every 3 years (based on model results of 34 months to clogged conditions) to ensure optimal performance.

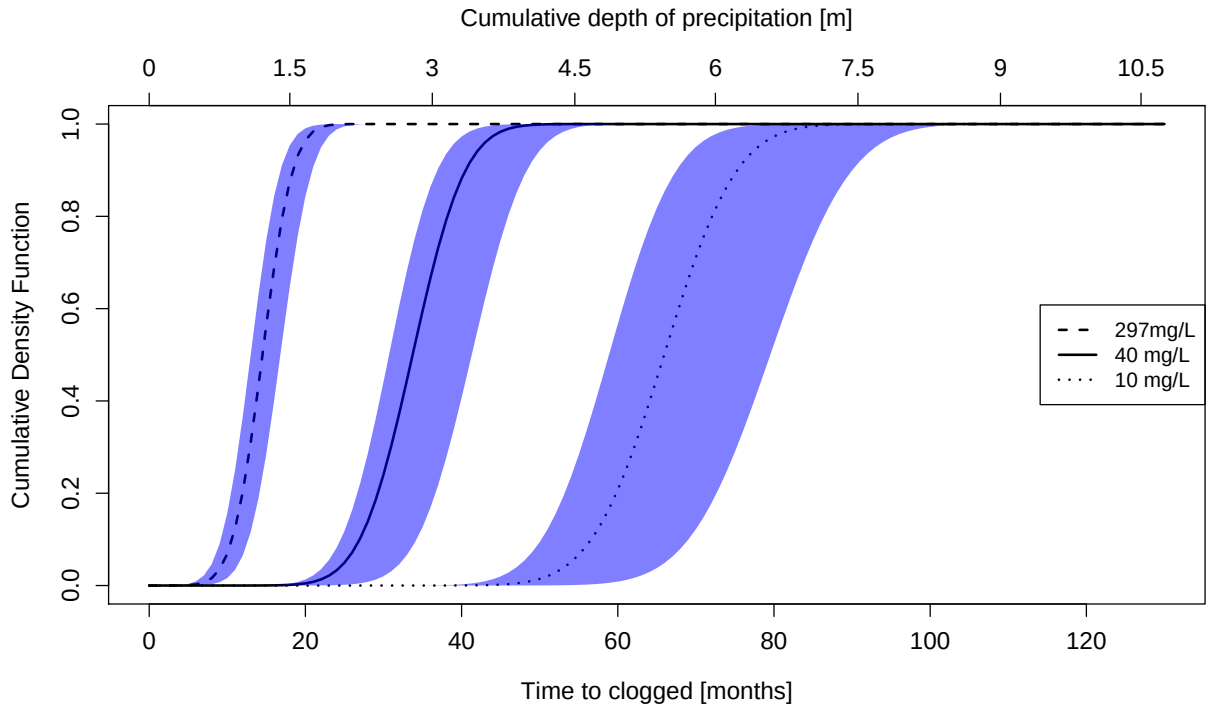

Figure 4.5: Changing the influent total suspended sediment concentration alters the cumulative probability density (CDF) of the time to clogged. The shaded areas correspond to the error bounds on the CDF. The CDF is given both is terms of time to clogged (bottom axis) and the corresponding mean cumulative precipitation (top axis).

Because clogging is highly determined by climate, these results will change depending on local rainfall distributions. Importantly, this analysis assumes a high performance standard for the considered rain garden since the garden was designed to retain and infiltrate the majority of the stormwater that fell on the property. Using a lower performance standard would help to increase the time window for maintenance.

Rain garden volumetric retention is greatly decreased for larger storm events, which reduces its overall future performance ability. Moreover, clogging increases the probability that smaller storms will begin to generate runoff. As expected, mean clogging time decreases with increasing influent TSS concentration. However, the standard deviation also decreases, implying that while rain garden pre-treatment does improve long-term performance, it also produces high performance variability due to the sensitivity of performance on rainfall distribution. Some examples of suggested stormwater pre-treatment include the use of forebays and drain inlet inserts to allow for the trapping of gross pollutants [86].

While *ksat* does significantly impact rain garden reliability, many of the effects are concentrated in larger storms. A large decrease in *ksat* thus does not necessarily translate into a large decrease in instantaneous reliability. Consequently, monitoring should comprise a holistic evaluation of the desired performance parameter rather than a single factor such as *ksat*. Performance parameters that might be relevant to effective monitoring and maintenance schedules could include volumetric runoff reduction, effluent turbidity, and the presence of long-standing ponded water. Many utilities already use some of these parameters in their maintenance regimes [87].

Although the model described here presents a first attempt at using a reliability-based approach to evaluate the performance of a rain garden over time, it is still highly simplified. The model assumes a uniform effect of clogging throughout the soil thickness, while literature suggests that clogging typically manifests in the top few inches of the bioretention column [82]. In addition, many other factors impact the change in *ksat* other than influent TSS. For instance, Le Coustumer et al. [80] indicate that the presence of coarse-root vegetation in the bioretention cell can help decrease the likelihood of clogging. Other studies [81] also show that while *ksat* decreases rapidly in bioretention cells within the first six months of planting, cells recovered functionality due to plant macropore processes. In addition, Mehring and Levin [88] suggest that rain garden ecology and a flourishing macrofauna can have important impacts on maintaining infiltration capacity. Earthworm burrows can increase infiltration rates by factors of 2 to 15 in terrestrial systems. In addition, their burrows create preferential flow paths under wet conditions. Other burrowing invertebrates such as termites and ants can also have the same effect [88]. While rain garden sizing can also be used to mitigate potential clogging [80], field inspections of bioretention cells in North Carolina revealed that over half of the bioretention cells were undersized [89].

Another factor that was not considered was the buildup of sediment in the upstream treated area between storm events, which could alter influent concentrations. The phenomenon of a greater proportion of pollutant loads being washed off surfaces early on in the storm, leading to variable influent concentrations, is known as 'first flush'. However, previous research has found that no correlation exists between first flush and antecedent dry weather period [90]. This study evaluates the effects of long-term clogging on rain garden

performance, and so excludes the first flush effect, instead assuming constant concentrations based on average reported concentrations from rainfall collected over several sizes of storms.

4.2.5 Implications for GSI Maintenance

The mean time to clogging is 34 months for a 9.3-m^2 (100 ft^2) sandy loam rain garden with 40 mg/L total suspended sediment loading, and a mean annual cumulative rainfall of around 1000 mm (40 in). The findings illustrate that TSS influent concentrations affect the mean and standard deviation of the time to clogging. Increasing the influent concentration decreases a rain garden's long-term performance, making a strong case for pre-treatment. However, results show that rain gardens with pre-treated influent runoff are more sensitive to the distribution of incoming rainfall, increasing uncertainty around the elapsed time to clogged conditions.

Many public utilities identify the significant build-up of sediments and debris along with long-term ponding as a cause for concern and immediate remedial maintenance [91]. Possible repairs to systems that are already clogged include the removal of the top layer of soil; because clogging tends to happen in the upper layer of soil, removing this upper layer immediately renews performance capacity. Another suggestion is to dig small pits within the garden to remove the soil, and naturally letting them fill in over time [92]. However, this restorative maintenance can be expensive [93, 94]. To avoid these high costs, some utilities suggest a routine maintenance schedule. If sediments are detected before they become a significant issue, then simply clearing out the excess debris and aerating the soil with a garden rake will avoid the need for restorative maintenance as a result of clogging. The University of New Hampshire Stormwater Center suggests checking for standing water biannually after the first year. Additionally, they suggest a biannual inspection to check for accumulated material in the filter bed [87]. Other organizations suggest annual inspections for accumulated sediment or debris [92, 95]. The Rutgers University rain garden maintenance manual suggests checking the rain garden for sediment accumulation after each major storm event [96]. These routine maintenance schedules are helpful, but remain ad-hoc and without a quantifiable reasoning for their suggested timings. This study presents a quantitative

metric that can be used to specifically highlight unique maintenance "windows" for which maintenance is most appropriate for a given location.

This study's findings are important because they present a first attempt at using a reliability-based approach to evaluate green infrastructure maintenance requirements. This analysis allows utilities to focus their efforts on the time period before the mean predicted time to clogging, and to take a proactive approach to long-term performance while avoiding excess expenses. Based on these findings, saturated hydraulic conductivity alone is not the only parameter that should be used to assess rain garden performance. Other possible indicators of rain garden performance could include a visual inspection for standing ponded water or for unexpected overflows during smaller rainfall events to determine whether the rain garden is draining adequately. A reliability-based approach with final performance metrics for the rain garden (e.g., volumetric retention) is a more holistic method that can be used to model and monitor long-term rain garden performance. Importantly, modeling rain garden maintenance using a probabilistic approach also allows for schedule customization to the design needs and unique soil characteristics for each rain garden location.

4.3 Predicting Green Infrastructure Performance Under Antecedent Moisture Conditions using SCLA[2]

Understanding the impact of antecedent soil moisture on hydrological performance metrics is another challenge for scientists studying green infrastructure. In their study of green roof hydrological performance, Locatelli et al. [97] highlighted that variables such as antecedent moisture and rainfall patterns make runoff analysis uncertain for single events. Other studies show that soil storage and antecedent moisture both play a role in the ability of rain gardens and other types of green infrastructure to reduce runoff [50, 98]. Brander et al. [99] indicated that both groundwater depth and soil type significantly impact the effectiveness of infiltration basins in highly urbanized environments. Apart from its impacts on runoff quantity, subsurface antecedent moisture also impacts water quality. The creation of a deep internal water storage zone can be helpful in stimulating denitrification processes within

[2]The content of this section is in revision for *Sustainable and Resilient Infrastructure.*

the green infrastructure, leading to the removal of nitrates [100]. Pearson et al. [101] used experimental evidence to confirm that antecedent moisture content significantly affects both runoff quantity and quality. Because antecedent soil moisture has a significant impact on performance, timing and inter-storm duration for smaller events can also be important metrics for assessing performance [102]. In other words, green infrastructure can underperform even for small storms if there is a short enough interstorm duration.

This study addresses the need for a probabilistic understanding and quantification of green infrastructure performance under back-to-back rainfall events. A stochastic life-cycle analysis framework is used to evaluate the extent to which interstorm duration impacts the ability of green infrastructure to reduce runoff both in short and long terms. The results are presented in two different forms. Wireframe fragility surface plots illustrate how the conditional probability of failure changes with interstorm duration and storm magnitude. Two fragility surfaces are presented, for small and large antecedent storms. To illustrate how antecedent moisture conditions affect rain garden performance over longer periods of time, the long-term changes in the probability of failure are plotted for time periods ranging from 1 to 24 months.

4.3.1 General Modeling Setup

Fragility surfaces for two different initial storm magnitudes (S_{k-1a} and S_{k-1b}) are generated for a test rain garden. The fragility surface is a 3D plot that depicts the probability of failure of the rain garden after different interstorm duration and under different second storm (S_k) magnitudes following a given storm S_{k-1}. Figure 4.6 illustrates the method used to create these fragility surfaces. Further details of the mathematical modeling used in each step are detailed later in this section, as shown in Figure 4.6.

To evaluate the long-term impacts of antecedent moisture on rain garden performance, changes in the probability of failure of the system over time are tracked. Figure 4.7 diagrammatically illustrates the methodology. To calculate the new antecedent moisture, random selections are made from the probability distributions of the storm magnitude and the interstorm duration. Using these values, relationships are developed between precipitation,

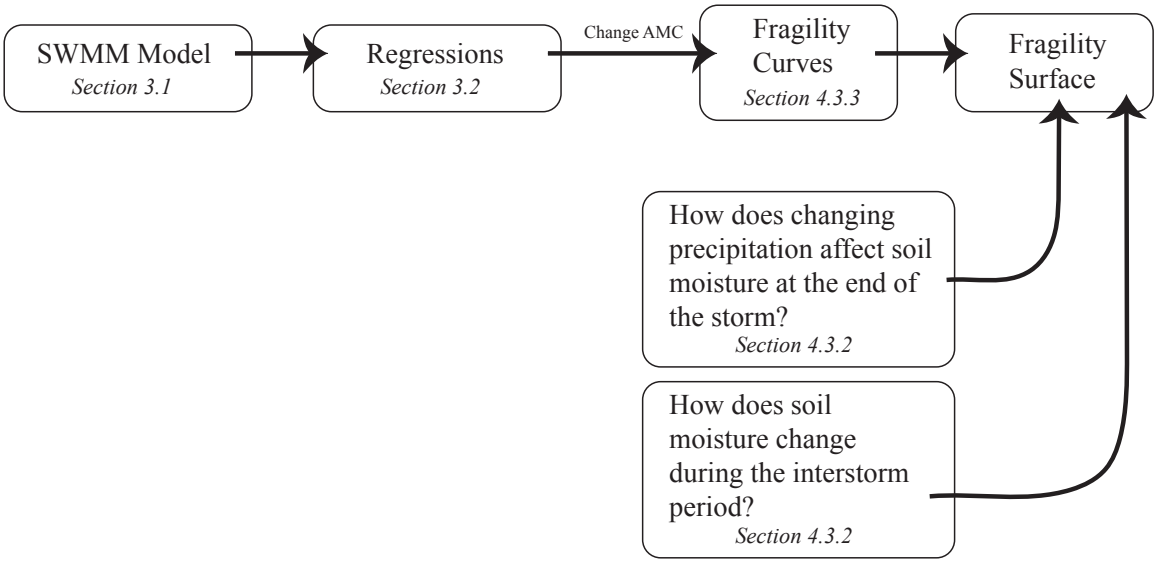

Figure 4.6: The fragility surface is created based on fragility curves representing the change in antecedent moisture content (AMC) and the change in the soil moisture over time.

interstorm duration, and antecedent moisture. After calculating the soil moisture content, the probability of failure is calculated using the preset fragility curves. A 'weighted coin flip' is conducted based on the calculated probability of failure, to determine whether or not the rain garden is in failure. The process is repeated until the given time period is completed, with all of the determined failures being summed. The probability of failure for the time period is the number of failures divided by the number of storm events. The process is repeated using a convergence criteria of coefficient of variance (COV) less than 0.05 for time periods ranging from 1 to 24 months to determine the mean and standard deviation of the probability of failure for each time period.

4.3.2 Temporal Changes in Soil Moisture Content

To understand how antecedent moisture and interstorm duration affect green infrastructure performance, it is important to understand how soil moisture changes over time. Because the seepage out of the rain garden into the surrounding aquifer is much lower than the infiltration rate into the rain garden, the runoff effluent from the rain garden is caused by

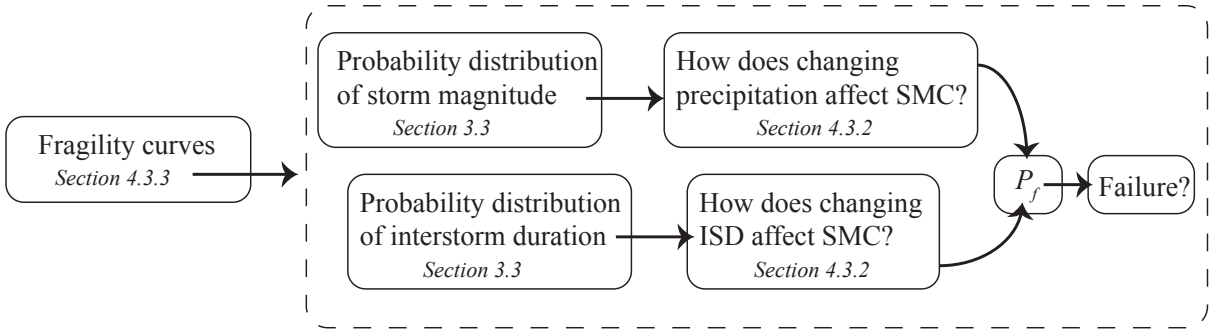

Figure 4.7: Several steps go into calculating the long-term probability of failure, as detailed in later sections, including the calculation of how changing precipitation and interstorm duration (ISD) affects the soil moisture content (SMC). The dashed line represents the algorithm inside the while loop for a given time period.

saturation excess runoff rather than infiltration excess runoff. In other words, runoff only starts happening when the soil pores in the rain garden are completely filled with water (i.e., the soil is saturated).

After the storm has passed, there are two possible cases:

1. There is no water ponded on the surface after the storm has passed. After the storm has passed there is no inflow into the mass balance, only outflow through drainage. At the interstorm duration timescales considered (i.e., <48 hours), losses through evapotranspiration are assumed to be negligible.

2. There is some ponded depth (H) at the ground surface after the storm is over. This ponded water needs to be removed before the soil can begin to drain.

   The controlling factor in how fast the water is removed from the system is the seepage rate. The time taken to drain the ponded water can be defined as t_d. The soil moisture content a time t after the storm has passed ($SMC(t)$) is given in Equation 4.2, based on a mass balance. Note that when no water is ponded on the surface, t_d =0 in Equation 4.2. From the calculated SMC, the initial saturated fraction ($sat.frac$) is calculated as required by SWMM, as shown in Equation 4.3, where n is the porosity, and WP is the wilting point.

$$SMC(t) = SMC_0 - \frac{seepage \times (t - t_d)}{thickness} \tag{4.2}$$

$$sat.frac = SMC \times \frac{100}{n - WP} - \frac{100 \times WP}{n - WP} \tag{4.3}$$

Based on the SWMM outputs, a relationship between the magnitude of the storm (r_1), t_d, and SMC_0 (the soil moisture content at the beginning of the interstorm period) is developed as shown in Table 4.1. There are four potential outcomes in calculating SMC: 1) the soil does not become fully saturated; 2) the soil is fully saturated, but there is no ponding such that t_d=0; 3) there is some ponding, but no runoff effluent from the top of the berm; and 4) there is both ponding and runoff. Plots of the best fit curves for these regressions can be found in Appendix A.

Table 4.1: Soil moisture content as a function of initial saturation ($sat.frac$) and precipitation (r_{k-1}) (in cm)

Case	**Model**	$\mathbf{R^2}$	**Range**
1 Not saturated	$SMC_0 = -0.0029 + 0.0036 sat.frac + 0.143 r_{k-1}$	0.96	$\frac{118.1 - sat.frac}{37.7} > r_{k-1}$
2 Saturated, no ponding	$SMC_0 = n$ $t_d = 0$	N/A	$\frac{118.1 - sat.frac}{37.7} \leq r_{k-1} < \frac{37.2 - 0.097 sat.frac}{13.7}$
3 Ponding, no runoff	$SMC_0 = n$ $t_d = -13.2 + 0.097 sat.frac + 13.7 r_{k-1} - 24$	0.99	$\frac{37.2 - 0.097 sat.frac}{13.7} \leq r_{k-1} < \frac{-47.9 + 0.097 sat.frac}{(0.95 - 13.7)}$
4 Ponding, runoff	$SMC_0 = n$ $t_d = 0.95 r_{k-1} + 34.7 - 24$	0.99	$r_{k-1} \geq \frac{-47.9 + 0.097 sat.frac}{(0.95 - 13.7)}$

4.3.3 Results

Figure 4.8 shows the resulting 24-hour duration as-built fragility curve, along with the 1-sigma error bounds. Fragility remains fairly low for the smallest storms, showing a rapid increase in the probability of failure after about 7.4 cm of precipitation to an asymptotic value. Although the error bounds remain fairly small, there is a slight increase in the error with higher rainfall. Overlaying the PDF of rainfall magnitude on top of this fragility curve showcases the ability of the rain garden to effectively deal with the vast magnitude of storms in this particular climate.

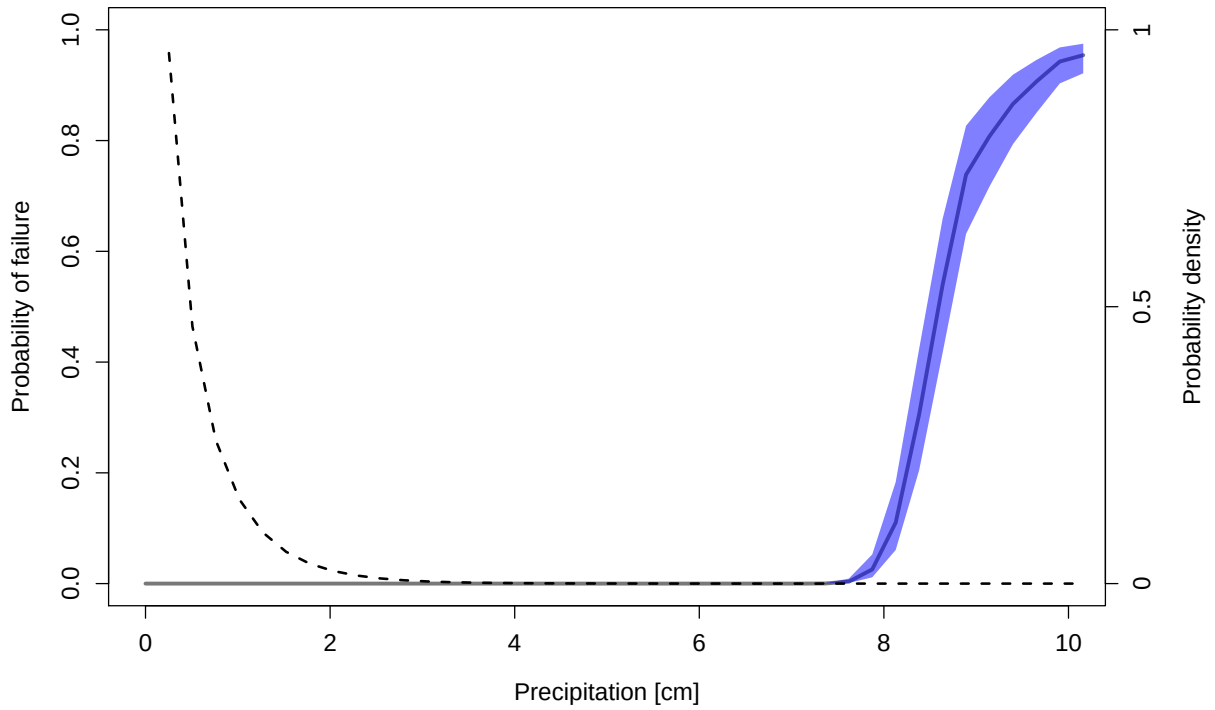

Figure 4.8: The as-built fragility curve for the rain garden shows that the garden is reliable over a wide range of storms. The dashed line represents the PDF of rainfall magnitudes for a temperate, humid climate.

To evaluate how $sat.frac$ affects the probability of failure for different storms, a family of fragility curves are created by changing the $sat.frac$ mean input into FERUM while keeping all other inputs constant. Figure 4.9 shows the family of curves, ranging from 40% initial saturation to 100% initial saturation. Although the overall shape of the curve stays the same, the curve shifts to the left with increasing initial saturation, indicating higher probabilities

of failure for smaller storms as the soil gets increasingly saturated. However, even when the soil is completely saturated, storms below 6.1 cm of precipitation still fail to produce significant quantities of runoff. This limited runoff is a result of ponding within the rain as a result of its built-in 6 inch berm. This finding is consistent with reported values from the USGS field site, which showed little to no runoff for the entire duration of its monitoring lifetime [103].

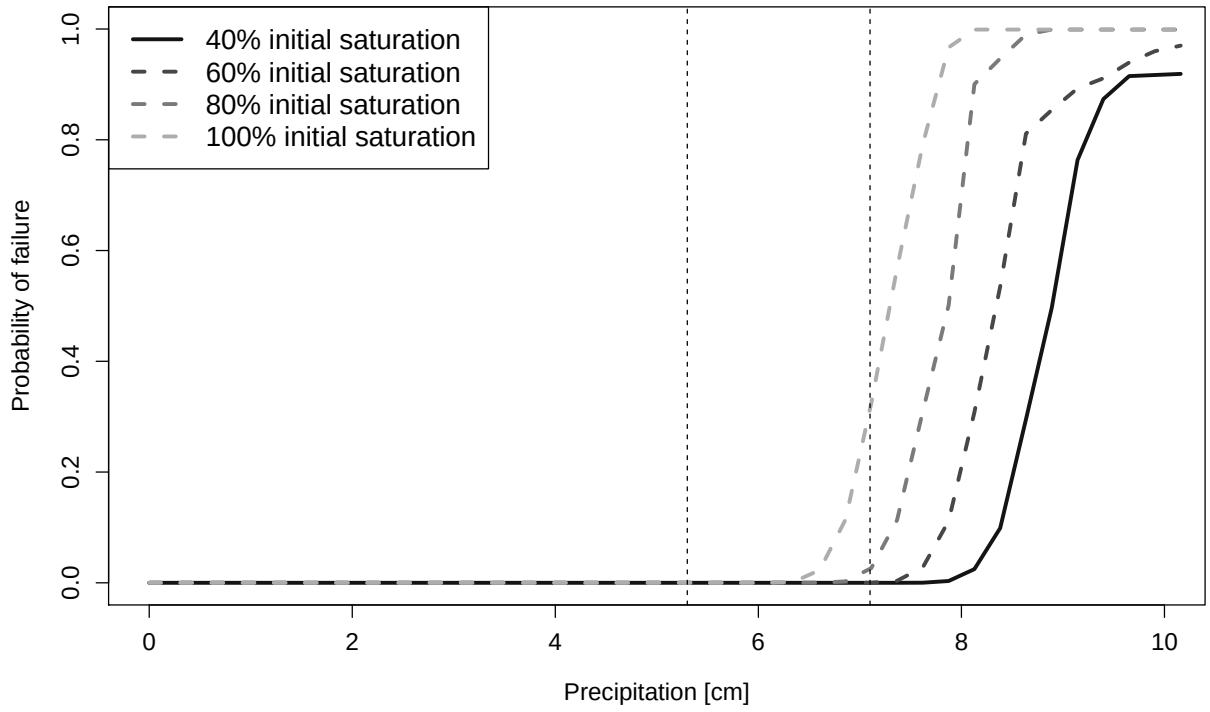

Figure 4.9: Increasing the initial saturation shifts the fragility curve to the left; the overall shape of the curve stays the same.

Figure 4.10 presents a 3D wireframe plot of the conditional probability of failure for the rain garden under storms with different magnitudes (S_k) and different interstorm durations, for a 2.5-cm magnitude preceding storm S_{k-1}. Interstorm durations were modeled up to 48 hours after the storm had subsided, and the soil initial saturation fraction before S_{k-1} was assumed to be 50%. As with the fragility curves in Figures 4.8 and 4.9, the probability of failure is generally very low for smaller magnitude storms. The probability of failure begins to significantly increase for very large storms. Increasing the interstorm duration decreases the magnitude of the probability of failure at the inflection point, and also slightly increases

the magnitude of the S_k required to increase the probability of failure above near-zero. The probability of failure for the largest magnitude storm also decreases with increasing interstorm duration.

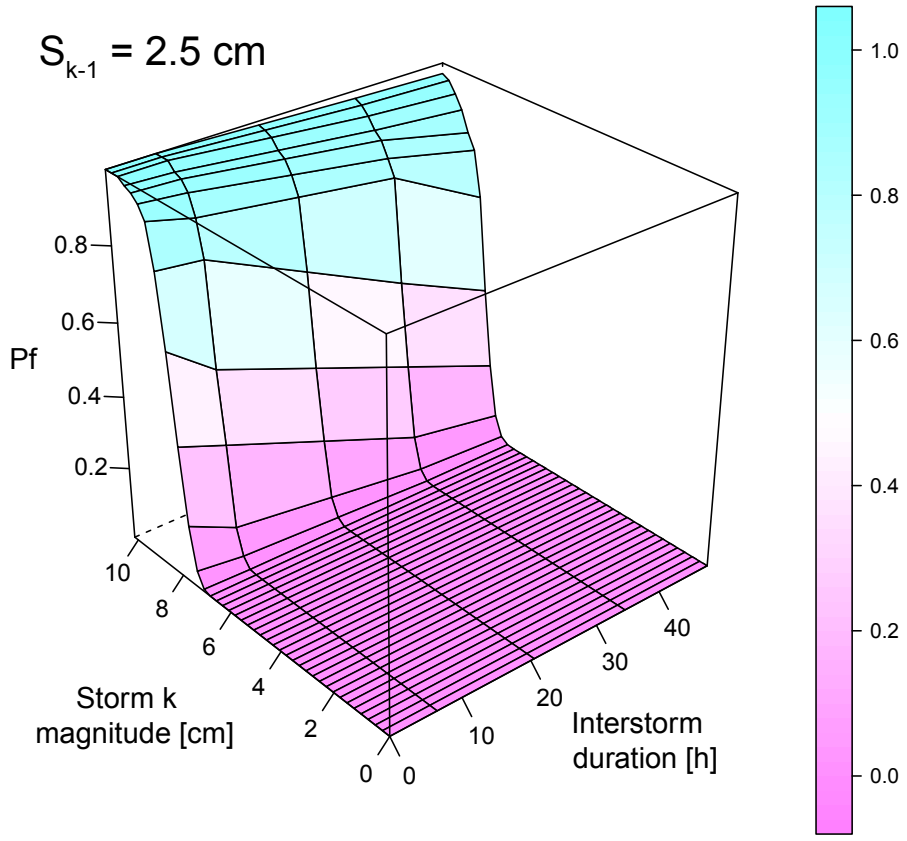

Figure 4.10: The fragility surface for a small magnitude S_{k-1} shows us that increasing the interstorm duration very slightly decreases the probability of failure.

Compare these results from Figure 4.10 with those presented in Figure 4.11, illustrating the results for a 7.6-cm magnitude preceding storm S_{k-1}. While the curvature of Figure 4.10 is less steep, Figure 4.11 reaches an asymptotic value more rapidly. In Figure 4.11, there is also little change in the probability of failure at different interstorm durations for the largest magnitude storms. Together, the two plots indicate that the probability of failure does not change dramatically over the time of the interstorm duration. The high volumes of water

required to increase the probability of failure also suggest that saturation excess processes are responsible for much of the runoff generation for long duration storms. In addition, the largest change in the probability of failure occurs during larger storms. In other words, he rain garden is most likely to fail if there are two large storms (> 6.5 cm) in succession with a small interstorm duration (< 24 hr), which is unlikely for the observed patterns of precipitation. This finding reflects other studies that show very few recorded rain garden failures for back-to-back rainfall events [102].

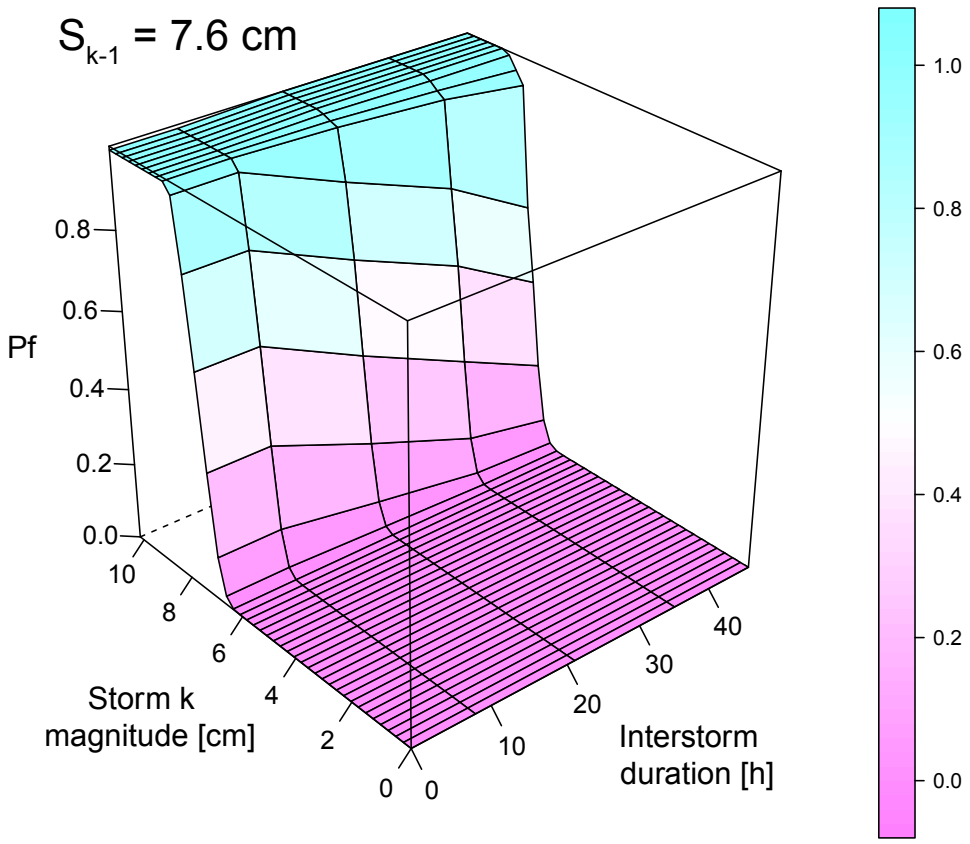

Figure 4.11: The fragility surface for a large magnitude S_{k-1} is much steeper than the fragility surface for a small magnitude S_{k-1}.

Figure 4.12 shows the change in the mean probability of failure (i.e., the total number of failures divided by the total number of storms within a given timestep, averaged over the number of iterations required to achieve COV≤ 0.05 over time; the shaded area shows the standard deviation of the probability of failure. In the long term, the probability of

failure decreases from 7.8% to an asymptotic value of 4.1%, around which it continues to fluctuate over time. The asymptotic decrease in the probability of failure indicates that if interstorm duration is incorporated into the analysis of rain garden performance, the model reaches equilibrium at a time scale of around one year of simulation. In other words, the approximate spin-up time for a rain garden model incorporating antecedent moisture conditions should be around one year.

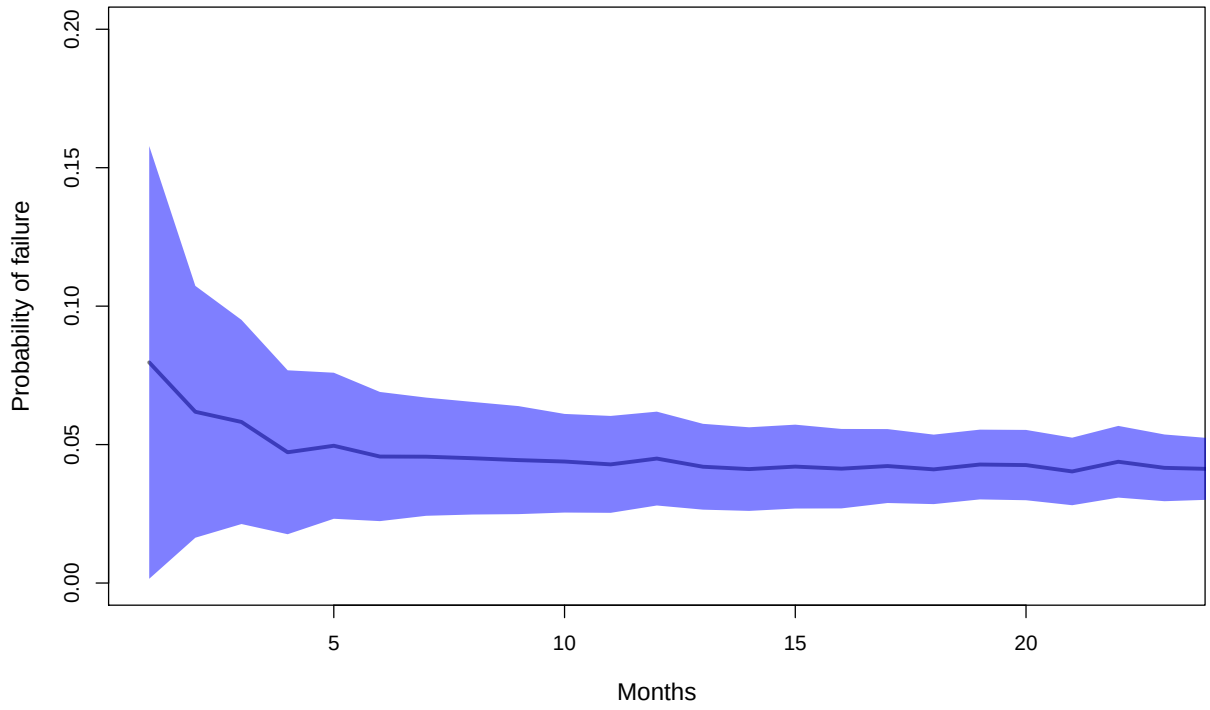

Figure 4.12: The spin-up time for a rain garden model incorporating back-to-back rainfall events is approximately one year.

4.3.4 Discussion

The 48-cm soil media depth selected in the initial model represents not only the rain garden medium (rototilled mulch and compost), but also a sandy layer surrounded by much more clayey soil. In practice, a 48-cm medium depth is much deeper than what is observed in a typical rain garden. It was possible that the highly reliable performance indicated by the initial rain garden fragility curve might be a result of the deep, sandy soil media. To

test this hypothesis, the same fragility curve analysis was conducted using a mean thickness of 23 cm, keeping all other variable parameters constant. The resulting fragility curve for a 50% initial saturated fraction is shown in Figure 4.13. The shape and position of this curve is similar to the 80% initial saturation fragility curve plotted in Figure 4.9. This result is expected since runoff is saturation excess driven: the amount of soil storage available with 23 cm of soil instead of 48 cm of soil is approximately half. Even at this lesser depth, the rain garden still shows high reliability under the smallest, most frequent storm events. Importantly, this analysis was conducted using a test rain garden with a fairly low loading ratio (1:5 ratio of rain garden to upstream impervious area). Because of the smaller influent volume into the rain garden, much better performance is observed than might otherwise be expected. However, many design guides for homeowners in similar climates suggest loading ratios in the same range as the one used for the Madison, WI rain garden. The University of Connecticut extension program suggests a 1:6 loading ratio despite their comparatively wetter climate [104].

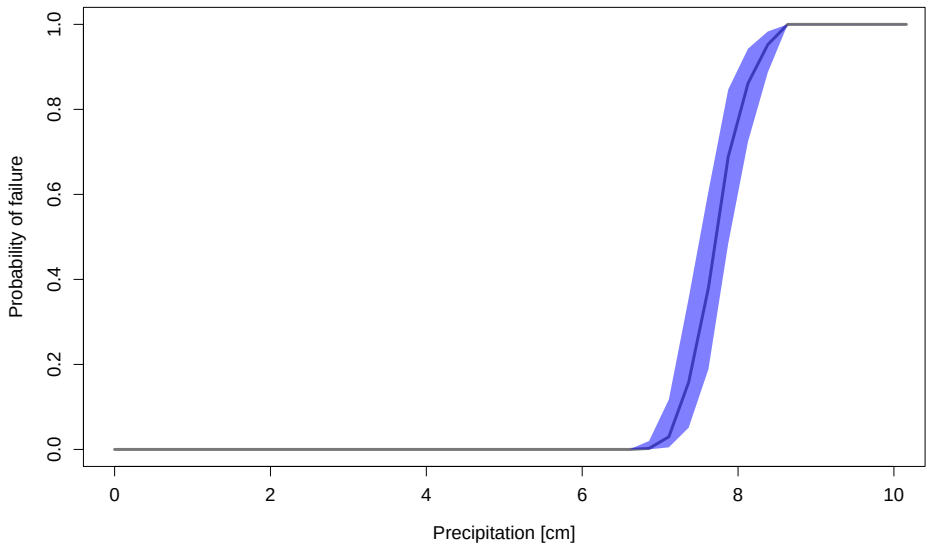

Figure 4.13: The shape and position of the half-thickness media fragility curve is similar to the 80% initial saturation fragility curve.

Despite these limitations, this analysis indicates that infiltration-based green infrastructure can be functional, even in clayey native soil. Other studies similarly find that bioretention installations in native soils with fairly low saturated hydraulic conductivity can lead

to large reductions in annual runoff, as long as the bioretention cell is properly designed [105]. In addition, the storage depth of the planting medium has been shown to have a much larger effect on bioretention flood reduction than the hydraulic conductivity of the native soils [9]. Because the as-built fragility curve shows very low probabilities of failure for small- to medium-sized storms, well-designed rain gardens have high performance reliability under the most frequently occurring storm events. Choosing to increase the planting media depth of a rain garden in less well-drained soils can be an effective technique in volumetric runoff reduction.

The results show that rain gardens can perform reliably in a variety of situations, including back-to-back rainfall events. While antecedent moisture does have some effect on performance, this effect is only visible for large storms, based on the shape of the fragility surface with increasing interstorm duration. In other words, only two large rainfall events in close temporal proximity can easily trigger a failure of the rain garden. Due to the probability distributions of both rainfall magnitude and interstorm duration, the likelihood of two large rainfall events occurring within a short period of time is unlikely. During the most likely scenarios, the rain garden shows little change in reliability during a two-day interstorm period.

The ability of rain gardens to cope with antecedent moisture both in back-to-back events and in the longterm has important implications for their design and relative importance in managing stormwater within a green-grey infrastructure network. Previous modeling studies suggest that antecedent moisture plays a major role in watershed-scale flooding [106]. However, both empirical and statistical modeling of back-to-back rainfall mitigation by green infrastructure indicates that events with the potential to create excess runoff are rare [102]. This analysis confirms this latter finding. Most importantly, the results suggest that the ability of the rain garden to adequately infiltrate ponded water during average interstorm periods more than compensates for any changes that that increased soil moisture has on the fragility curve. The low probability of failure of the test rain garden, both in the case of small- to medium-sized individual storms indicates that this rain garden is well-designed. Interestingly, this point synergizes well with the argument made by Wadzuk et al. [107] that existing design standards for rain gardens need to be mathematically proven, either using

numerical or analytical approaches.

While the study of antecedent moisture and back-to-back rainfall is of primary concern for runoff modeling, the ponding of surface water in rain gardens and bio-infiltration cells can also provide habitats for disease vectors such as mosquitoes. Studies in temperate and tropical regions indicate that mosquitoes show varying preference for different types of green infrastructure [108, 109]. A study of green roofs, traditional roofs, and ground-level blue-green spaces at the University of Hong Kong showed that traditional roofs have more ponding – and correspondingly more mosquitoes – than green roofs [110]. A characterization of sustainable urban stormwater management systems in Lyon, France indicates that systems where water is drained within 5 days are typically not significant breeding sites for mosquitoes [108]. The results indicate that back-to-back rainfall does not lead to large quantities of ponded water for long periods of time, implying that there is not an opportunity for mosquito breeding.

The recovery of green infrastructure during the interstorm period plays an important role in the modeling of green infrastructure over extended timeframes. The SLCA approach allows for a quantification of the variability inherent in green infrastructure performance, providing a useful complement to the continuous simulation approach used by Avellaneda et al. [111] and others. This analysis provides a unique analytical framework for probabilistically analyzing the performance reliability of green infrastructure under different storm magnitudes and interstorm periods. Notably, the method presented in this analysis provides a corollary to the analytical probabilistic approach suggested by Guo and Guo [112].

4.4 Spatial Variability in Green Infrastructure Performance Under Different Native Soils

One of the the largest predictors of rain garden performance is the native soil surrounding the garden. Multiple studies have shown that green infrastructure performance varies significantly with soil type as well as rainfall distribution [5, 113]. Moreover, urban soils are highly heterogeneous, varying both as a result of natural variability and anthropogenic interactions [114]. Studies in urban areas in China, the United States, and Poland reveal that urban soils

vary significantly in their physical and chemical makeup [114–116]. Some of this variation is a result of soil compaction, building rubble admixture, and soil contamination by waste products.

Despite this built-in variation, many modeling studies continue to use broad-base Soil Survey Geographic Datasets (SSURGO) national soil datasets without considering local spatial variability as a factor in rain garden performance. This section demonstrates the use of fragility curves to evaluate rain garden performance under different soil classes, showcasing the impact of varying native soils under different levels of precipitation. The effect of rain garden design parameters on performance is also evaluated. Specifically, the effects of upstream loading ratio and soil media thickness on rain garden reliability are quantified. This analysis is incorporated into the methodology of Objective 2, which uses the concept of fragility curve "families" to evaluate the effects of green infrastructure at the network scale.

4.4.1 General modeling setup

As part of the RainReady Initiative, towns across the south side of Chicago have been working to evaluate potential locations for green infrastructure. A collaboration between Landscape Architecture, Civil and Environmental Engineering, and the Illinois State Geological Survey at the University of Illinois at Urbana-Champaign resulted in a large-scale project to understand, map, and evaluate native soils in this area, focusing on the Calumet Corridor, to assess their suitability for green infrastructure implementation.

Data from locations across the Calumet Corridor were used to determine soil types throughout the region. More specifically, amoozemeter analysis was used to obtain saturated hydraulic conductivity readings for key implementation sites in Calumet City, IL and Milothian, IL. Figure 4.14 indicates the locations of measurement sites within Midlothian, IL. The amoozemeter allows for in situ testing of saturated hydraulic conductivity using a constant head test. Field measurements were taken June through September of 2018. At the same time, soil borings were extracted for lab analysis at the University of Illinois to determine porosity and more detailed soil profiles. Soil textural data that had already been collected for other purposes (such as construction and drinking water wells) were combined

into a single public database. The combination of these two datasets allowed the classification of soil types into rough classifications based on their saturated hydraulic conductivity and textural class. Figure 4.15 shows the box plots with designations of "coarse", "mixed", and "fine" soils [117].

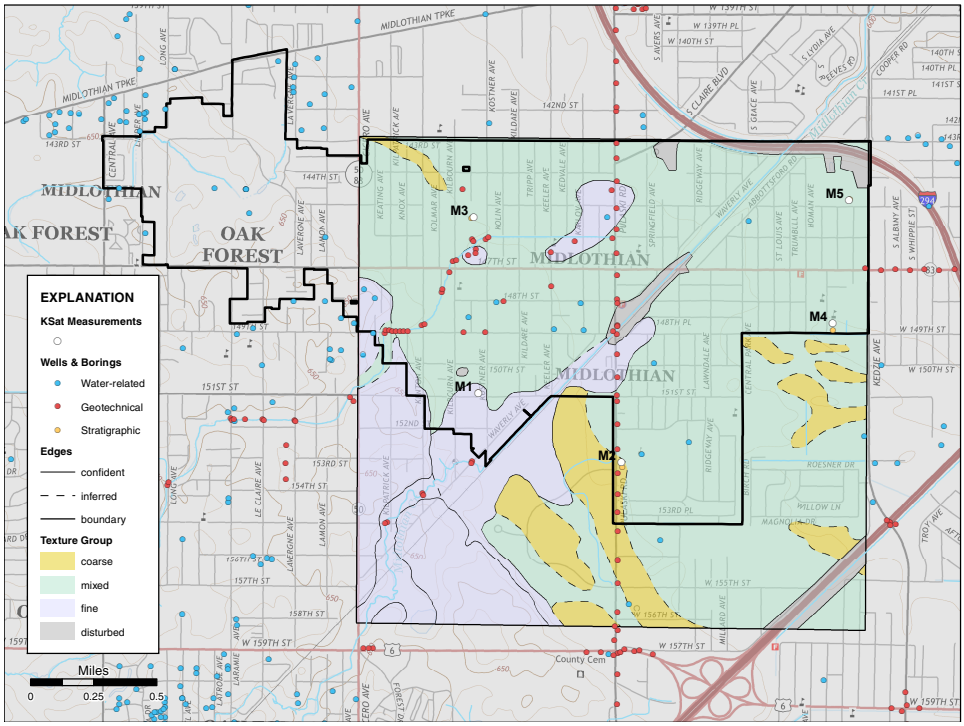

Figure 4.14: Locations from across the Calumet Corridor were selected for soil borings, amoozemeter tests, and textural analysis (reproduced from [117]).

Regression analyses were generated using a similar methodology to the one detailed in Chapter 3. However, because the study was focused on understanding the implications of rain garden implementation on the broader urban environment, loading ratio and storm duration were also included as parameters in the analysis. Hydraulic loading ratios have long been considered an important characteristic of green infrastructure sizing. Loading ratios are defined as the ratio between the area of the green infrastructure and the area of the upstream impervious cover. For example, the Madison, WI rain garden that was used as the template for this analysis has a loading ratio of 1:5. While loading ratios of up to 1:8 may be used for infiltration-based green infrastructure, the risk of clogging and the extra required upkeep makes this option not ideal. Although loading ratios of up to 1:10 were

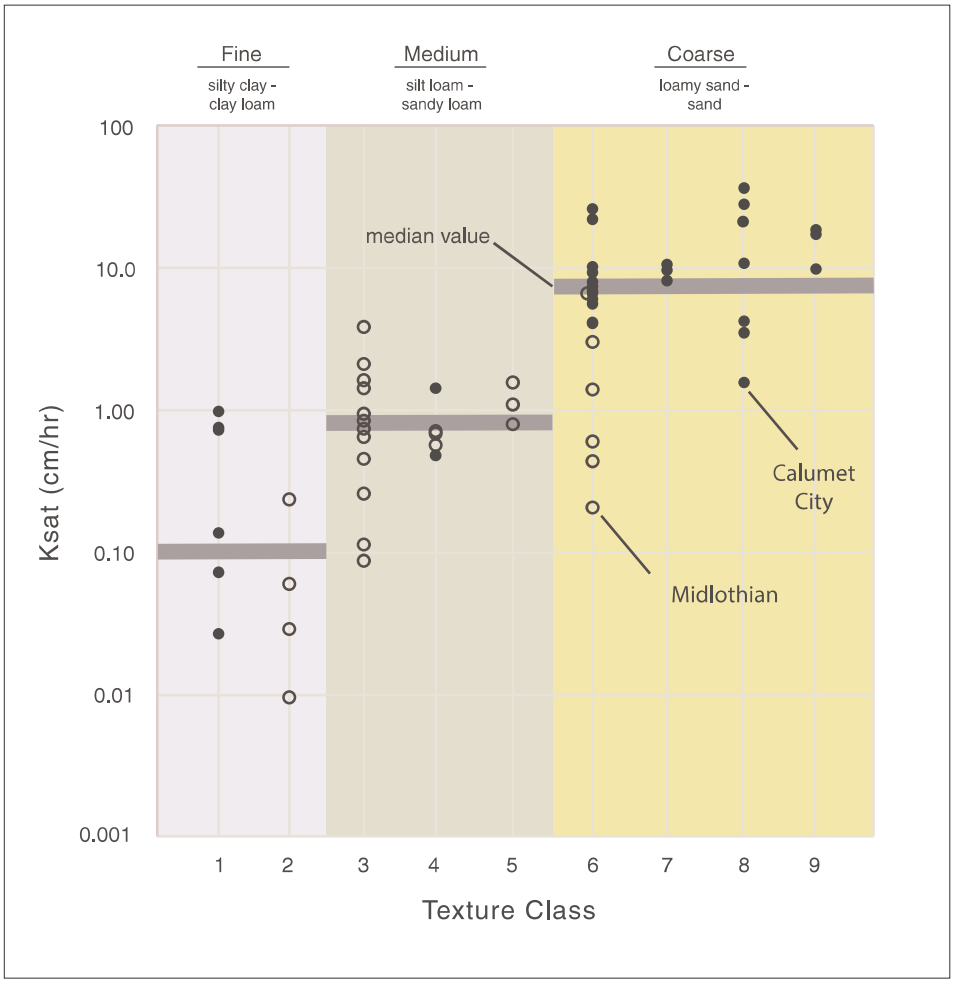

Figure 4.15: Soil types found in the Calumet Corridor were classified by soil texture and saturated hydraulic conductivity to create three rough soil groups that could be used for reliability analysis (reproduced from [117]).

tested, the largest recorded loading ratios are not reported here for this reason [104].

Due to the overlapping distributions of the soil parameters, the mixed and fine soil classifications produced very similar regression results. Table 4.2 shows the forms, coefficients, and fits of the regression equations determined for coarse and mixed/fine soils. Plots of the best fit regressions are shown in Appendix A. To show the effects of media thickness on rain garden efficiency, the mean soil thickness used in the final reliability calculations was changed in increments of 6 inches from 12 inches to 30 inches.

Table 4.2: Model form, coefficient values and R-squared for coarse and fine/mixed soils (all units in imperial)

Soil Class	**Model form**	**Coefficient values**		**Model Fit**
Coarse	$h = \frac{1}{1+e^{-10.5+0.36ksat+1.43duration+1.00seepage+0.11thickness+5.50porosity+54.5loading-6.11r}}$ $V^{0.42} = \theta_0 + \theta_1 duration^{0.5} + \theta_2 ksat^{0.5} + \theta_3 seepage + \theta_4 thickness +$ $\theta_5 porosity + \theta_6 loading + \theta_7 r^{0.5}, h > 0.7$	θ_0	1.59	Accuracy = 0.96 R^2=0.78
		θ_1	-0.845	
		θ_2	-0.281	
		θ_3	-0.121	
		θ_4	-0.028	
		θ_5	-1.264	
		θ_6	-11.20	
		θ_7	3.45	
Fine/mixed	$h = \frac{1}{1+e^{2.60-0.18duration+1.93seepage+0.09thickness-3.52r}}$ $V^{0.67} = \theta_0 + \theta_1 duration^{0.5} + \theta_2 ksat + \theta_3 seepage^{0.5} + \theta_4 thickness +$ $\theta_5 porosity + \theta_6 loading + \theta_7 sat.frac + \theta_8 r^{0.5}, h > 0.8$	θ_0	-2.07	Accuracy = 0.85 R^2=0.87
		θ_1	-0.44	
		θ_2	-0.012	
		θ_3	-1.26	
		θ_4	-0.018	
		θ_5	-2.63	
		θ_6	-25.8	
		θ_7	0.029	
		θ_8	7.35	

4.4.2 Results

Figure 4.16 graphically displays the conditional probability of failure for a rain garden using an 80% volume reduction standard, under different planting media thicknesses, native soil types, and loading ratios. As expected, the probability of failure increases with storm magnitude, with finer-textured soils showing steeper increases in the probability of failure. However, it is important to note that the results indicate that rain gardens with deep planting media can perform well, even under native soil conditions. With a planting depth of 2.5 feet, even a rain garden with a high loading ratio in a "fine" native soil has a high reliability when dealing with runoff from a 3-inch magnitude storm.

Equally importantly, the results highlight the importance of using multiple metrics to characterize soil permeability outside of soil textural classes. The fragility curves for "mixed" and "fine" soils appear similar because the distributions of the two textural classes overlap considerably, as shown in Figure 4.16. In terms of rain garden design, the results indicate that planting medium thickness is an important parameter for rain gardens in mixed- to fine-textured native soils. While planting medium thickness does have some impact on rain garden performance in coarse-textured native soils, storage within the rain garden plays a less crucial role, since the water is easily drained out of the rain garden and into the surrounding soil. Finally, the fragility curves show that loading ratio is a critical factor in improving rain garden performance. Rain gardens with the lowest loading ratio (1:2) show almost no failure, even under sizeable storms.

The probabilistic quantification of rain garden performance remains important for modeling volumetric reduction in real urban environments due to the highly heterogeneous nature of urban soils. Recent studies indicate high variability in saturated hydraulic conductivity within city roadside swales in Minnesota [118]. Other studies show that urban soil profiles are significantly altered from their original, natural states [119], and that soil properties vary considerably between fill and non-fill areas in urban environments [114]. Furthermore, differentiated soil compaction can significantly alter the ability of urban soils to infiltrate water, making construction and maintenance practices important considerations [120].

Creating fragility curves for a given soil "family" allows the incorporation of these het-

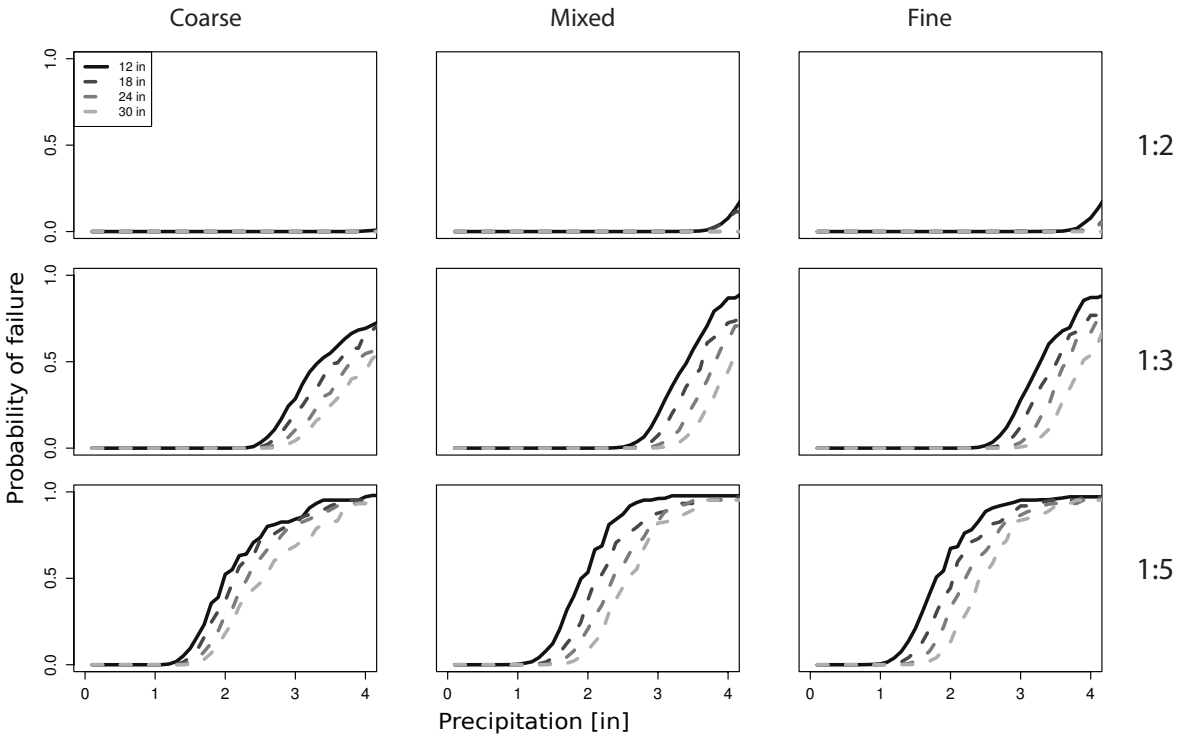

Figure 4.16: Fragility curves for the Calumet corridor show variability in rain garden performance as a result of native soil type, planting medium thickness, and loading ratio.

erogeneities through a probability distribution of soil characteristics. Using these families of curves can inform the assessment of how well rain gardens and other green infrastructure practices affect volumetric retention without mandating a detailed soil analysis of any given site. These rough classifications can allow us to perform large-scale evaluations of city-wide green infrastructure implementation using existing SSURGO datasets. However, more detailed soil characteristics can also be incorporated into the model by adjusting the underlying probability distribution. These fragility curves provide the building blocks for further analysis, incorporating and acknowledging the uncertainties inherent in green infrastructure performance, without compromising model rigor.

4.5 Summary

In this chapter, a fragility curve approach is adopted to approach multiple concerns related to the performance of infiltration-based green infrastructure under spatial and temporal variability. An adapted SLCA approach is used to evaluate the effects of temporal changes on rain garden performance. Firstly, SLCA is used to model long-term clogging in rain gardens. The clogging process was modeled as a shock deterioration with no recovery. Results indicate that a maintenance window of approximately 3 years should be followed to avoid clogging in a temperate, humid climate.

Next, SLCA is used to evaluate the effect of back-to-back rainfall events on rain garden runoff. Rainfall events were modeled as shock deterioration, while drying during interstorm periods was modeled as gradual recovery. Antecedent moisture is not likely to affect this particular rain garden unless two large storms happen within a very short time period of each other. Based on the probability distributions of rainfall magnitude and interstorm duration, this scenario is possible yet unlikely. Indeed, the long-term simulation of rain garden performance shows that including antecedent moisture conditions actually increases overall rain garden reliability, because the soil has time to recover its capacity during long interstorm periods.

The spatial variability of green infrastructure performance is modeled using a "family" of fragility curves. The infiltration associated with the native soil surrounding the rain garden is modeled by changing the seepage parameter in the SWMM model. Fragility curves are created with different textural classes of soils for different storm magnitudes and durations. These fragility curves indicate that the rain garden performs well for small- to medium-sized storms even in fine native soils. Importantly, the rain garden on which the SWMM model was based is overdesigned: during the period of study, there were very few events that generated effluent from the rain garden [103]. The overdesigned nature of this rain garden correspondingly leads to very low probabilities of failure in the model results. Creating fragility curves for different soil textural classes allows the categorization of uncertainties associated with urban soil heterogeneity. These fragility curves inform the modeling framework for Objective 2.

The use of fragility curves to evaluate temporal and spatial variability is a powerful tool for green infrastructure planning and management. This chapter showcases a probabilistic approach to address the challenges of green infrastructure performance quantification, and to help provide evidence-based quantification of risk to allow decision-makers and managers to better understand when and where green infrastructure will be most effective.

CHAPTER 5

NETWORK-SCALE RELIABILITY ANALYSIS OF GREEN INFRASTRUCTURE IMPLEMENTATION

5.1 Introduction

The concept of catchment-scale green infrastructure implementation has become near-ubiquitous in many urban environments. Madison, WI has committed to the installation of 1000 rain gardens throughout the city [121]. Philadelphia, PA has adopted a 25-year plan that aims to use green infrastructure to reduce the total annual amount of pollution entering streams and rivers by 85% [122]. Chicago has pledged $50 million to the installation of an additional 10 million gallons of green stormwater storage [123]. With the rise of these impressive, city-wide green infrastructure goals comes an obvious question: Where should green infrastructure be located to achieve the best stormwater reduction benefits with limited coverage?

Catchment-scale studies of green infrastructure implementation and performance have become increasingly common. Between 1990 and 2018, the scale of the study of green infrastructure hydrology has increased both temporally and spatially [124]. While site-specific studies are still the most common scale of analysis for experimental and monitoring studies, numerical modeling has expanded to incorporate scales ranging from neighborhoods [125] to entire cities [124].

These studies have revealed a range of important – and sometimes unexpected – benefits to scaled green infrastructure implementation. Studies have shown that significant reductions in runoff volume are possible even with small increases in the amount of green infrastructure coverage. Ahiablame et al. [126] show that annual decreases in runoff volume of up to 12% were possible even when green infrastructure implementation was confined to a small percentage of the total watershed area. Another study shows that a green infrastructure retrofit

of 0.5% of the total available area was sufficient to reverse the effects of mansionization on catchment runoff for a low intensity, long duration storm [127]. A green infrastructure retrofit of less than 10% of total catchment area has been shown to fully capture runoff from small storms [125].

These impressive runoff reductions correlate with large reductions in combined sewer overflow (CSO) events in combined sewersheds, both in modeled results and in field experiments [128]. In Lisbon, the implementation of GSI interventions on only 5% of all available impermeable public space led to a modeled annual reduction in runoff of 8000 m^3 entering the combined sewer [129]. Autixier et al. [130] show that green infrastructure implementation can lead to a 60% reduction in CSO volumes. The impact of green infrastructure on CSOs can be further improved by using a hybrid approach that combines green and grey infrastructure [26].

Green infrastructure implementation at the catchment scale can have significant impacts beyond hydrology. Some modeling studies show that catchment scaling of GSI is effective at reducing pollutant loading as well as reducing runoff volume [131]. However, field scale experiments conducted in 2017 [128] indicated that the peak concentration of certain pollutants actually increased in effluent measured after the construction of test rain gardens. Zhang and Chui [124] showed that there are several important linkages between hydrological and bioecological benefits at the catchment scale. For example, improved hydrological connectivity leads to greater stability in the hydrologic regime, which in turn improves climate resilience and ecological integrity. Overall, scaled green infrastructure approaches tend to be more robust under a wider range of future scenarios than grey infrastructure alternatives [132].

Design and network location can affect green infrastructure at the catchment scale. Multiple studies have shown that integrating different types of GSI leads to the largest decreases in runoff volume [111, 133]. Qin et al. [9] support this claim, showing that different types of GSI react differently to different types of storms. Using 'controlled' or 'smart' green infrastructure to manage flows and ponding times can significantly improve catchment-scale performance [25]. Zellner et al. [125] evaluate green infrastructure placement at a neighborhood scale. They show that with limited layout options, a randomized assignment of

GSI results in better volume reduction than clustered assignment. However, if layout is not constrained, the best placement of green infrastructure follows existing flow paths. In other words, adding green infrastructure in high flow accumulation areas leads to a greater reduction in runoff [51].

Catchment scaling is thus an important next step in green infrastructure research, but also presents a range of emerging questions. Existing research suggests that the efficiency of LID practices vary widely across sites [23]. The question that naturally arises is what factors contribute to variability in green infrastructure scaling [23]. Studies have shown that green infrastructure tends to perform better on a subcatchment scale than at a catchment scale. However, larger-scale modeling studies have typically not captured the uncertainty and "noise" from smaller-scale processes [133]. To what extent can scaling be used to quantify and predict temporal and spatial variability in green infrastructure performance?

A variety of different factors affect how the performance uncertainty is manifested at the catchment scale. While other researchers (notably Lim and Welty [51] and Li et al. [133]) have incorporated this variability into their analyses, they do so from a capacitance rather than a probabilistic perspective. In this chapter, a scaled-up version of the fragility curve approach developed in the previous chapter is used to determine how rain gardens respond to different types of storm events in a case-study catchment area located in West Baltimore, MD. Results from a small 'block-scale' model are compared to findings from the watershed-scale network. Two different approaches to rain garden placement are evaluated: a 'randomized' approach and a 'clustered' approach. In doing so, this study evaluates the effects of scale and location on the impacts that green infrastructure has on a larger network from a stochastic perspective.

5.2 Study Area

The Gwynn's Run watershed, located in southwest Baltimore, MD, was selected because its unique combination of socioeconomic, land use, and environmental challenges make it an interesting case study on the potential effectiveness of green infrastructure. Figure 5.1 shows a map of the Gwynn's Run watershed, along with the stormwater distribution network used

in this analysis. Gwynn's Run is a fairly large urbanized watershed with an area of 2.5 mi^2 [134]. Nearly 80% of the land use within this area is residential and industrial. Gwynn's Run itself is a stream that suffers from high levels of nitrate contamination [134]. As a part of the larger Chesapeake Bay watershed, Gwynn's Run is part of Baltimore's effort to encourage the use of green infrastructure to reduce potential contaminants reaching the Bay. Although a 2018 Chesapeake Bay Program study indicated that the watershed is on track to meet targets for phosphorus and total suspended sediments, it has fallen behind on reductions in nitrogen [135].

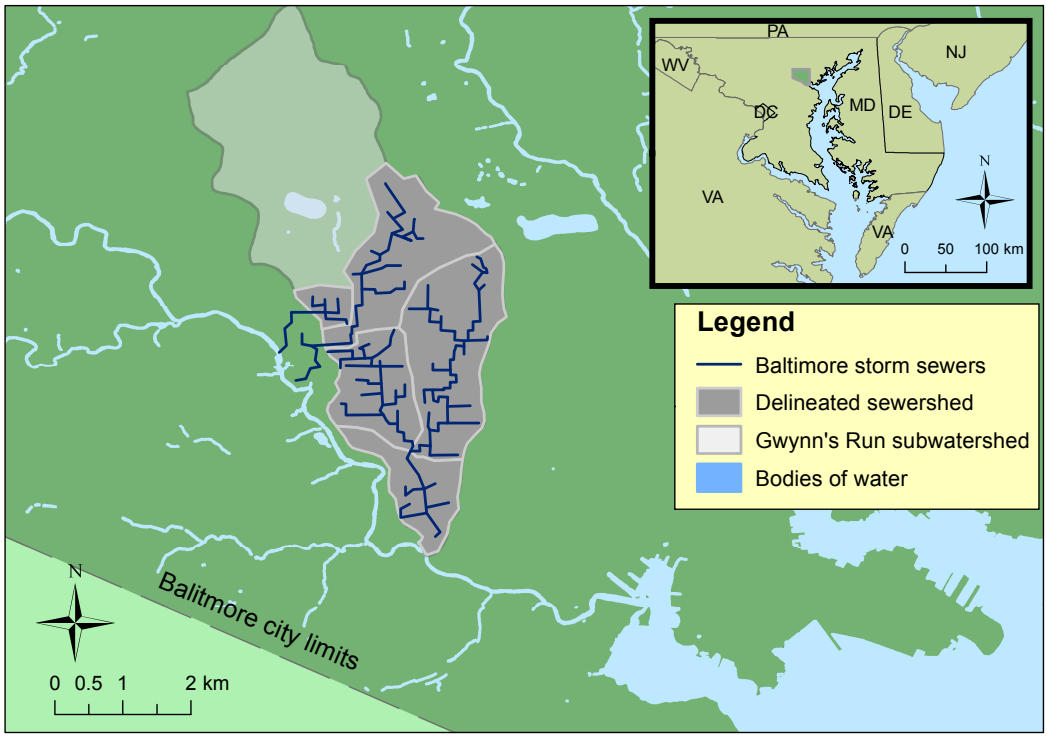

Figure 5.1: The case study is located in the Gwynn's Run subwatershed in West Baltimore, MD.

The area surrounding Mill Hill and Shipley Hill, the locus of this research, ranks among the lowest in socioeconomic status within Baltimore [136]. Many of the neighborhoods located within the Gwynn's Run watershed are predominantly African American or other minority

groups [137]. Moreover, the percentage of the population below the poverty line in southwest Baltimore is 26.2% compared to the city-wide average of 15.2% [137]. Multiple efforts have advocated for urban greening within southwest Baltimore as a means to equitably distribute access to green space within the city.

From a geographic standpoint, the Gwynn's run watershed is made up of a diverse combination of land use types and soils. Although many of the sites captured in this location are single-family residential units, the site also encompasses multi-family apartments buildings and retail facilities. Soils range from well-drained sandy loams to denser sandy clays and urban complexes. Finally, the separated stormwater is well-defined and easily discretized into smaller sections. Gwynn's Run is thus an ideal case study location for the appropriate placement of green infrastructure within an existing urban network.

5.3 Methods

A four-stage process was used to generate the network model used in the analysis. Firstly, geographic watershed data are pre-processed within ArcGIS to define catchment properties needed for hydrologic and hydraulic modeling. Next, the data are integrated into a coherent stormwater network using the SWMM engine within MIKE URBAN. At the same time, a Python script is used to collate GIS data on rain garden characteristic and property parcels to assign rain gardens to watersheds either at random or using a nearest-neighbor protocol. Finally, a weighted coin flip algorithm is used to integrate all pieces of the model for final calculations. Figure 5.2 diagrammatically illustrates the overall method.

5.3.1 GIS Pre-Processing

Inlets, junctions, and sewer pipe data were provided by the City of Baltimore. The network data were verified and corrected to ensure that consistency in pipe elevation, size, slope, and flow direction were maintained. Light Detection and Ranging (LiDAR) rasters at 0.7 m horizontal resolution were used to delineate catchment areas for each inlet using the ArcHydro toolset in ArcGIS; the inlets were burned into the post-processed raster as 'sinks'

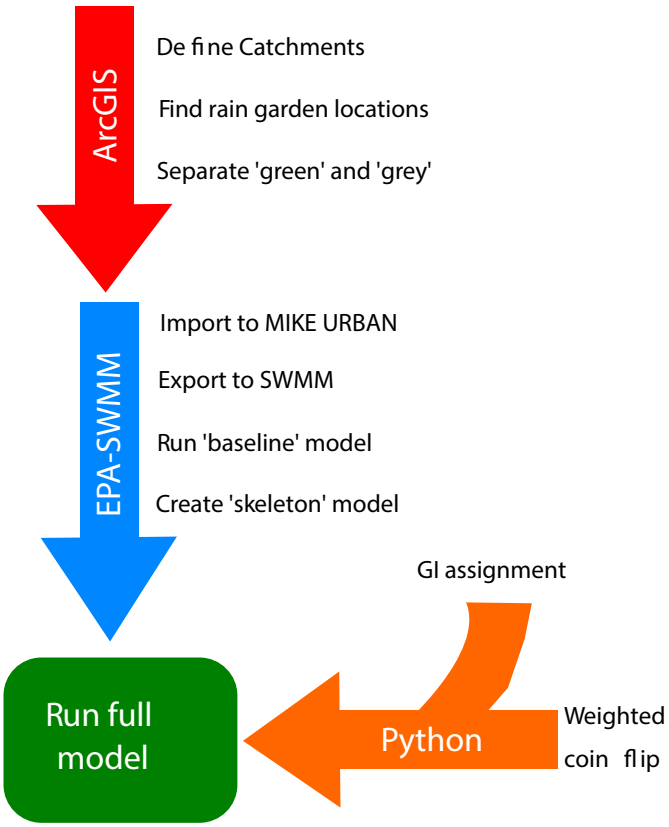

Figure 5.2: The network-scale analysis is completed using a four-stage modeling process within ArcGIS, SWMM, and Python.

to ensure that all overland flow was routed to an inlet. Four-band orthophoto rasters of the watershed were processed to identify and cluster areas of impervious and pervious land use, using the methodology developed by Thanapura et al. [138]. These areas were then spatially joined to identify regions that were directly connected impervious areas versus those that were 'islands' of impervious area within larger pervious spaces. Catchments were further divided into proportionally-sized 'grey' (i.e., directly connected impervious area) and 'green' (i.e., combined pervious and indirectly connected impervious area) subcatchments for modeling in MIKE URBAN, a GIS-integrated water management software. Green catchments were routed to grey catchments, which were then routed to the corresponding inlet. Multiple studies have shown that an uncalibrated, highly detailed SWMM model that appropriately

captures the routing of water between impervious and pervious areas within each subcatchment can reach similar predictive performances to calibrated models [71].

The National Resources Conservation Service (NRCS) national WebSoil Survey was used to acquire information on soil types within each catchment. Four typical soil types were identified for the Gwynn's Run subcatchment: sandy loams, loams, legores, and urban complexes. Based on borings provided by the Baltimore Department of Transportation, a sandy clay was assessed to be an appropriate approximation for fill in urban complexes within Baltimore. Soil, slope, slope length, and land use data were spatially joined to the watershed shapefiles. Two different spatial scales were selected for the analysis, based on Strahler Stream Ordering of the different sewer pipes: 1) second order branching (block-scale) and 2) the entire watershed. Figure 5.3 shows the location of each of the different scales within the network.

5.3.2 Modeling in MIKE URBAN/SWMM

MIKE URBAN, a proprietary software developed by DHI, was used as an interface between ArcGIS and SWMM. MIKE URBAN is designed to model both 1D and 2D flows within urban catchments. Because the software can model water quality, wastewater, drinking water, and stormwater systems, MIKE URBAN is often used to evaluate integrated urban water management systems. MIKE URBAN can use two different engines: DHI's MOUSE engine and SWMM. The software has the ability to read in catchment, pipe, and node parameters based on existing, formatted GIS shapefiles, as well as the capacity to create and modify shapefiles within the program itself. For the purposes of this analysis, the SWMM engine was used to facilitate later Monte Carlo simulations. The network generated and verified within MIKE URBAN was exported to SWMM to generate the text-based .inp file that was used by the coin-flip algorithm in the final analysis.

The initial .inp file contained all subwatersheds generated during model creation. Triangular hyetograph two-hour duration storms of magnitudes ranging from 1 inch to 4 inches were passed through the SWMM model. The resulting runoff hydrographs for flow into each inlet node were read and saved as .txt files using the R swmmr package. The peak flow

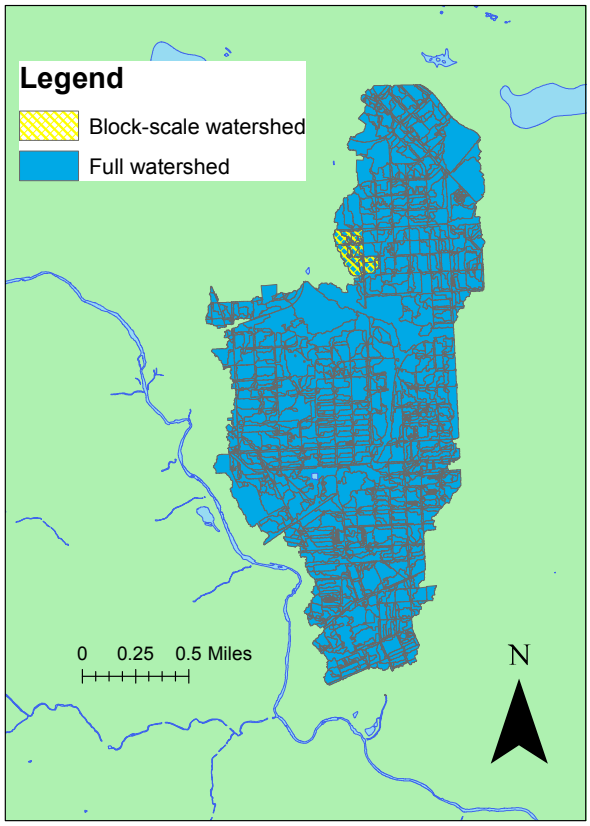

Figure 5.3: Two different scales of green infrastructure modeling analysis were completed based on Strahler Stream order of the sewer pipes.

and total runoff volume for the system hydrograph were also calculated and stored. A new 'skeleton' SWMM model was then generated containing only the pipe and node information, with no subcatchment data.

5.3.3 Random and Clustered Assignment of Rain Gardens

Rain garden potential locations were selected within ArcGIS using criteria commonly used by many municipalities. Rain gardens must be situated at least 10 feet away from any buildings to avoid potential seepage into basements and foundations. This criterion was modeled by creating a 10 foot buffer around building footprint data provided by the City of

Baltimore. Parcel data were also available through the same service. Rain gardens should not be placed on sites with slopes exceeding 12%, or in areas where mean water tables lie within 2 feet of the ground surface. Slope raster data were calculated using LiDAR and spatially joined to individual watersheds to exclude areas that were inappropriate. Finally, rain gardens without underdrains should be sited in areas with relatively well-drained soils. Because of the typical soil types found within West Baltimore, none of the watersheds were excluded as a result of this criterion [139].

In addition to these criteria, the study assumed that rain gardens would primarily be located on existing permeable land. This assumption was made because the study aimed to model the impact of rain gardens on private property, negating a common removal of impervious surfaces. Once selected, rain garden potential locations were numbered and spatially joined to both their relevant parcel and inlet watershed.

ArcPy was used to create an algorithm that would select rain gardens to be implemented based on the database of potential locations. The random selection algorithm chose rain garden locations by using a random number generator to select parcel ID numbers within the catchment. The clustered selection algorithm chose rain garden locations using randomized seed sites within the catchment, and using a nearest-neighbor approach to select rain gardens in parcels adjacent to the seed sites. Both algorithms were set to terminate when the total selected rain garden area was equal to a given percentage of the total available rain garden area. Percentages of 100%, 50%, 25%, and 0% implementation were used in this analysis. Figure 5.4 shows a comparison of the clustered and randomized approaches to GSI.

The loading ratio was calculated for each subwatershed within the model based on the ratio of impervious upstream area to selected rain garden area. Upstream pervious area was factored into the calculation using a relationship developed empirically within EPA-SWMM, shown in Equation 5.1, where the "Equivalent Loading Ratio" is the final loading that is input into the algorithm. Appendix A presents the regression plot used to develop this relationship. Due to the general layout of land use within the watershed, rain gardens were assumed to act in parallel, rather than in series. As a result, the assumption that two adjacent rain gardens of a given area perform similarly to a single rain garden of twice that area is valid.

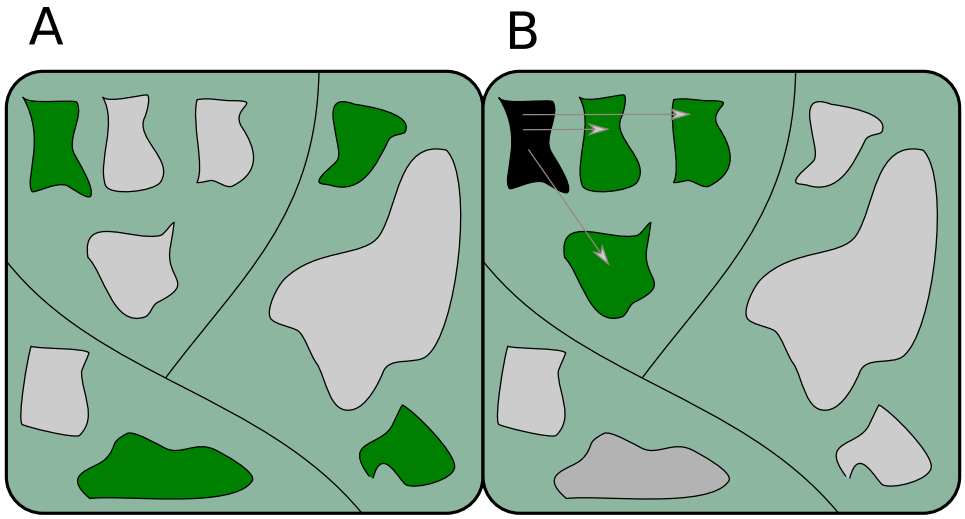

Figure 5.4: The randomized approach (A) used a random number generator to select random parcel ids for green infrastructure implementation throughout the network. The clustered approach (B) used a randomly selected 'seed' site (shown in black), and selected rain gardens in adjacent parcels based on closest distance.

$$\frac{\text{Loading Ratio}}{\text{Equivalent Loading Ratio}} = 1.67 \times \frac{\text{Impervious Area}}{\text{Total Area}} - 0.67 \tag{5.1}$$

5.3.4 Weighted Coin Flip Analysis

As shown in Section 4.4, fragility curves can be used to compare the effects of native soil type and loading ratio on the ability of green infrastructure to reduce runoff volume. In the Baltimore watershed, fragility functions were generated for the four different dominant soil types following the form of the general equation presented in Equation 5.2.

$$F = P([\alpha V_{paved}(\mathbf{x}, r, LR) - V_{GSI}(\mathbf{x}, r, LR)] \leq 0 | R = r, LR = LR) \tag{5.2}$$

The fragility curves were created for different loading ratios, different storm durations, and different levels of reduction. Loading ratios were tested ranging from 1:10 through 1:2. Standards of volume reduction (α) were implemented at 80%, 75%, 70%, 60%, 50%, and 40%. Volume reduction below this level was deemed insignificant and not tested. Figure 5.5 shows an example plot of the fragility curves for sandy loam at 80% reduction and different

loading ratios.

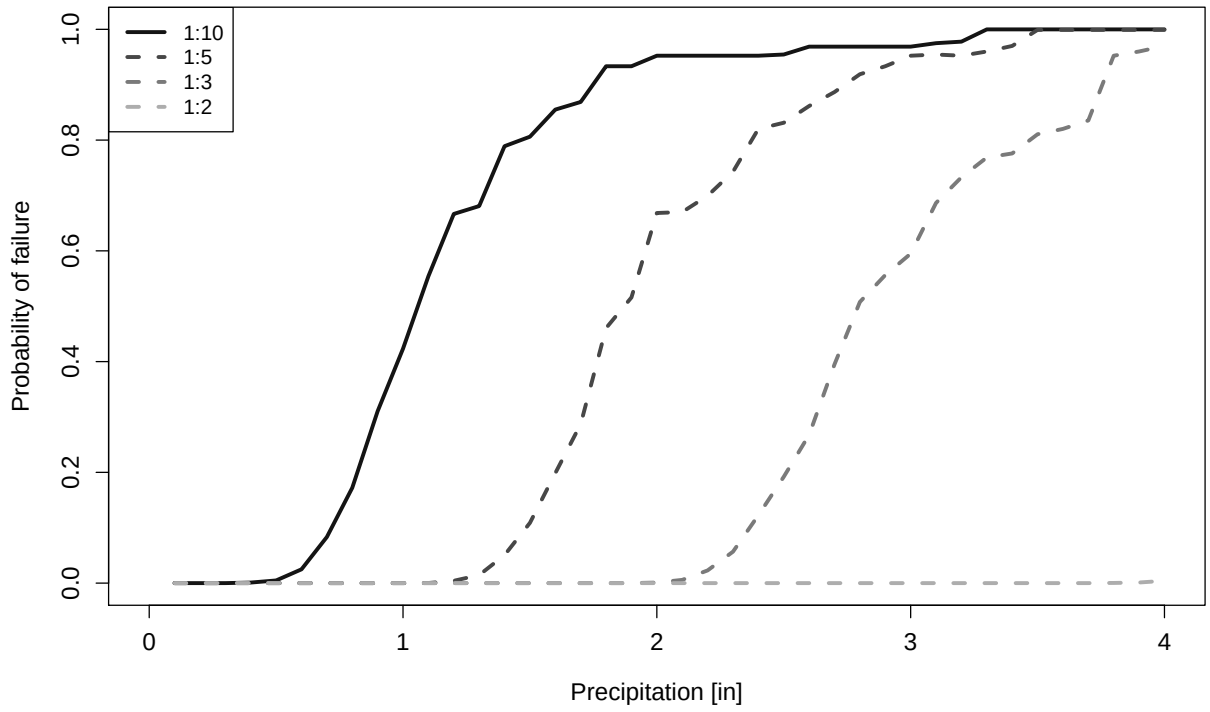

Figure 5.5: Fragility curves were created for different loading ratios and standards of failure for each of the native soil types within the Gwynn's Run watershed. This plot shows fragility curves for a sandy loam soil under different loading ratios.

The fragility curves for the different soil types were input into Python as matrices. For each watershed, the dominant soil type was used to determine which fragility curve matrix to use for the calculation. Then, based on the calculated loading ratio and the precipitation magnitude, the probability of failure was interpolated from the fragility matrix for the highest standard of reduction. A weighted coin flip algorithm was used to determine whether or not the rain garden succeeded in reducing runoff by the desired amount. If not, then the next highest standard of reduction was used, until either a successful reduction was recorded, or the algorithm ran out of potential reduction standards.

The fraction by which the implemented rain gardens successfully reduced runoff volume was recorded for each watershed. The inflow hydrographs (determined in Section 5.3.2) were multiplied by the calculated corresponding fraction. The new hydrographs were input into the SWMM skeleton model. Output system peak runoff and total volume were recorded for

each iteration.

The process was then iterated for a given rainfall magnitude until the COV of the total volume was < 0.1. The same process was repeated seven times to allow for different randomized spatial configurations. The mean and standard deviation of the volume were recorded and synthesized across all seven spatial iterations. Both randomized and clustered allocation approaches were compared across 50% implementation and 25% implementation regimes for each rainfall magnitude. The process was then repeated for rainfall magnitudes between 1 inch and 4 inch. Figure 5.6 shows a flow chart of the weighted coin flip analysis process.

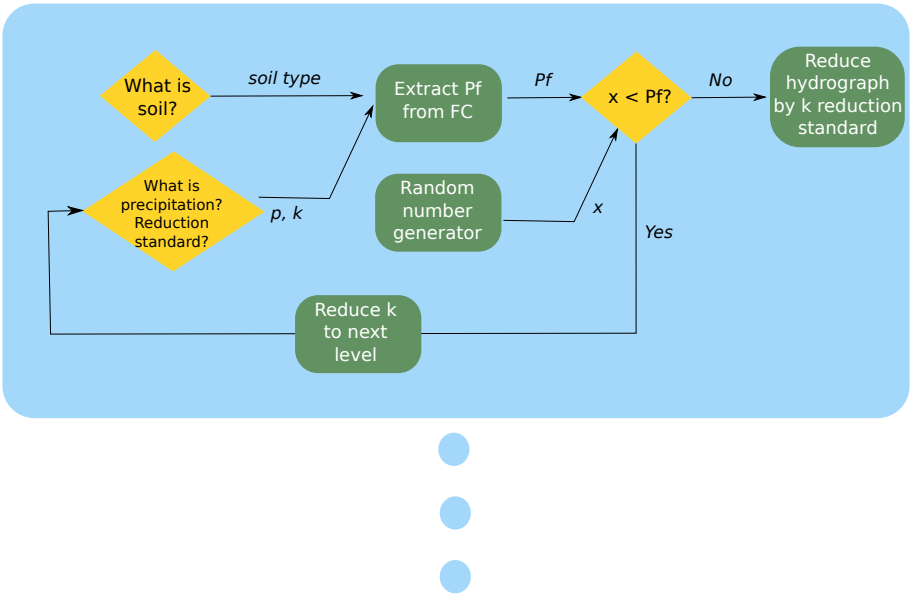

Figure 5.6: The Python weighted coin flip algorithm extracted data for each watershed on soil type, precipitation magnitude, and selected standard of reduction. These values were used to interpolate a probability of failure for the rain garden based on input fragility curves. A random number generator was then used to determine whether the rain garden succeeded ($x > Pf$) or failed ($x < Pf$) to reduce runoff by the targeted amount.

5.4 Results

5.4.1 Block-Scale Analysis

Figure 5.7 shows the mean percent volume reduction within the smallest-scale network. The 100% implementation regime is shown as a solid black line, while the 50% and 25% regimes are shown in blue and orange respectively. The shaded areas on each of the graphs represent one standard deviation away from the mean.

The results indicate that green infrastructure implementation has a significant impact on volume reduction for low rainfall magnitudes. As expected, the greatest values of volume reduction occur at 100% implementation. However, volume reduction decreases significantly at higher rainfall magnitudes. Volume reductions for 100% implementation range from 28% at lower rainfall magnitudes to 11% at higher rainfall magnitudes.

Rainfall magnitude also affects the impact of clustering on reduction capacity. For smaller rain events, clustered approaches are a significant improvement over random green infrastructure allocation. At 1 inch of precipitation, a 50% clustered implementation is nearly twice as effective at volumetric runoff reduction as a 50% random implementation. However, as rainfall magnitude increases, the discrepancy between clustered and randomized approaches becomes insignificant. In fact, at larger rainfall magnitudes, the 25% clustered implementation appears to offer less volume reduction potential than the randomized approach.

The standard deviations in the 25% and 50% implementation regimes are derived from two different sources. The first source is the built-in convergence criterion for the Monte Carlo analyses, which is based on whether or not each of the rain gardens extracted for the run is in failure. Per the algorithm stopping criterion, this value is always less than 0.1μ, where μ is the calculated mean value for the all algorithm iterations. The second source of variability is a result of where the rain gardens are placed in the network. This location-based variability is often much larger than the former type; in general, the randomized location selection results in a higher variance than the clustered location selection. This variability highlights the importance of rain garden location selection for efficient volume reduction.

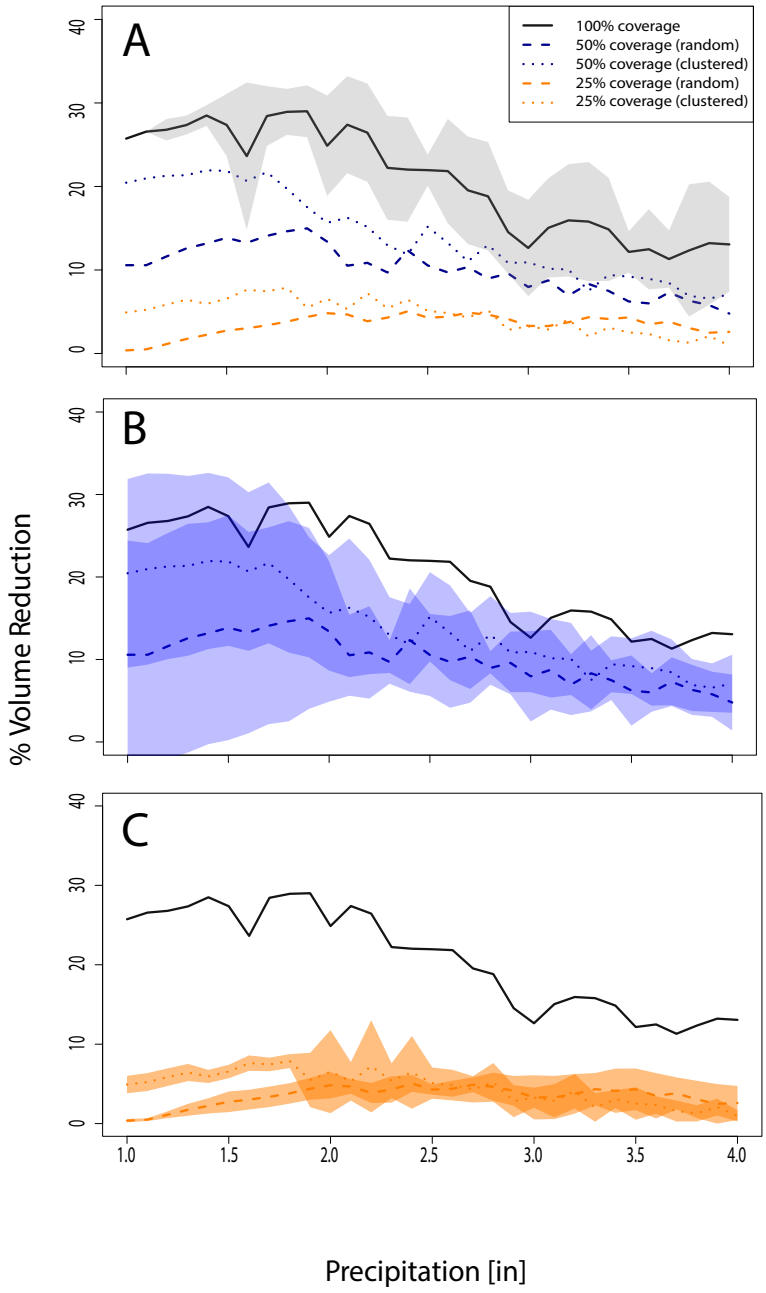

Figure 5.7: For the smallest network scale, green infrastructure has a significant effect on volume reduction at lower rainfall magnitudes. This figure shows the mean volume reduction for 100%, 50%, and 25% implementation. The standard deviations on the figures show the standard deviation away from the mean for: (A) 100% implementation; (B) 50% implementation; and (C) 25% implementation

5.4.2 Watershed-Scale Analysis

Figure 5.8 shows the mean percent volume reduction within the large-scale network. At this scale, the amount of volume and peak reduction that occurs is highly dependent on the level of green infrastructure coverage that is implemented. At 100% coverage, the reduction values are comparable — and in some cases slightly higher — than the reduction for equivalent storms for smaller networks. For example, at 100% coverage for the watershed-scale network, volume reductions can exceed 35% during small magnitude storms. However, volume reduction decreases at a much more rapid rate as storm magnitude increases, compared to its counterpart in the smaller network; volume reduction approaches near-zero levels of reduction at around 2.9 inches of precipitation. In contrast, for the smaller network, the volume reduction metrics still shows some capacity even at the largest tested storm magnitudes.

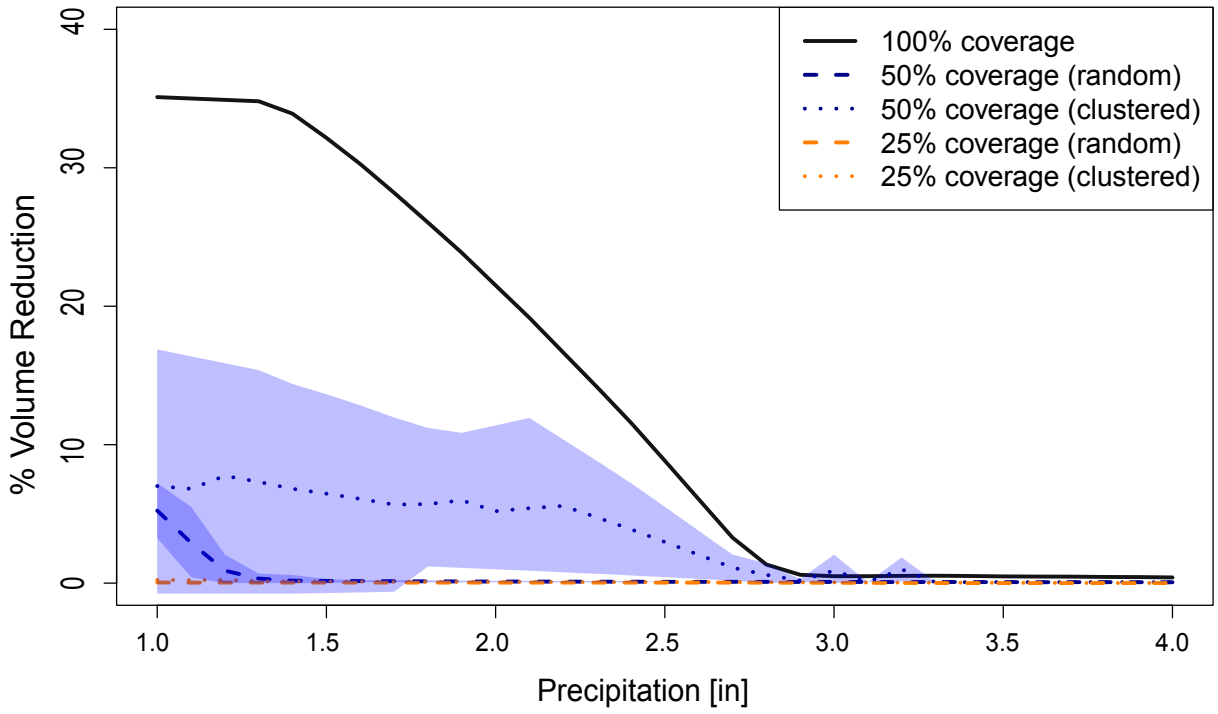

Figure 5.8: Mean volume reduction for 100%, 50%, and 25% implementation within the watershed-scale network decreases with increasing precipitation. Shaded areas represent the standard deviation around the mean for 50% implementation. The 100% and 25% implementation standard deviations are small enough that they are not visible on the plot.

For smaller levels of coverage, green infrastructure does not have a large impact on volume reduction. Even for small storms, a 50% implementation only leads to a maximum volume reduction of 8%. At a 25% implementation, volume reduction is small enough that it is scarcely visible on the plot. In both cases, there continues to be some advantage in a clustered approach compared to a random approach to green infrastructure placement. However, the difference in magnitude between the two options is much less than that observed for smaller networks.

Studying the standard deviations of the plots reveals the reasons for some of these discrepancies. In the case of 100% implementation, the standard deviation is so small that it is not visible in the figure. As previously mentioned, the only type of variance associated with the 100% reduction is due to Monte Carlo analysis. In the case of the 50% implementation, large variance is observed, comparable in magnitude to those observed in the plots for the block-scale network. This large variability is attributable to location within the network of either the randomly selected GSI placement sites (in the case of the random algorithm), or the randomly attributed 'seed' site (in the case of the clustered algorithm). Because the locations were selected by chance, rather than chosen to optimize the hydrologic impact of green infrastructure on the network, the mean effect is dampened because some configurations lead to almost no volumetric reduction. Similarly, although the 25% implementation regimes show little variance, their consistently low reduction values signify that the impacts of singular rain gardens are being dispersed throughout the model, leading to much lower volumetric reduction overall.

5.4.3 Validation

A test SWMM model was used to validate the use of the weighted coin flip analysis to predict the impact of green infrastructure allocation on network efficiency. The model was based on the block-scale catchment-delineated model created in SWMM to generate the runoff hydrographs used in the rest of the analysis. The existing ArcPy algorithm was use to assign rain gardens to different catchments based on a random or clustered approach. Rain gardens were added to the appropriate catchments using the SWMM LID module;

the size of the rain garden was based on the area allocated by the ArcPy algorithm. Each rain garden was assigned parameters based on the 'test' rain garden described in Chapter 3. The seepage rate was varied between rain gardens based on numbers randomly selected from the variable distribution for the soil type in each catchment. Table 5.1 lists the volume reduction for a block-scale system tested with 100% coverage, 50% random coverage, and 50% clustered coverage for a 1 inch and a 4 inch magnitude storm.

Table 5.1: Volume reduction from a test block-scale SWMM model using built-in LID module

Precipitation [in]	**Volume reduction 100% coverage**	**Volume reduction 50% random coverage**	**Volume reduction 50% clustered coverage**
1	37.5%	10.9%	27.8%
4	8.2%	0.0%	0.0%

For this particular iteration, the volumetric reduction for the 1-inch storm at 100% coverage is slightly higher than expected from the weighted coin flip analysis. Conversely, the volumetric reduction for the 4-inch storm at 100% coverage is slightly lower than the calculated mean, but is within the bounds of error for the weighted coin flip analysis. The volumeteric reduction for 50% random coverage is around what is expected for the 1-inch storm, but is lower than expected for the 4-inch storm. The volumetric reduction for 50% clustered coverage is higher than the predicted mean, but is within the bounds of error for the model. Importantly, these results are for a single iteration, both in terms of the distribution of seepage rate and the location of the rain gardens within the network. This analysis is intended to show that a direct implementation of rain gardens into the network using the SWMM LID module produces similar results to the runoff hydrograph reduction methodology presented in this chapter.

5.5 Discussion

The findings from this study are corroborated by existing modeling studies and field experiments. As with site-scale studies of green infrastructure, catchment-scale green infras-

tructure performance is highly contingent on the type of storm that the green infrastructure experiences. Garcia-Cuerva et al. [140] showed that stormwater strategies that incorporate either centralized or decentralized bioretention cells can be highly effective, even in extreme events. However, the impact of green infrastructure options on volume reduction is typically much greater for smaller storms than larger ones because the amount of volume retention decreases greatly as precipitation increases [10]. Field experiments by Woznicki et al. [141] support this finding with in situ monitoring of four catchments in Maryland, three containing traditional curb-and-gutter drainage and one containing vegetated swales. Runoff only commenced at 6 mm of rainfall for the green catchment, but was produced for even small storm events in the grey catchments. However, the authors stated that the differences between the green and grey catchment hydrographs were insignificant for rainfall events with depths greater than 20 mm.

In this modeling study, the largest reductions in both runoff volume and peak are observed at low-magnitude rainfall events, with both metrics decreasing with increasing storm magnitude. At the same time, storm magnitude impacts the effect that green infrastructure location has on performance. For example, while clustered green infrastructure tends to show improved volume reduction compared to randomized green infrastructure, the difference between these two approaches becomes insignificant at higher magnitude storms. Other researchers, including Garcia-Cuerva et al. [140], have shown that different mechanisms control volumetric reduction at the catchment scale, dependent on storm size. In this study, both catchment scale and the selected green infrastructure allocation algorithm control runoff volume reduction.

As shown by this analysis, and by existing literature, the amount of space that is available to convert to green infrastructure has a significant impact on reduction potential. Total impervious area is the driving determinant of peak discharge as well as water storage in the catchment [28]. As a result, the amount of impervious area that is converted to green infrastructure impacts its efficiency. Multiple studies have shown that the available area for green infrastructure is a major determinant of its efficacy at the catchment scale. Green infrastructure stormwater benefits double when green infrastructure goes from 2% to 10% of total catchment coverage [142]. Liu et al. [143] showed that pervious pavement has a

significant impact on certain catchments because the use of permeable pavement rather than bioretention opens up more possible areas for green infrastructure installation. For decentralized bioretention cells, watershed coverage and the percentage of the upstream area routed to the bioretention are the most significant indicators of volume reduction [140].

The modeling results from this study indicate that watershed coverage is particularly important at larger catchment scales. While the 100% implementation results from the watershed-scale study are comparable to the 100% implementation results from the block-scale analysis, the same cannot be said for the 50% or 25% implementation results. At the watershed scale, 50% implementation has limited impact on runoff reduction for clustered implementation; the limited effectiveness is even more pronounced for randomized implementation. The collective effect of multiple rain gardens working together to reduce runoff is dispersed across many different subwatersheds, leading to suboptimal outcomes. One key finding of this analysis is that the relative placement of green infrastructure within the network is a significant contributor to their collective success. Increasing implementation coverage is one potential approach to increase watershed-scale effectiveness. Another approach could be to cluster rain gardens by watershed, rather than using a nearest-neighbor 'social diffusion' approach. In practice, this type of concerted implementation strategy would likely only be possible under the auspices of a designated watershed governing body. One potential option for creating such an entity is discussed in Chapter 6.

This study provides a useful means to incorporate risk into spatial green infrastructure modeling without the need for an intensive, spatially-variable Monte Carlo model. The incorporation of built-in green infrastructure fragility curves, developed at the modular level to study other phenomena, as shown in Chapter 4, creates a 'short cut' that can be used to evaluate the appropriate placement of green infrastructure within the network. Moreover, the use of fragility curves allows the classification and quantification of different sources of uncertainty, differentiating those associated with environmental factors, such as native soil type, from those associated with network placement. In this study, the variance observed as a result of environmental factors was dwarfed by the variance that resulted from how green infrastructure was distributed across the network. These findings again highlight the importance of careful location selection for green infrastructure, both relative to other

infrastructure and in terms of position within the watershed as a whole.

5.6 Conclusion

This chapter builds on the fragility curve methodology developed in Chapter 4 to provide a stochastic framework to analyze the impact of location and scale on green infrastructure network performance. The Gwynn's Run watershed in west Baltimore, MD was selected as an illustrative case study site. Two different network scales were selected to test both clustered and randomized approaches to green infrastructure implementation. A weighted coin flip analysis was implemented using Python to determine the effects of allocated green infrastructure on subcatchment runoff hydrographs input into a 'skeleton' EPA-SWMM model of the network.

The findings from the model indicate that, as in the case of modular fragility functions, rainfall magnitude plays a significant role in the runoff reduction effectiveness of green infrastructure. Green infrastructure implementation coverage is also important, although the effect is much more pronounced at larger catchment scales, as the distribution of green infrastructure at lower implementation levels dilutes its effectiveness. Finally, the method used to assign green infrastructure location also changes its effectiveness, although the difference between clustered and randomized approaches is negligible for higher-magnitude storms.

CHAPTER 6

THE POLICY AND LEGAL IMPLICATIONS OF GREEN INFRASTRUCTURE INTEGRATION INTO THE BUILT ENVIRONMENT

6.1 Overview

While green infrastructure has many potential benefits for urban environments, the net effect that it has on cities is contingent on private citizens' willingness to implement it on their own properties. This chapter explores some of the policy, psychological, and legal implications of this private-public integration on green infrastructure performance. Section 6.2 uses a game theoretic framework to analyze how different municipal policies change agents' behavior with regard to green infrastructure implementation. These findings also have implications for aspects of environmental justice, and suggest some potential policy strategies. While game theory is a useful framework for modeling agent behavior, it assumes selfish rationality, and thus does not accurately represent human behavior. Section 6.3 reviews the Economic Self-Interest model used in current practice, proposes an alternative framework for human motivation, and suggests some practical methods to use this new psychological model to influence green infrastructure uptake. Finally, in Section 6.4 some of the implications for green infrastructure monitoring and maintenance are evaluated under the current legal framework of the Clean Water Act.

6.2 A Game Theory Analysis of Green Infrastructure Stormwater Management Policies[1]

6.2.1 Introduction

The USEPA estimates that urban runoff is the leading cause of impairment related to human activities for ocean shoreline waters, and has led to significant degradation of nearly 30,000 miles of river [2]. As a result, the EPA has begun to implement strict standards on stormwater quality. Cities need to meet these standards to avoid fines, or the loss of federal grant money. It is up to individual municipalities to meet downstream regulations by implementing urban land-use policies that enable individual landowners to decrease the amount of contaminants being washed off their property. The USEPA encourages MS4s to meet their required minimum control measures using green infrastructure as much as possible, by allowing them considerable flexibility in choosing what approach to take under the current rules. Partly as a result of these regulations, green infrastructure has been incorporated into stormwater management plans in cities across the United States: of the 27 major cities studied by Chini et al. [16], 24 incorporated green infrastructure into their stormwater plans.

Cities thus need to provide incentives to encourage private individuals to 'opt in' to green infrastructure projects [144]. Diverse green infrastructure initiatives have been adopted by cities around the world, with varying degrees of effectiveness [16]. Cerra [145] summarizes some of the most popular strategies for encouraging voluntary environmental stewardship on private property, classifying them into four main categories. The first category includes the use of indirect incentives or regulations administered by a municipality as a part of a policy or ordinance. The second category encompasses market-based certifications that encourage ecological enhancements during site development in return for formal recognition from a third-party certification agency. Community-based initiatives form a third alternative approach: citizens are driven by a "bottom up" interest in a shared ecological goal, rather

[1]The content of this section is published as William, R., Garg, J.,and Stillwell, A.S. (2017). A game theory analysis of green infrastructure stormwater management policies. *Water Resources Research, 53*(9), 8003-8019.

than by market forces. Finally, some parties use the concept of ecosystem services — the aspects of ecosystems utilized to enhance human well-being — to quantify and monetize some of the multiple benefits conferred by green infrastructure implementation [146]. For example, the temperature regulation benefits provided by green roofs can be monetized in terms of seasonal building energy savings [39]. This concept can be used to encourage direct public or private payments for the services rendered by green infrastructure. Thus, the complex dynamics between the economic, social, and hydrological characteristics inherent in its design and implementation makes green stormwater infrastructure an intriguing example of socio-hydrology within the urban nexus.

Across the country, municipalities are moving to direct financial incentives, such as Chicago, IL's private sector Green Roof Grant Program, using block grants to help incentivize green infrastructure implementation [147]. The Green Roof Grant Program awarded up to $5000 to residential and small commercial landowners who chose to invest in green roof technology on their property [148]. On the other hand, many cities (including Baltimore, MD) use stormwater remediation fees to control runoff. The fee rates are typically proportional to the impervious area in each lot, and go toward maintaining the stormwater utility and restoring and protecting the local watershed. Fee credits are available to discount the stormwater fee for lots that make use of green infrastructure, but are typically capped at some upper bound [149]. Another approach is to use municipal regulatory power to mandate technology standards for certain types of development. For instance, Toronto, ON, Canada mandates that all new industrial development with a gross floor area of over 2000 m^2 have green roofs [147]. In this analysis, stormwater management approaches — grants (direct incentives), regulations, and fees and credits — are evaluated in the context of green infrastructure installations using game theory to model landowners' likely actions. This analysis thus addresses both a major gap in the literature and in real life implementation by providing a quantifiable means to evaluate the suitability of stormwater management policy practices for different urban areas.

6.2.2 Background

Game theory is a field of study that aims to model conflict and cooperation in scenarios where two or more agents make decisions that will affect each other's welfare [150]. In a game theory framework, all agents are assumed to be rational and intelligent: each agent aims to maximize his or her own expected payoff. Cooperative game theory incorporates this individual rationality while also allowing for cooperation and bargaining between different agents [150]. Multiplayer cooperative games with more than two agents can be modeled using coalitional analysis, where a coalition is defined as any non-empty subset of the set of all agents. A grand coalition is simply a coalition made up of the set of all the agents. A multiplayer cooperative game can be specified by the characteristic function $c : 2^N \rightarrow \mathbb{R}$, where N is the set of all the agents and $c(S)$ is the total cost of coalition S when the agents in S cooperate and do not take any help from the agents outside of S. The payoff allocation (or cost allocation) for these games can be determined using the concepts of the *core* and the *Shapley value*. The core and Shapley value are the main solution concepts in cooperative games that are analogous to the Nash Equilibrium in non-cooperative games. The core is the set of all allocations in which no coalition of agents has an incentive to secede and obtain a better payoff; that is, an allocation (with respect to costs) in the core satisfies the constraints described in Equation (6.1) [150].

$$core := \left\{ \begin{array}{l} \sum\limits_{i \in N} x_i = c(N); \\ \sum\limits_{i \in S} x_i \leq c(S), \forall S \subseteq N \end{array} \right\} \tag{6.1}$$

While the core provides an interesting perspective on individual agents' power, it might also be empty or quite large, making it difficult to apply as a concept in practice. On the other hand, the Shapley value uniquely distributes the total cost of the grand coalition among the agents. It is based on the natural properties that a solution should be expected to satisfy (symmetry, the zero value of a dummy player, and additivity), and can be calculated using the formula stated in Equation (6.2), where $\phi_i(c)$ is the Shapley cost allocation for agent i, S is a given coalition, $c(S)$ is the cost function of coalition S, and n is the total number of agents in the grand coalition N [150].

$$\phi_i(c) = \sum_{S \subseteq N \setminus \{i\}} \frac{|S|!(|N| - |S| - 1)!}{|N|!}(c(S \cup \{i\}) - c(S)) \tag{6.2}$$

Game theory has historically been used to model economics, political science, and social science problems; however, the field has a wide range of potential applications in biology, computer science, and other engineering disciplines [150, 151]. Within the field of water resources engineering, a game theory approach can be used to characterize multi-objective and multi-decision maker problems to generate a more realistic simulation of stakeholder behavior [152]. In other words, game theory provides a useful approach in realistically approximating interactions between water resources technology, human behavior, and the natural environment: a crucial component of the socio-hydrological framework [153]. Historically, cooperative game theory applications have been more common among water resources researchers than non-cooperative applications [151, 152]. Several studies that have modeled water resource questions using both cooperative and non-cooperative approaches have identified cooperative strategies as having more utility than non-cooperative strategies [154–156]. Game theory applications in this field include transboundary water resources management, reservoir management, and water infrastructure operations [154, 157, 158]. However, the applications most pertinent to this analysis relate to the issues of runoff quality management and pollution control.

The use of game theory to model different approaches to pollution control has a long history. Hardin [159] publicized the concept of the "tragedy of the commons" to describe the fact that individual users acting independently according to their own self-interest behave contrary to the common good of all users by depleting a shared resource. More recent studies have investigated game theory approaches to modeling pollution control in transboundary river basins. Within the field of natural resource distribution, Teasley and McKinney [160] used a cooperative game theory framework to analyze water and energy resource allocation in the international Syr Darya river basin. A Nash-bargaining approach was successfully applied to model the allocation of pollution control measures on the U.S.-Mexico border [161]. Fernandez [162] extended this analysis to dynamically incorporate asymmetries in power between Tijuana, Mexico and San Diego, CA, United States. These asymmetries lead

to the need for coordinated binational abatement involving payment transfers between the players, because Mexico needs to be incentivized to cooperate.

Other researchers have addressed similar issues of river basin water quality management for more than two players. Studies have investigated the use of cooperative game theory approaches to model point and non-point source pollution mitigation efforts on rivers in Australia, Korea, and China [155, 156, 163] . In particular, Shi et al. [163] used a Shapley value approach to investigate the cost effectiveness of reducing water pollutant emissions in different regions of the Jialu River. The authors also evaluated each of the solutions obtained in terms of fairness and solution stability (i.e., the sustainability of cooperation).

However, few researchers have used a game theory approach to model green stormwater infrastructure allocation in an urban setting, and in particular the impact of policy-making decisions on implementation. In addition, limited literature currently exists to quantifiably evaluate the benefits and drawbacks of different municipal policy approaches to encouraging the implementation of green infrastructure for stormwater management on private property. This analysis uses cooperative game theory to model the allocation of green infrastructure within an urban setting for different stormwater management public policy frameworks. The Shapley value and core give an indication of key players in the coalition, thus indicating how network location and player size impacts player importance in controlling green infrastructure implementation.

6.2.3 Methods

Problem setup

The analysis setup is a simplified representation of the Gwynn's Run subwatershed located within the Gwynn Falls watershed in west Baltimore, MD. The setup involves five players (A, B, C, D, and E), located within the same MS4 sewershed. Figure 6.1 shows a diagram of the simplified representative setup. The players with the two largest amounts of impervious area are B and C, followed by E, A, and D, as shown in Table 6.1. While some player areas are arranged in parallel to the storm sewer network (e.g., A and B), others are arranged

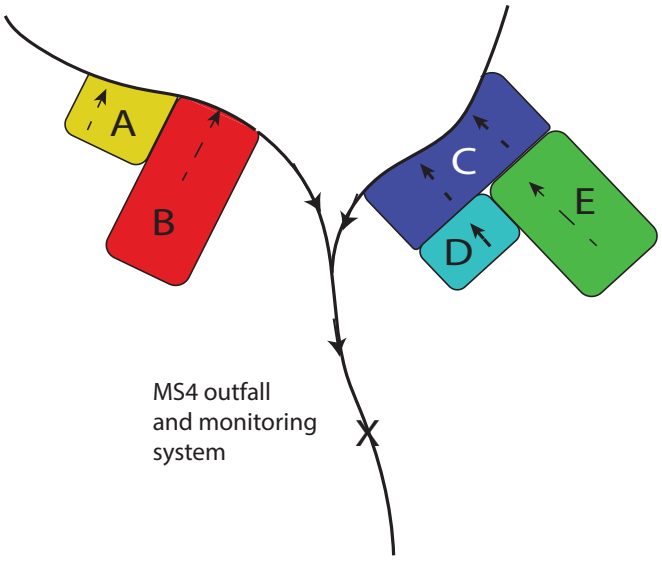

Figure 6.1: This analysis uses a simplified representation of the watershed studied in Objective 2. The watershed is comprised of five players connected to a municipal separated storm sewer (MS4) system. While players A and B are connected in parallel, players C and D, and C and E are connected in series.

in series (e.g., D and C, meaning that water first flows across D, and then across player C before entering the storm sewer). To test the importance of location on the allocation of green infrastructure between the players, two additional scenarios are tested: one with all five players in parallel; and another with all five players in series (in alphabetical order, with E being the downstream-most player). The allocation of green infrastructure in the watershed is modeled as a single iteration game, since infrastructure is typically a one-time installation.

Table 6.1: Agents in the network own different amounts of impervious area

Agent	**Impervious area (ac)**
A	1
B	2
C	2
D	0.5
E	1.5

Loading and treatment

The case study is modeled based on the policies currently used to manage the high levels of total suspended sediment (TSS) in the Chesapeake Bay Watershed (CBW). Under the CWA, Maryland, along with other states in the CBW, is required to develop TMDLs to help to maintain the specified uses of its rivers and the Chesapeake Bay. One of the most critical concerns, particularly for states with large urban areas, is the presence of high levels of TSS in the river downstream of the town (*Anacostia Riverkeeper Inc. v. Jackson, 2011*). Based on prior investigation and the designated use of the river, the government sets a control λ on the amount of sediment being washed into the river by the city's MS4. If the city's load exceeds λ, then the government can withhold certain funds that have been offered to the city. This withholding is equivalent to a 'penalty' being imposed on all five agents, as shown in Equation (6.3), where ψ is a penalty, λ is the load limit, and L_i is the load of the pollutant from player i. Note that although the penalty is assessed when the total loading is greater than λ, there is no reward for the city further reducing below the pollutant cap requirements. The sensitivity of the Shapley values to the values of ψ and λ are also assessed.

$$Penalty = \begin{cases} \psi \times (\sum_i L_i - \lambda)^2, \text{if} \sum_i L_i \geq \lambda \\ 0, \text{otherwise} \end{cases} \tag{6.3}$$

Each player contributes sediment into the system at a rate proportional to the amount of impervious area on its land. The exact relationship between the annual sediment loading for a given player i, L_i (in lbs), with the impervious area, A_i (in ac), is given by the Schueler [164] Simple method shown in Equation (6.4). Because the Simple method is empirical, the units required for the calculation are a combination of imperial and metric: P is the precipitation (in inches), C is the pollutant concentration (in mg/L), P_j is the fraction of rainfall events that produce runoff, and I is the fraction of impervious area. This case study assumes that P, C, P_j, and I remain constant. The annual precipitation P is estimated to be the U.S. average of 30 in. The concentration C is 297 mg/L, based on the estimation by Fuerhacker et al. [84] of the mean runoff concentration of TSS from a 3-ac parking lot. P_j is set to the default suggested value of 0.9, and I is assumed to be equal to 1.

$$L_i = 0.226 \times (P \times P_j \times (0.05 + 0.9(I)) \times C \times A_i \tag{6.4}$$

Estimating the treatment capability of an individual green infrastructure module is challenging, given that green infrastructure performance varies based on storm type and other factors, including media depth, water table height, and soil type [15]. However, a weighted averaging of reported treatment values suggests that bioretention cells (a common form of green infrastructure) can help to reduce TSS loadings by 80% [165]. Because TSS reduction is only based on physical processes taking place within the soil rather than additional biological or chemical processes, treatment is superadditive for units in series, as illustrated by Figure 6.2. However, green infrastructure cannot remove pollutants below certain irreducible thresholds, due to limitations of particular removal pathways, and possible internal production of nutrients and turbidity [166]. Brown et al. [29] suggest an irreducible concentration of 10.3 mg/L for stormwater best management practices that utilize filtration. The effluent concentration coming out of each individual bioretention cell was checked against the value from Brown et al. [29], to confirm that treatment capability was not being over-estimated.

The recommended sizing for a bioretention cell draining an area of 0.25 ac — 1 ac is 25 ft × 50 ft (around 0.03 ac) [167]. As the size of the area being drained increases, the required surface area of the bioretention cell increases as a step-wise function. The decision being made by each player is whether or not to implement a single 'unit' of green infrastructure meeting the requirements as described (i.e., the decision for a given player is a binary variable).

Problem definition

The cost for a bioretention cell is based on estimates by Narayanan and Pitt [168], adjusted to 2016 dollars. While these costs do date from 2006, they remain relevant and have been incorporated into more recent work, most notably the City of Austin's EnVision Tomorrow green infrastructure app [169]. For bioretention cells implemented in sandy soil, implementation costs can be estimated as shown in Equation (6.5), where A_i is the total upstream impervious area being drained to the bioretention cell. The green infrastructure

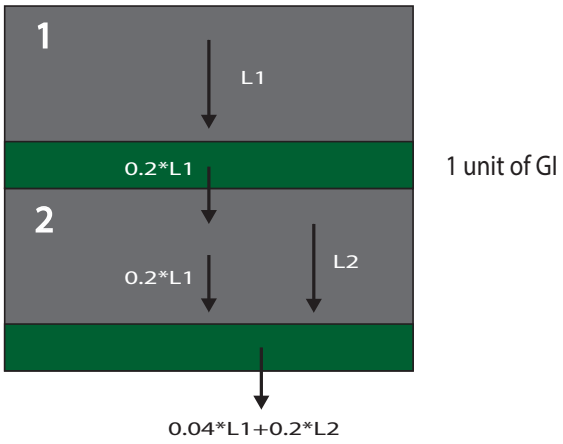

Figure 6.2: Bioretention cells can be used to remove excess total suspended solids (TSS) via physical mechanisms such as filtration. The use of a 'treatment train' of two appropriately-sized units of GSI in series leads to superadditive pollutant removal, illustrated here with loadings L1 and L2.

installation cost is summed across all agents, and added to the assessed load exceedance penalty to determine the total cost for the system. Municipalities often use financial incentives or regulatory fines to encourage the use of green infrastructure. Equation (6.6) adds together all of these costs and benefits to create a single total (net) cost for the system to be minimized. A tradeoff thus exists between the penalty assessed for exceeding the stated system load limit, and the individual cost to each player for installing green infrastructure.

$$\text{GSI Cost}_i = 2861 \times A_i^{0.438} + 3437 \times A_i^{0.0152} \tag{6.5}$$

$$c(S) = \sum \text{GSI Cost}_i + \text{Penalty} + \text{ Regulatory fines} - \text{Financial incentives} \tag{6.6}$$

This analysis is modeled as a cooperative game by assuming that the different agents can work together in different coalitions to minimize costs. The 'cost' assigned to each coalition, $c(S)$, is the total cost paid by the entire MS4. The agents in S choose whether or not they will each install green infrastructure so as to minimize the system cost, assuming that all other agents not in S chose not to install green infrastructure. In other words, $c(S)$

addresses the 'worst possible case' when considering the actions of agents outside of the coalition. Using what we know about $c(S)$ for all possible coalitions (including the grand coalition), the Shapley value can be calculated for different scenarios (described in the next section). Each scenario is evaluated based on how well it meets pollution control standards.

Scenarios

Four different scenarios were evaluated, showcasing the different policies most commonly used in the United States to incentivize green infrastructure implementation in urban environments. The values for regulatory fees and incentives were chosen to be representative of actual programs currently in place in cities around the country, and to be comparable in value to each other and to the cost of green infrastructure installation.

1. **Business as usual (BAU).** This scenario models what would happen in a situation without any additional benefits to players who install green infrastructure or regulatory fines to agents who do not.

2. **Direct grant.** An additional bonus amount is given directly to each agent based on the amount of space it dedicates to green infrastructure. A $3000 benefit is given to smaller players who install green infrastructure (i.e., less than 1 ac), while a $6000 benefit is given to larger players. The values approximately reflect the value of comparable grant programs implemented in other U.S. cities [148].

3. **Municipal regulation.** The city requires that a certain percentage of each agent's area be converted to green infrastructure. The government penalizes agents who fail to meet this condition with a uniform fine of $4000, a value chosen to be on the same order of magnitude as the other rewards and fines.

4. **Stormwater fee and credits.** Each agent is charged a stormwater remediation fee that is a function of the impervious area of the property. This function is linear, and is based on the Baltimore, MD stormwater remediation fee of $2500 per acre per year [170]. Additionally, properties are eligible for stormwater credits, which are a

percentage reduction in the stormwater fee. The credits are non-linear and increasing: agents with the highest green infrastructure cost receive a 50% credit, while smaller agents receive a credit proportional to their costs, as shown in Equation (6.7). Note that in reality, municipalities typically use revenues generated by stormwater fees to maintain storm sewer networks and other important municipal services. However, this particular public benefit is not reflected in this analysis.

$$\text{Credit} = 50\% \times \frac{\text{GSI cost}}{max(\text{GSI cost})} \times \text{Stormwater fee} \tag{6.7}$$

6.2.4 Results

Original test case

A game theory model with no benefits or fines for the coalition was used to assess a baseline business as usual (BAU) scenario,. As expected, increasing the number of agents in the coalition does, in general, decrease the coalition cost. However, the cost of the grand coalition might not necessarily be less than the cost of the sub-coalitions. In other words, the cost function is non-negative, monotonic (Equation (6.8a)) and subadditive (Equation (6.8b)), but not strictly decreasing, and a smaller coalition might have the same cost as the grand coalition (i.e., the grand coalition might not be the 'optimal' solution). This observation indicates that the optimal choice of green infrastructure allocation does not necessarily produce the lowest levels of pollution. An example of this situation is shown in Table 6.2, which shows an abridged version of the cost function $c(S)$ calculated for each possible coalition for the BAU, 3000 lbs/yr load limit, \$5 per 1000 lbs scenario. In this case, $c(ABC) = c(ABCD) = c(ABCE) = c(ABCDE)$. To check submodularity (Equation (6.8c)), we can use an example where $S = \{A, B\}$ and $T = \{A, C\}$. From the calculated costs in Table 6.2, $c(S \cup T) = 23,600$, while $c(S \cap T) = 625,500$. Because $c(S) = 291,600$ and $c(T) = 88,100$, the constraints of submodularity are violated. The game in this BAU case is thus not convex, because its characteristic function $c(S)$ is not submodular [171]. Because the game is formulated in the same way for all other scenarios, the characteristic

function is unlikely to be submodular in these scenarios either.

$$c(S) \geq c(S \cup T),\ \forall S \subseteq N, S \neq \emptyset. \tag{6.8a}$$

$$c(S) + c(T) \geq c(S \cup T),\ \forall S, T \text{ subject to } S \cap T = \emptyset \tag{6.8b}$$

$$c(S \cup T) + c(S \cap T) \leq c(S) + c(T),\ \forall S, T \subseteq N \tag{6.8c}$$

It is important to note that the properties of monotonicity and subadditivity are generalizable for all of the different scenarios because of the way the game is formulated. As previously stated, the algorithm seeks to minimize the overall cost for each coalition over all agents. This condition implies that adding an extra agent i to a coalition S can only decrease the cost (provided that S is not the empty set). For some coalition $S \cup i$, if asking i to implement green infrastructure would increase the cost, i would simply not implement green infrastructure, implying that $c(S \cup i) = c(S)$. Importantly, this reasoning does not preclude the existance of positive Shapley values, since it only holds true when $S \neq \emptyset$. In other words, the intial marginal cost of adding the first player will be non-negative, because $c(\emptyset) = 0$.

Because of the monotonic and subadditive properties of the cost function, the core of the game for each of the scenarios is non-empty. This property can be proven intuitively: if we assign the entire cost of the grand coalition to any given agent (for example, A), all of the inequalities that make up the core are satisfied. However, there are many different allocation variations that are also in the core. This fact implies that the Shapley value is a more precise method than the core of evaluating cost allocations between the different agents. The Shapley value will thus be used in all following discussions regarding the "optimal" solutions suggested by the game.

Figure 6.3 shows the calculated Shapley values for the BAU scenario for baseline, all parallel, and all series cases, with a pollutant limit of 3000 lbs/year and a penalty of \$5 per 1000 lbs. An interesting finding is that the Shapley values for agents B and C are negative in the baseline and all parallel scenarios. In this case study, the Shapley value is the allocation

Table 6.2: An abridged table showing cost $c(S)$ for a given coalition S, for a pollutant load limit of 3000 lbs/year and a penalty of \$5 per 1000 lbs in the original configuration. The lowest possible cost is underlined

S	$c(S)$ [\$]	S	$c(S)$ [\$]	S	$c(S)$ [\$]	S	$c(S)$ [\$]
(A)	625,500	(AB)	291,600	(ABC)	<u>23,600</u>	(ABCD)	<u>23,600</u>
(B)	439,200	(AC)	88,100	(ABD)	232,100	(ABCE)	<u>23,600</u>
(C)	168,600	(AD)	531,900	(ABE)	130,900	(ABDE)	97,000
(D)	730,100	(AE)	363,100	(ACD)	86,000	(ACDE)	73,200
(E)	527,500	(BC)	36,500	(ACE)	74,400	(BCDE)	32,900
(AB)	291,600	.....		.....		(ABCDE)	<u>23,600</u>

of the different costs among all five agents. A negative Shapley value is thus a 'benefit'. Hence, the negative Shapley values indicate that agents A, D, and E all pay their shares into a collective pool, and then use some of that money to help incentivize agents B and C to put in green infrastructure on their land. In the baseline configuration, the Shapley value allocation to agent C is an order of magnitude larger than agent B ($-\$170,400$ as opposed to $-\$36,400$). Because the average cost of green infrastructure installation for C is around \$10,000, the money provided to C would more than completely reimburse C for any costs incurred from its installation of green infrastructure. Thus, C stands to benefit a great deal by being part of a cooperative game with the other agents, and also holds substantial power in the coalition. The reason for C's powerful standing is its strategic position in the watershed, see Figure 6.1. As the downstream-most agent in a set of agents in series, having C install green infrastructure helps to decrease loads not just from its land, but from D and E as well. Moreover, B and C have two of the largest impervious areas (at 2 ac each); adding green infrastructure to either of these lots greatly decreases the overall pollutant load going into the river.

Figure 6.4 shows the percentage discrepancy from the BAU scenario for each of the different policy scenarios: direct grant, municipal regulation, and stormwater fee. As expected, the direct grant acts on the Shapley values in the opposite direction from the other two scenarios; rather than penalizing bad behavior (as in the case of the regulatory or fee scenarios), the direct grant rewards good behavior. The direct grant also has the greatest impact on the Shapley values of the individual agents. However, in the original configuration, the

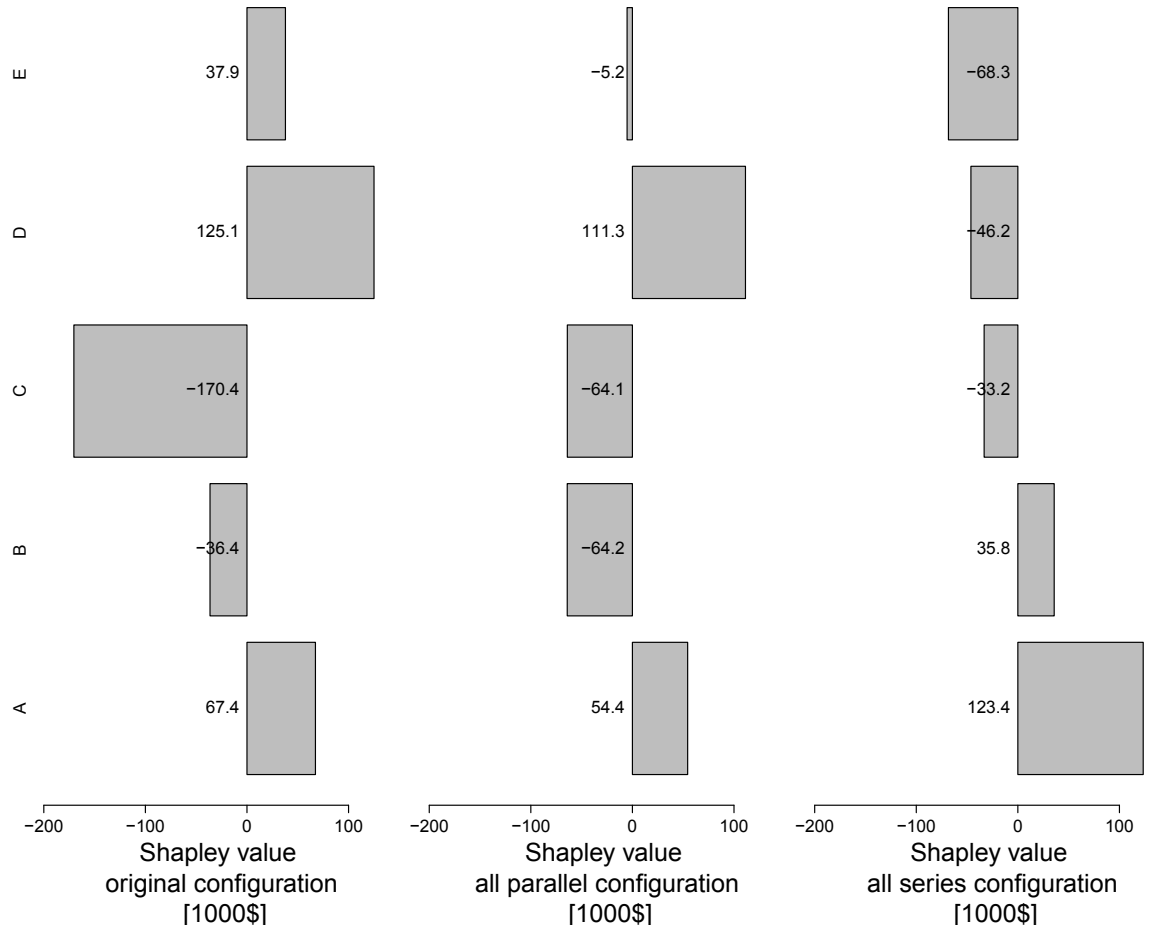

Figure 6.3: Bar charts comparing the Shapley allocations for the BAU scenarios for the original, all parallel, and all series configuration illustrate the impact that network location has on the Shapley values, shown for pollutant limit of 3000 lbs/year and a penalty of $5 per 1000 lbs.

overall changes to the Shapley allocation made as a result of policy changes are not large in magnitude.

An interesting consequence of the optimal allocation in the original configuration from Figure 6.1 is that both the BAU and stormwater fee scenarios fail to reduce the level of pollution in the river below the required threshold, as shown in Table 6.3. In both scenarios, the optimal allocation of green infrastructure is for agents A, B and C to put in green infrastructure, leading to a final loading of 3124 lbs/year. However, the stormwater fee scenario leads to the higher cost overall. In other words, the stormwater fee scenario leads to no additional environmental benefit compared to BAU. The direct grant scenario reduces

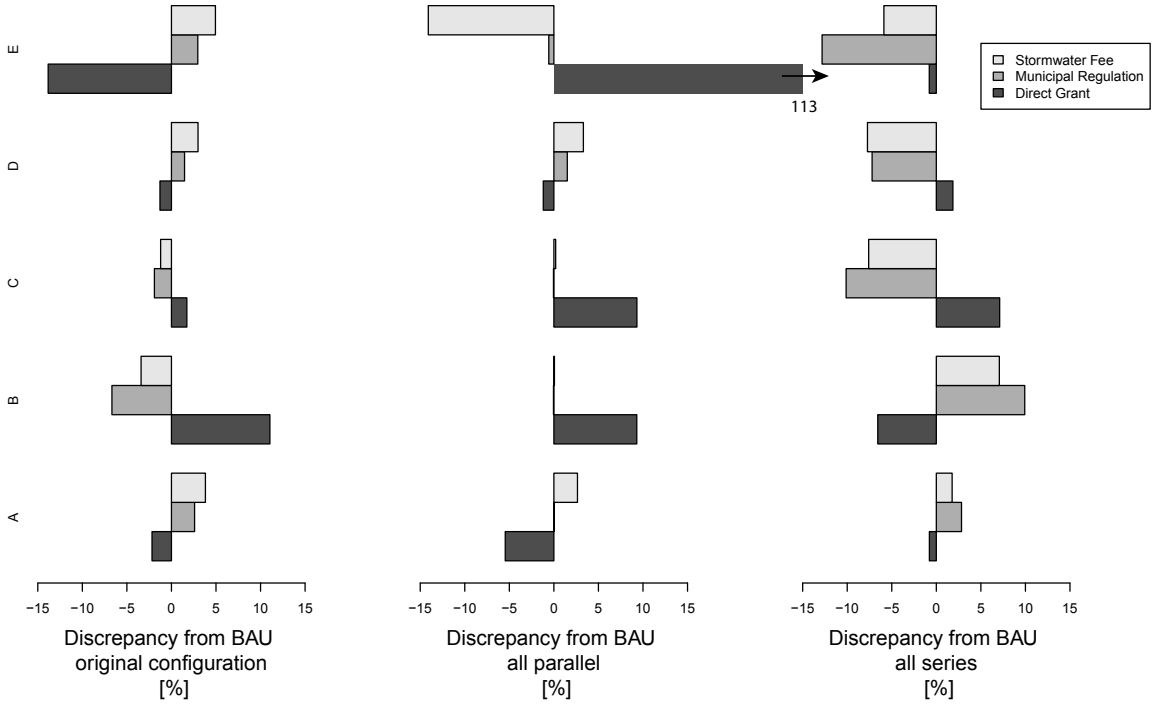

Figure 6.4: Percentage discrepancy from the BAU scenario for the stormwater fee, municipal regulation, and direct grant scenarios varies based on location and configuration. The original, all parallel, and all series configurations are represented. The relative impact that each scenario has on the agents is strongly affected by the type of configuration. Since Shapley values are an allocation of costs in this case, a negative Shapley value is a 'benefit' to a given player.

the loading into the river to 2572 lbs/year, and also leads to a reduction in overall cost. The municipal regulation scenario leads to the lowest optimal loading into the river (2387 lbs/year), since all five agents installing green infrastructure is the optimal configuration (i.e., lowest cost) for this scenario. However, the municipal regulation also has the highest overall total cost in comparison to the other scenarios.

Effect of spatial configuration

In the different spatial configurations considered, the Shapley value distribution for the all parallel case was dramatically different from the distribution for the original test case (see Figure 6.4). As expected, the Shapley values for the different actors are influenced by the size of the impervious area, with larger actors having a more negative Shapley value. In this

Table 6.3: Optimal loadings and allocations for the baseline configuration

		Optimal allocation agents					
	Scenario	**A**	**B**	**C**	**D**	**E**	**Optimal load [lbs/ year]**
3000 lbs/year, $5 per 1000 lbs	BAU	✓	✓	✓			3124
	Direct grant	✓	✓	✓		✓	2572
	Municipal regulation	✓	✓	✓	✓	✓	2387
	Stormwater fee	✓	✓	✓			3124
6000 lbs/year, $5 per 1000 lbs	BAU		✓	✓			4930
	Direct grant		✓	✓		✓	4410
	Municipal regulation		✓	✓	✓	✓	4225
	Stormwater fee		✓	✓			4930
3000 lbs/year, $2.5 per 1000 lbs	BAU	✓	✓	✓			3124
	Direct grant	✓	✓	✓		✓	2572
	Municipal regulation	✓	✓	✓	✓	✓	2387
	Stormwater fee	✓	✓	✓			3124

setup, B, C, and E have negative Shapley values because they are the three largest agents; it makes sense for other agents to pay them to more rapidly reduce the pollutant load of the overall system. Interestingly, the direct grant scenario has the largest impact on all of the agents except agent D, who is most strongly affected by the stormwater fee scenario. As shown in Table 6.4, the optimal solution for the direct grant, municipal regulation, and stormwater fee scenario is to have all five agents install green infrastructure. Although this allocation does not reduce the loading below the 3000 lbs threshold, it does reduce the pollution by nearly 1000 lbs compared with the BAU scenario.

Table 6.4: Optimal loadings and allocations for the all parallel and all series configurations

		Optimal allocation agents					
	Scenario	**A**	**B**	**C**	**D**	**E**	**Optimal load [lbs/ year]**
All parallel	BAU	✓	✓	✓		✓	4010
	Direct grant	✓	✓	✓	✓	✓	3084
	Municipal regulation	✓	✓	✓	✓	✓	3084
	Stormwater fee	✓	✓	✓	✓	✓	3084
All series	BAU					✓	3166
	Direct grant					✓	3166
	Municipal regulation	✓	✓	✓	✓	✓	754
	Stormwater fee					✓	3166

The Shapley value distribution for the all series case makes clear that network location, not agent size, has the largest impact on the Shapley value allocations. Although all five agents are the same size as in the all parallel case, the distribution of allocations is starkly different. In the all series case, downstream agents have more negative allocations than upstream agents, as shown in Figure 6.3. This result implies that the downstream-most agent, E, has notable bargaining power. In this test case, the municipal regulatory scenario has the largest impact on all agents, but has the greatest impact on the agents with negative

Shapley value allocations. As shown in Table 6.4, in three out of the four scenarios, the optimal coalition is to simply have agent E install green infrastructure. Interestingly, this allocation does not reduce the pollutant loading below the 3000 lbs threshold concentration. However, the optimal coalition in the municipal regulatory scenario is to have all five agents install green infrastructure, contributing a pollutant loading of only 753 lbs.

Effect of penalty and load limit values

To test the sensitivity of the results to changing the pollutant load limits and the penalty assessed for exceeding that limit, two additional cases were tested. The first case increased the load limit to 6000 lbs/year, but maintained a $5 per 1000 lbs penalty. The second case maintained a 3000 lbs/year limit, but decreased the penalty to $2.5 per 1000 lbs. The BAU Shapley values for the two cases are summarized in Figure 6.5. As expected, the total cost decreases by about half in both of the additional sensitivity cases. However, the general allocation framework for the Shapley values remains consistent. Halving the penalty decreases the magnitude of the Shapley values for all actors more than doubling the load limit does.

As shown in Table 6.4, the optimal pollutant loadings are in general much larger in the load limit sensitivity test case than in the original case. The optimal allocation in the BAU scenario for the increased load limit case is to allocate green infrastructure to only B and C, leading to a loading of 4930 lbs/year. In the decreased penalty case, the optimal allocation for the BAU scenario is to allocate green infrastructure to A, B, and C, leading to a loading of 3124 lbs/year. This value is above the designated load limit for the second scenario. Interestingly, the coalitions for the optimal allocation are typically larger in the case with the lower penalty and original load limit (i.e., $2.50 per 1000 lbs and 3000 lbs/year respectively), than in the case with the original penalty and higher load limit (i.e., $5 per 1000 lbs and 6000 lbs/year respectively). In both cases, the municipal regulatory scenario provides the best environmental protection in terms of optimal load.

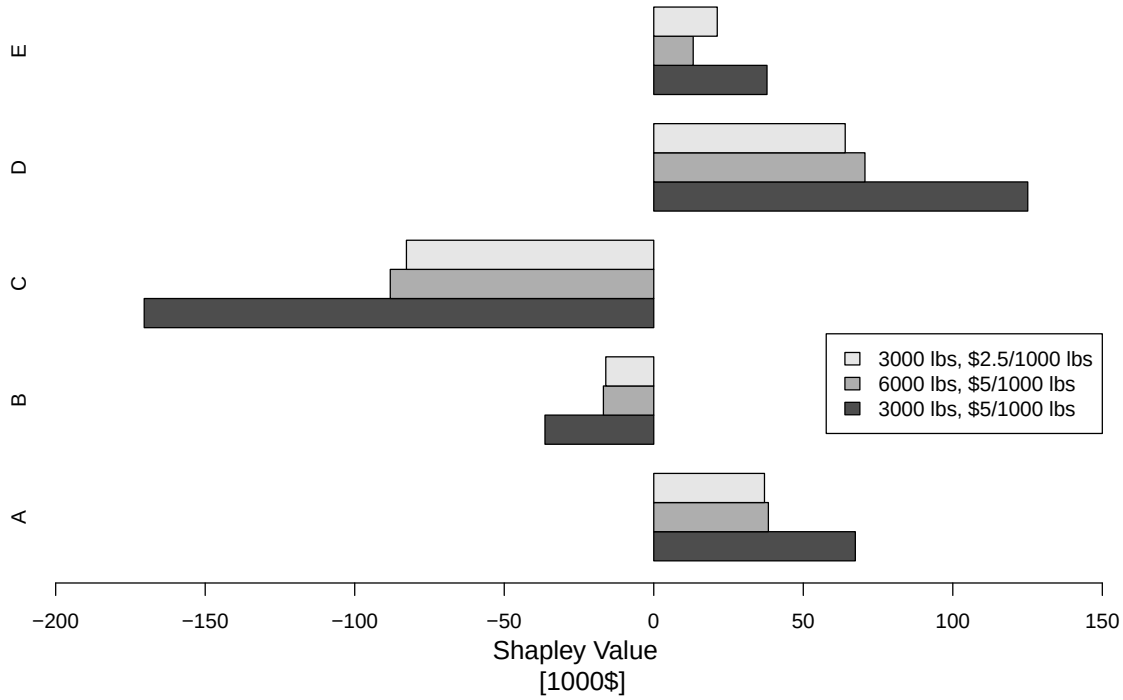

Figure 6.5: A sensitivity analysis of the Shapley value to the penalty and the load limit indicates that both variables have a similar impact on the green infrastructure installation results.

6.2.5 Discussion

The question of which stormwater management policy is most appropriate for a given city is dependent on multiple factors. In this analysis, the municipal regulatory approach leads to the lowest environmental impact in all test cases. In general, using a regulatory approach also does not have a very large impact on the calculated cost allocations of individual agents. However, municipal regulation is not necessarily a politically popular option, and might require larger investments of human capital than some of the other suggested policy approaches. The direct grant program has an environmental impact that is nearly as favorable as the regulatory approach, but it might not be financially sustainable in the long-term. Multiple policy studies in integrated urban water management have highlighted that financial sustainability and a steady source of revenue is vital to the long-term viability of water infrastructure projects [172–175].

Network layout and location greatly affect the impact of different stormwater management

policies by disproportionately allocating coalition bargaining power to downstream agents in a network. For example, agent E has the highest amount of bargaining power in the all series case as the downstream-most agent, although it is not the agent with largest impervious area. Keeping this discrepancy in mind, network layout greatly affects the choice of policy that has the greatest impact on individual agents' calculated cost allocations (i.e., their Shapley values). The regulatory scenario overall has the largest impact on agents' calculated cost allocations in the all series case, but has the greatest effect on agents with the highest bargaining power. This result implies that although the overall cost in this scenario is not greatly increased by municipal regulation, the downstream players are not getting paid as much to put in green infrastructure. In contrast, the direct grant policy scenario has the largest impact on cost allocations in the all parallel layout. In this layout, although having some municipal policy incentivizing green infrastructure does help to reduce pollution from BAU, the type of policy that is implemented makes little difference in terms of environmental protection since the direct grant, municipal regulation, and stormwater fee scenarios each have optimal allocations involving all five agents.

A comparison of the Shapley values to the costs incurred by agents in the optimal allocations for each of the different scenarios reveals a discrepancy in which agents are shouldering the burden of the costs. This observation is most evident in the all parallel test case. Agents C and B are more than adequately reimbursed for the expenses they incur in installing green infrastructure. However, agents A and D are not: even though they too are required to install green infrastructure under the optimal allocation, they are also required to pay into the collective "pool" used to reimburse agents C and B. This result is due to the allocation rewarding agents who can contribute the most to the overall system. Hence, the largest polluters, who have the greatest impact on the overall pollution load if they install green infrastructure, are incentivized to install green infrastructure while other agents bear the brunt of the cost. In the all series case, the cost allocation distribution appears to be fairer, as agent E is the only agent actually putting in green infrastructure in most scenarios, and is adequately reimbursed for doing so. On the other hand, it is important to note that in this case, agent E is essentially responsible for cleaning up the pollution from all of the other upstream agents.

This issue of agent equity is central to understanding both the social component of the sustainability triple bottom line and the human-environment interactions governing urban water. Based on the results, agent location and network configuration play significant roles in shared cost allocation among agents. The all series test case illustrates that location within the network is a much better indicator of allocation framework than agent size. The significance of the downstream-most agent in helping to reduce system pollution should imply that this player has substantial bargaining power in the Shapley value allocation process. However, the game theory model setup assumes that each agent comes to the table with a fairly equal level of negotiating power. This assumption does not hold true in practice. In fact, environmental equity literature suggests that lower-income, vulnerable populations are the ones more likely to be located near potential environmental nuisances. Studies show that low-income populations are statistically more likely to live in areas that are more polluted by various sources compared with environments where higher-income people live [46]. Lower-income populations are also less likely to be able to effectively participate in the formulation of laws, policies, and environmental regulations [46]. These factors indicate that the downstream-most agent is not likely to have a high amount of power entering the negotiations. However, the same literature also provides a strong motivation for continuing work to ensure that disadvantaged populations in urban areas do have access to green space, in the form of stormwater management best management practices. A study by Wendel et al. [176] concluded that green space access improvements do not necessarily require large increases in the overall quantity of green space, but could rather be achieved via more equitable distribution of smaller spaces. In other words, the proper implementation of green infrastructure in urban environments has the potential to address at least some of the issues of environmental inequality facing urban residents at the local scale.

While this work provides an interesting first attempt at using a game theory framework to allocate green infrastructure within an urban environment, there remain many avenues for future potential work. In this analysis, the agents in the MS4 network are modeled as being a part of a single cooperative game. In reality, there are few instances where agents would have an opportunity to work together as a 'coalition' to distribute the payoffs or costs associated with green infrastructure. The issue arises from the fact that green infrastructure

installation costs typically rest on the individual, whereas the 'penalty' associated with not meeting a pollutant threshold is distributed. Ideally, this situation could be modeled as a combination of a cooperative and a non-cooperative game. However, there is no guarantee that a pure Nash equilibrium exists. While a mixed Nash equilibrium always exists for any game with a finite series of actions [177], using a mixed Nash equilibrium does not make sense for this particular scenario: a mixed Nash equilibrium involves an agent choosing a particular strategy to play with some probability.

The results imply that a sub-watershed level committee or other communal structure could be advantageous in helping to facilitate communication between agents and allocate resources to ensure collaboration between agents in the MS4. Stormwater managers could learn from the example of groundwater conservation districts, which are used to locally manage and protect groundwater resources in states such as Texas [178]. Alternatively, homeowners' associations (HOAs) could step in to help coordinate private landowner involvement in managing their local watershed. Section 6.3 elaborates how HOAs can be a key component of the process of green infrastructure implementation. Cooperative game theory thus provides an innovative framework to explore the environmental-economic trade-offs between invidual private agents with regards to green infrastructure, but also reveals new areas for improvement and collaboration.

HOA presence is not necessarily strongly correlated with water demand, suggesting that geographical, social, and policy-related contexts are more important than institutional types in predicting environmental impacts [179]. As a result, HOAs can be incentivized to create positive green infrastructure implementation policies, scaling up the game from individual private agents to HOAs and neighborhoods. Similarly, developers can be incentivized to consider implementing green infrastructure in new developments at the building phase. Including developers as well as existing private homeowners adds an extra dimension to the game due to the inherent differences in cost between new-build green infrastructure versus retrofit green infrastructure. Interestingly, one important side-effect of including new development into the game might be to reduce the bargaining importance of network location: downstream land costs will typically be lower, meaning that developers will already be in prime position to implement new green infrastructure where is needed most. Several cities

are already taking steps in this direction. For example, Toronto, ON, Canada has a mandatory green roof requirement for all developments over a certain square footage. Similarly, Atlanta, GA requires all new homes and large additions to manage the first 1.0 inch of runoff on their site using green infrastructure [180]. However, the long-term environmental and economic benefit of these aggressive regulations on new structures remains to be seen.

6.3 Environmental Psychology: A Review

While a game theoretic approach provides useful insights into policies that might be used to motivate green infrastructure implementation in urban environments, the method has limitations due to its underlying assumptions about human psychology. The field of environmental psychology offers some practical guidance on how to convince urban residents to make long-term sustainable change, including the implementation of small-scale green infrastructure on their properties. This section discusses potential flaws in current frameworks currently used in practice, research into the factors that prompt human engagement, and some practical suggestions for GSI implementation.

6.3.1 Our Current Framework: Economic Self-Interest

The Economic Self-Interest model states that individuals systematically evaluate choices, and then act in accordance with rational self-interest. This framework drives game theory, and also motivates many municipal programs that use financial incentives to encourage green behaviors. However, there are proven reasons why an Economic Self-Interest model might be sub-optimal. The model focuses on the use of extrinsic rewards (i.e., monetary benefits). However, multiple sustainability efforts that focus on underscoring the monetary efforts of sustainability have failed. McKenzie-Mohr [181] suggests that the reason is that the Economic Self-Interest approach overlooks "the mixture of cultural practices, social interactions, and human feelings that influence the behavior of individuals, social groups, and institutions."

More particularly, the model's focus on extrinsic financial rewards can actually lead to

decreased motivation and long-term sustainability. Research indicates that overuse of extrinsic rewards can lead to decreased intrinsic motivation. This phenomenon, known as the "over-justification effect", implies that reducing or removing a financial reward leads to a reduction in the desired behavior, unless another, more powerful motivator, such as habit, has been put in place. Other studies complement these findings, indicating that extrinsic, financial rewards might not be as powerful motivators as previously thought. In a comparative study of recycling programs that used written commitments versus incentives techniques, the commitment-based study group showed more of the target behavior than the incentives-based group [182].

Another phenomenon that causes similar sub-optimal performance in rewards-based programs is "reactance". Reactance is cause by the perceived limitation of autonomy by an authority figure or society at large, and can manifest itself in views, positions, or behaviors contrary to what was originally intended. The classic example of reactance is that underage college students drink more than their legal-age peers; an increase in the legal drinking age in 1992 led to a rash of underage drinking violations, as drinking suddenly appeared more 'attractive' [183, 184]. In the context of rewards, a 1990 study showed that government-supplied rewards aroused reactance in managers, while parent company rewards did not [185]. Other studies indicate that above a certain monetary threshold, an increase in monetary reward actually leads to a decrease in performance for cognitively challenging tasks [186].

6.3.2 The Psychology of Drive: Factors that Prompt Human Engagement

Given that the Economic Self-Interest model cannot fully explain human motivation, we turn to other potential frameworks. Self-Determination Theory (SDT) was developed in the 1980's and creates a model of human motivation that is contingent on three factors: autonomy, relatedness, and mastery [187]. Autonomy is the urge to be a causal agent in one's own life. In other words, autonomy represents the need to be self-directed. Relatedness is the urge to feel connected to other people. In particular, relatedness is strong between members of similar social circles. Mastery is the feeling of accomplishment that comes from overcoming a challenge, or perfecting a skill. A good example of the power of mastery as a

fundamental human drive is the ability of games to keep us engaged for long periods of time through the rewarding of effort with rapid, clear feedback [187].

The flipside of autonomy is reactance. Because reactance is so prevalent in many arenas of human interaction, many psychologists have made detailed studies of reactance, what induces it, and how it can be avoided. While certain groups (e.g., teenagers, farmers, fishermen) are more prone to reactance than others, some rules governing reactance appear to be widely applicable. Certain behavior-modification approaches, for instance, seem more likely to elicit reactance than others, because they are perceived as limiting the target audience's autonomy. The most obvious of these approaches are laws and regulations, as well as direct threats. However, as previously mentioned, tangible rewards can also elicit reactance in certain cases. Combative situations or conversations can elicit reactance [188], as can the perception of a higher authority limiting choice [189]. Choosing an appropriate approach to incentivize behavior-modification is thus important to limiting the negative consequences of reactance. Other factors, including how a message is delivered, and who delivers it, can be equally consequential. In general, the more distant socially the messenger is from the intended audience, the more likely an approach is to induce reactance [190]. For this reason, community-created rules and initiatives are much more likely to be followed. Another potential trigger for reactance is how invested the messenger is in the outcome: a messenger who is perceived as neutral is much less likely to elicit reactance than someone who clearly has a vested interest [191].

Relatedness is another key driver of human motivation. One of the best examples of the power of relatedness is the impact of social norms on behavior. Social norms, in the form of positive role models, have a powerful effect on behavior. A study of student water conservation indicated that student compliance in saving water in the shower jumped to 49% (from 6%) in the presence of a positive role model. After the addition of a second role model, compliance rose to 67% [181]. Social norms can be divided into two different types: injunctive norms and descriptive norms. Injunctive norms evaluate societal approval or disapproval for a certain behavior, while descriptive norms define what behaviors (positive and negative) are typically engaged in. An important aspect of ensuring the social norms are as effective as possible is ensuring that injunctive and descriptive norms do not accidentally

cancel each other out. If negative behaviors are common, then negative descriptive norms might encourage further unsustainable behaviors [192]. Conversely, the confluence of positive injunctive and descriptive norms can be powerful: using praise as a motivator when someone is doing above average can lead to further behavioral improvements, not just for that particular person, but for their neighbors. Importantly, studies also show that social norms are most likely to stick if they are presented as coming from peers and other members of similar social circles [192]. Social norms are also most likely to create positive change when examples of the desired change are present in close proximity to the changes that need to be made in behavior [181].

The final component of SDT is mastery. The ability of mastery to modify behavior is epitomized by the phenomenon of "gamification". Games have several approaches to keep players engaged and motivated. Many games use progress bars to track status, experience, or the learning of new skills. Players can set and meet multiple short- and long-term goals, a concept that also ties into the concept of autonomy. Effective games provide rapid, clear feedback. They also reward effort, whilst adding an element of uncertainty in how rewards are distributed through a "reward schedule" which can be adapted based on player skill [193]. Increasingly, these concepts from the world of gaming are being adapted as potent behavior-modification tools, in everything from educational interfaces, to museum design, to customer data acquisition. In the world of sustainability, gamification has shown promise in helping to reduce energy consumption, particularly for high-energy users. Ro et al. [194] show that with gamification, a change in attitude is not necessary to motivate a change in behavior.

Outside of SDT, two other principles are useful in describing how humans moderate behavior: the creation of habits, and perceptions of convenience. Habits are defined as behaviors that are triggered by environmental cues, repeated, and have been reinforced in the past by rewarding experiences. Research suggests that habits can be powerful shapers of behavior: a 2011 study of dietary behavior suggests that up to 18% of the variance in eating behavior may be attributed to habit [195]. While many models of human behavior assume that intention is an important aspect of behavior [196], this assumption does not hold true for all habits. In particular, strong habits are typically not influenced by intention. For-

tunately, behaviors can be changed by changing situational cues; changing implementation intentions; and creating opportunities for positive reinforcement. For people who are already pre-disposed to accepting the target behavior, the first of these approaches can be easily managed through the use of prompts, in and of themselves a powerful predictor of behavioral change [181]. While habit creation may not be relevant to the initial desired behavior of green infrastructure installation, it is crucial for regular upkeep and maintenance of existing green infrastructure on private property.

Utilizing SDT can help to remove many of the internal, motivational barriers to GSI implementation. However, many people often face external barriers to sustainable behavior. Making sustainable behaviors convenient (or conversely, making unsustainable behavior inconvenient) can be another approach to helping to motivate behavioral change. The outcomes of lowering the external barriers to sustainability are heartening: a recent study of composting alternatives in Halifax, Canada indicates that introducing curbside pickup led to a 99% participation rate amongst households [181].

6.3.3 Practical Suggestions for GSI Implementation

Although game theory suggests that municipal regulation leads to the most positive environmental outcomes, environmental psychology literature cautions that overly heavy-handed approaches can lead to reactance. Strong regulatory schema might not lead to long-term, sustainable behavioral change, and at worst might lead to homeowners seeking out 'loopholes' in the regulations. Without the manpower to ensure adequate upkeep and maintenance of green infrastructure on private property, cities may struggle to enforce unpopular ordinances [197]. Cities that mandate green infrastructure on new development may thus find themselves falling short of long-term sustainability goals. Similarly, direct incentives programs are only likely to lead to change so long as the incentives are kept in place. These programs thus do not provide for the long-term, organic diffusion of green infrastructure and sustainable ideology into different parts of the city not specifically targeted by the initiatives program.

Instead of relying on one sole mechanism for fostering GSI uptake, cities should instead rely on a variety of approaches, to target each of the different factors of human motivation.

Relatedness is a powerful tool for fostering sustainability. Creating a network of peer-to-peer neighborhood role models can provide guidance to their local communities and help create templates to show what works and what does not. This approach relies on traditional models of social diffusion, targeting information about green infrastructure at early adopters within host communities to ensure reasonable community uptake. Importantly, it facilitates several factors that have been identified as drivers of social diffusion: simplicity and ease of use, trialability, and observable results [198]. Peer role models can help to 'test drive' green infrastructure and applicable tool kits, providing communities unique pilot sites within their own neighborhoods so that they can have better indications of final outcomes, aesthetics, and costs. In action, real-world practitioners have found this approach useful, suggesting that identifying 12-15 key group influencers early in the planning process is key to success [199, 200].

Leveraging existing institutions such as HOAs can help to more widely spread positive social norms (both descriptive and injunctive), whilst also allowing community buy-in and rules creation. This last factor is important in helping to mitigate reactance, which might occur if outside authorities were to impose such rules. Studies show that HOAs can have a significant impact on environmental factors such as residential water consumption in arid areas, with HOAs that require the use of turf grass using much more water than HOAs that allowed alternative landscaping [201]. In a stark example of the adverse impact that HOAs can have on environmental commons issues, the HOA in Blackhawk, CA drew ire from local government officials after threatening to fine homewoners for brown or dead lawns despite the continuing state drought in 2016 [202]. However, HOAs, when properly incentivized, can also be a powerful mediator in regulating urban water demands [179]. HOA involvement in stormwater management is a logical extension of their current impact. In fact, HOAs in Montgomery County, MD are already being used to coordinate institutional parcel rebates as a part of the RainScapes Rewards program [203].

In practice, because green infrastructure is highly visible, social norms dictate whether their presence positively or adversely affects the perceived value of a home. Nassauer [204] surmises that the 'halo effect' is particularly strong with regards to green infrastructure: not only does the appearance of neighbors' yards have marked impacts on individual preferences,

but examples of "care" and maintenance are also contagious. HOAs or neighborhood associations are also a useful means of gaining commitments from local residents. Commitment-based approaches have been shown to be especially effective if they are voluntary, public, and written down, and taken as a group. Outside of neighborhood associations, faith-based organizations (such as Faith in Place), education-based institutions (such as local public schools), and community-centric organizations (such as local YMCAs), often play a key role in ensuring the GSI is an understood and accepted part of communities.

City engagement programs (in collaboration with local educational institutions) can be used to allow local residents to develop new skills associated with maintaining and caring for shared green infrastructure. Learning new skills helps to bolster a sense of mastery, and can thus translate into behavioral change. The process of learning these skills also helps lead to long-term changes in attitude through changes in behavior: repeated behaviors often lead to beliefs that become strongly held [181]. These same repeated behaviors also can lead to the formation of habits, which can then be reinforced using prompts for appropriate maintenance on private property. Training is also key for proper installation – and ultimately long-term performance – of green infrastructure. Although green infrastructure is becoming normalized amongst designers and planners, training for proper GSI installation and upkeep is rare, leading to a plethora of challenges [205]. The current national roll-out of the National Green Infrastructure Certification Program (NGICP) might help to offset some of these challenges, and could offer an interesting long-term study on the impact of training on enthusiasm for green infrastructure implementation within urban communities.

6.4 Green Infrastructure and the Legal Framework for U.S. Urban Stormwater Control

6.4.1 How did we get here?

The aim of the CWA is to protect "the physical, chemical, and biological integrity of the nation's waters" [206]. However, it took a surprisingly long time for urban stormwater, a significant source of pollution for many U.S. streams, lakes, and rivers, to come under the

purview of the CWA. Specifically, it was the Supreme Court's ruling on *NRDC v. Costle* (1977) that forced the EPA to include urban stormwater as a part of the National Pollutant Discharge Elimination System (NPDES) permitting process. It took a further ten years for Congress to pass substantial amendments to sections 301 and 402 of the CWA, highlighting the need to manage stormwater and create stormwater permit programs for urban areas and industry. The first set of CWA MS4 regulations came into effect in 1990 [207].

Stormwater is legally defined by the USEPA as all "stormwater runoff, snow melt runoff, and surface runoff and drainage" not including infiltration into pipes or street wash waters [207]. Urban stormwater scientifically is classified as a non-point source pollutant (i.e., distributed flow rather than channeled). That urban stormwater is legally considered a non-point source pollutant before it enters the sewer system is evident throughout case law. In *Ecological Right Foundation v. Pacific Gas and Electric Company* (2013), the court found that leachate from urban utility poles containing toxic substances could not be regulated under the CWA because it was not a "point source". However, legally, stormwater that flows into an MS4 is classified as a point source discharged into a water of the United States (WOTUS). In other words, MS4 discharges are regulated under the Clean Water Act through the same permitting process that is used to regulate wastewater treatment plant discharges [208].

MS4s are regulated through NPDES permits that are allocated to the sewer network based on ambient, state-controlled water quality standards, rather than effluent limitations. The water quality standard is determined based on the intended use of the impaired water. Water quality standards are intended to be supplementary provisions to ensure that waters meet minimum water quality standards, regardless of individual compliance with technology-based limitations. The MS4 permitting structure was implemented in two phases: Phase I (implemented in 1990) required individual NPDES permits for MS4s serving over 100,000 people, while Phase II (implemented in 1999) required general permits for all MS4s not covered by Phase I. While Phase I permittees are required to submit detailed information and quantitative data sampling of stormwater discharges collected during storm events, Phase II permit requirements are significantly less stringent. Both Phase I and Phase II MS4s are required to meet six "minimum control measures": i) public education and outreach, ii)

public participation, iii) illicit discharge detection and elimination, iv) construction runoff control, v) post-construction runoff control and pollution prevention, and vi) good housekeeping [209]. The final measure is intended to create protocols for municipalities to inspect whether control practices are working in the long-term as designed. These measures are recorded and updated in a municipal stormwater management plan.

Total maximum daily loads (TMDLs) are another alternative regulatory strategy used to control MS4 discharges. Section 303(d)(1)(A) of the Clean Water Act requires states to identify waters within their jurisdictions that fail to meet established water quality standards. States are then mandated under Section 303(d)(1)(C) to create TMDLs subject to review by the EPA. TMDLs are tools designed to help plan and implement strategies for both point and non-point sources within a watershed to work together to manage pollutant loadings. If technology-based pollution controls are insufficient to maintain the designated standards for a water body, the state is obligated to develop and submit to the USEPA for approval TMDLs for the pollutants in that water body [206]. Per *Pronsolino v. Nastri* (2002), the TMDL provides a blueprint for federal, state, and local agents to work together to implement pollutant controls to improve water quality standards.

One of the most complex and comprehensive TMDLs created to-date is based in the Chesapeake Bay watershed in the northeastern United States. The precedent-setting Chesapeake Bay TMDL allocates loadings in a highly detailed fashion, even to the level of separating load allocations (LAs) and waste load allocations (WLAs) for non-point and point sources, respectively (see *American Farm Bureau v. USEPA*, 2013). It is also unique in that it encompasses multiple states, and gives the USEPA the authority to reinforce state watershed implementation plans (SWIPs) if the states fail to meet their own benchmarks. As per *Friends of the Earth v. EPA* (2006), all established TMDLs need to have calculated daily loads rather than seasonal or annual loads. Based on a post-decision guidance memo from the EPA [210], many TMDLs calculate these daily load allocations based on seasonal loadings if the agency deems these more appropriate than meeting the ecological goals for the TMDL.

6.4.2 A Point Source Solution to a Non-Point Source Problem

The type of pollution discharged by MS4s is inherently difficult to control since urban runoff is non-point source pollution, which is then channelized into a network of pipes before final discharge (see *NRDC v. County of Los Angeles*, 2011). In other words, it is challenging to identify precisely who is responsible for what component of the contamination entering the storm sewers (see *NRDC v. County of Los Angeles*, 2011). In practice, federal or state regulation is most feasible at the downstream end of the pipe. It is up to individual municipalities to meet downstream regulations by implementing urban land-use policies that enable individual landowners to decrease the amount of contaminants being washed off their property. Moreover, stormwater pollutant discharges are by their nature inherently uncertain. As discussed in previous chapters, stormwater runoff volumes vary based on storm magnitude, duration, and intensity. These challenges are magnified for non-point source pollutant loadings, which are effected by other factors such as construction, traffic patterns, topology, and land use [211].

While the efforts that are being made to manage stormwater effluent on a federal level are commendable, there remain multiple challenges with the existing legal framework. The biggest cause for confusion remains the conflation of stormwater (a non-point source pollutant) with a point-source legal framework. The awkward combination of different legal paradigms is most obvious in the fact that stormwater NPDES permits are largely based on water quality standards: an area that is typically the purview of the TMDL. Multiple EPA memoranda and other guidance documents point towards the fact that the agency expected municipal stormwater discharges to comply with existent water quality standards, particularly when a TMDL was already in place. In 1991, the EPA Office of General Consul issued a memo stating that permits must require that MS4s reduce stormwater pollutant discharges to maximum extent practicable and also comply with water quality standards [211]. More recently, EPA's TMDL stormwater policy states that stormwater permits must include permit conditions consistent with the assumptions and requirements of existing WLAs [211].

The development of effluent standards for point source industrial users and publicly owned treatment works (POTWs) stemmed from reasoning that advances in technology could in-

directly enable improvements in the quality of receiving water bodies. Congress' intent with regards to these effluent standards was that they be uniform throughout the nation, in order to avoid the potential for a geographic "race to the bottom" [206]. For this reason, the DC Circuit court argued in *Weyerhaeuser Co. v. Costle* (1978) that the condition of the receiving waters should not be taken into account in establishing effluent limitations. Rather, effluent control technologies would be regulated on a progressively more stringent set of expectations over time, beginning with the implementation of "best practicable technology" (BPT) in 1977 and proceeding to a "best available technology" (BAT) standard by 1983. While the creation of these technology-based standards has significantly improved water quality, environmentalists argue that they are limited by their lack of incentives for industry to develop better pollution control technology. Equally importantly, technology-based standards do not guarantee that water quality and associated health-related goals will be met [206].

These challenges to a technology-based standard for point sources are even more pertinent to the regulation of non-point sources (such as municipal stormwater) through the use of stormwater control measures (SCMs). Within the industrial context, the entities causing the pollution can assume the responsibility for its end-of-pipe treatment. In the case of municipal stormwater, the uncertainties associated with variability in pollutant loading in time and space mean that municipalities might not have direct control over flows from individual properties within the city that contribute to water-quality standard exceedances. Many of these same issues have arisen in contexts outside of urban stormwater. In 2017, the Iowa Supreme Court ruled that the Des Moines Water Works did not have standing to bring suit against upstream drainage districts because the drainage districts had no statutory authority to mandate the requisite changes in farmers' nitrate management that would have brought relief to Des Moines' strained water treatment facility [212]. The key difference between the Des Moines case and the challenge facing many municipalities is that the Iowa Drainage Districts only had legal responsibility for maintaining drainage ditches and existing streams (rather than drainage tiles); municipalities take responsibilities for all stormwater conveyance structures within their jurisdiction (see *NRDC v. County of Los Angeles*, 2011).

Besides the public-private regulatory challenges that inevitably ensue from this paradigm,

the point source/non-point source dichotomy leads to issues associated with monitoring and compliance. EPA's guidelines require that Phase I MS4s conduct analytic monitoring of pollutants of concern in discharges from outfalls that are 36 inches or greater in diameter or drain more than 50 ac (Phase II monitoring is discretionary) [207]. Needless to say, few municipalities are able to effectively comply with this requirement. Stormwater discharge monitoring for all major municipal outfalls would be time-intensive and expensive. Moreover, because storm discharges are highly dynamic in nature, it is difficult to evaluate whether or not an MS4 is in compliance with existing WQS limits. The National Stormwater Quality Database (NSQD), is a broad survey of water quality samples gathered as a part of NPDES monitoring requirements for MS4s across the country. Of the 100 MS4s participating in the database, 58% reported issues with monitoring. The majority of these problems related to meeting sampling requirements for specific rainfall conditions or land use types. Another significant problem was equipment failure: a particular challenge for automated samplers [211].

Although the exceedance of effluent limitations technically constitutes a permit violation, permitting authorities have thus far not taken this approach in interpreting MS4 discharge data. In the case of *County of Los Angeles v. NRDC* (2013), the seven mass emission monitoring stations designated by LA County's NDPES permit were located in channelized portions of the MS4 controlled by the LA County Flood Control District that fed into the natural channel of the LA River. The location of the gaging stations (within the channel rather than at an outfall), coupled with the sheer number of municipalities draining into the river upstream of the District's gaging stations, made it difficult to attribute pollution directly to LA County. The discrepancies in how and where monitoring was conducted ultimately led to the contradictory rulings made by the Central California District court, the Ninth Circuit Court, and eventually the U.S. Supreme Court.

6.4.3 Stochastic Outcomes, Pre-Determined Implementation

To afford municipalities more flexibility in addressing stormwater pollution, the EPA has taken the approach of allowing the use of stormwater control measures (SCMs) in creating

effluent limits and guidelines. For all other NPDES permits, the CWA requires either numeric pollutant limits (i.e., water quality-based standards) or technology performance standards. Water quality-based effluent limits are typically used where technology-based limits are insufficient to achieve applicable water quality standards. In *Defenders of Wildlife v. Browner* (1999), the federal court upheld EPA's policy to issue stormwater permits to MS4s that use SCMs rather than numeric discharge limits. The court held that the CWA unambiguously demonstrates that Congress did not require municipal stormsewer discharges to comply strictly with its requirement that NPDES permits comply with state water quality standards. As a result, effluent limits often use SCMs when numeric limits are infeasible or for discharges where monitoring data are insufficient to carry out the purposes and intent of the CWA.

However, the use of SCMs as effluent limits in NPDES permits bumps up against the CWA's requirement that MS4s treat their discharges to the "maximum extent practicable". The term itself is inherently vague: according to the CWA, it means "fully consistent with the enforceable policies of management programs unless full consistency is prohibited by existing law applicable to the Federal agency" (15 CFR §930.32). While this flexibility is useful for municipalities in tailoring how to meet their goals for stormwater mitigation, it creates a legal headache for stormwater practitioners. Particularly in the realm of green infrastructure, pollutant removal (particularly of nutrients) is determined by other compounding factors such as soil moisture, native flora and fauna, and network location. Large-scale green infrastructure implementation is a delicate exercise in public-private partnerships, and might lead to sub-optimal placement or design of stormwater management infrastructure given private landowners' personal preferences. While some states (such as California) have made concerted efforts to quantitatively define "maximum extent practicable", others retain the original loose definition, making enforcement of water quality standards challenging, particularly for larger watersheds [213–215].

From a technical standpoint, the use of SCMs to define effluent standards runs into a much larger issue: the regulation of non-point source runoff using technologies that themselves have a high degree of performance uncertainty associated with them. Scientific uncertainty plays a large role in the definition of TMDLs. For example, the Chesapeake Bay TMDL acknowl-

edges that "on the basis of probability analysis, a loading that will be achieved 100 percent of the time cannot be calculated" and thus chooses a 95 percent probability as appropriate [174]. Moreover, the TMDL also builds in a margin of safety on its load allocations and waste load allocations, to account for any "lack of knowledge" regarding relationships between loads and downstream water quality. The modeling of the loadings for MS4s thus takes into account fluctuations in seasonality and other factors driving downstream discharges [174]. However, the use of SCMs (particularly the large-scale implementation of green infrastructure such as rain gardens) in discharge permits ignores similar changes in control measures. Without appropriate downstream monitoring, it is challenging to determine whether designated SCMs for MS4s are simply fulfilling the letter of the law rather than its spirit.

6.4.4 A Path Forward

While green infrastructure affords many potential opportunities to municipalities seeking to meet their legal obligations under the Clean Water Act, it does sit at an uncomfortable intersection between several different philosophies. Green infrastructure is explicitly designed to regulate a non-point source pollutant — urban stormwater — yet its implementation is often incorporated into legal regimes designed to deal with point source pollutants. Its performance is often highly variable, contingent on both natural and human-made factors including appropriate maintenance and design. Yet green SCMs are often used as deterministic stand-ins for the numeric effluent standards demanded by most other point source polluters.

To ensure that green infrastructure meets its potential in helping urban environments truly embrace the lofty goals of the Clean Water Act, much work remains. Adequate maintenance of green infrastructure is a mandatory requirement of many SWIPs. However, certified training programs for long-term green infrastructure maintenance (such as the newly introduced NGICP) need to be a mandatory component of all MS4 NPDES permits. Monitoring is also an essential component of any program that seeks to include green infrastructure as a part of a holistic management strategy for stormwater. General best management practices for MS4 stormwater monitoring should be observed, including the use (and appropriate cali-

bration and upkeep) of automated sampling as far as possible. Monitoring stations should also collect flow and precipitation data to avoid the use of regional precipitation data for large watersheds. Flow-composite data should be collected for the entire duration of the storm event to avoid bias. More importantly, long-term data collection efforts need to be made at the watershed scale to evaluate the effects of green infrastructure implementation on runoff. A semi-permanent network of collection stations can be used to evaluate urban runoff over concentrated time periods before, during, and after large-scale implementation of green infrastructure [211].

At a larger scale, innovative legal and management frameworks such as watershed permitting could help to alleviate some of the challenges associated with the non-point source/point source dichotomy. According to a 2003 EPA report, watershed-based permitting is "an approach that produces NPDES permits issued to point sources on a geographic or watershed basis" [211]. Assigning NPDES permits based on local ecology and geography rather than political or institutional boundaries has several benefits. Permits would be more closely aligned with the water quality goals of TMDLs. Using a watershed approach to permitting also allows for a more flexible, integrated approach to water management, and encourages the participation of all stakeholders within the region. As a result, a watershed permit would also encourage water quality trading, providing a cost-effective strategy to achieve environmental goals. Most importantly, from the perspective of this research, watershed permitting avoids the blame attribution squabbles often associated with urban stormwater disputes by delegating a sole authority responsible for water quality within the watershed.

6.5 Summary

This chapter explores how green infrastructure can be integrated into the urban environment from three policy perspectives: game theory; environmental psychology; and environmental law.

A game theory approach is used to compare the four types of policy incentives that are most commonly used by municipalities to encourage green infrastructure implementation by private stakeholders. Municipal regulation leads to the greatest reduction in pollutant

loading for all of the different network configurations tested. In comparison, stormwater fees are shown to have no effect on pollutant loadings, but did increase agent costs. The 'best' scenario to choose will depend on factors including political necessity and long-term financial viability. However, the minimal environmental impact attributed to the stormwater fee scenario is important for policy-makers to keep in mind when planning implementation strategies for their cities. Spatial layout and location within the network also have a significant impact on agents' bargaining power. The impact of location also raises important questions of social and environmental equity, which are critical to addressing the sustainability triple bottom line. While downstream agents might potentially have a strong bargaining position in determining the value of green infrastructure on their property, historically, populations living in areas affected by environmental 'nuisances' are usually low-income individuals. Finally, the results highlight the value of creating governance entities to help facilitate the negotiations and dialogue critical to cooperative games in a green stormwater infrastructure setting.

The second component of this analysis, an environmental psychology literature review, builds on this final finding. This study begins by exploring the current framework of economic self-interest that underlies both the game theory study and many existing green infrastructure incentives programs. While this framework offers a good starting point for mathematically evaluating user behavior, it fails to account for other, more powerful motivators of human behavior, including reactance. The framework of Self-Determination Theory is used to contextualize three alternative motivators of human drive: autonomy, relatedness, and mastery. Finally, the study offers some concrete suggestions of how to incorporate this theoretical framework into practical means to improve green infrastructure integration into urban communities.

The final component of this policy analysis focuses on the position of green infrastructure within the legal context of the U.S. Clean Water Act. After a brief history of the development of the MS4 program, the study puts forward two legal conundrums that could limit green infrastructure efficiency in meeting the goals of the Clean Water Act as a whole. Firstly, the MS4 program is a point source solution to what is inherently a non-point source problem. The resulting confusion over pollutant attribution has lead to multiple court cases

over the years, as well as challenges for MS4 monitoring. The second challenge is that green stormwater control measures are commonly used as 'built in' components of NPDES permits (in lieu of numeric effluent standards), although the end outcome of treatment using green infrastructure is inherently stochastic. The study puts forward some suggestions for watershed-scale monitoring and maintenance of green infrastructure, as well as a potential new paradigm for a permitting structure that might more successfully and holistically integrate urban stormwater into existing legal frameworks.

CHAPTER 7

CONCLUSION

Green infrastructure, the use of nature-based solutions to manage stormwater at its source, offers a lot of potential benefits in terms of dealing with the plethora of water quality and flood control challenges facing urban environments. However, green infrastructure performance is notoriously variable, a fact that has led it to be viewed as a 'risky' investment by many developers. Climate, soil type, maintenance, and plant type can all impact green infrastructure performance. As more cities begin adopting green infrastructure in response to changing climate and demographics, a characterization of green infrastructure uncertainty at both the individual and network scale is more important than ever. In this dissertation, a reliability-based framework is used to answer the over-arching motivating question *How does incorporating uncertainty into the impacts of green infrastructure implementation affect the performance of an existing system, from engineering and policy perspectives?* This question is further divided into three objectives, addressed below.

1. Characterizing GSI modular fragility

Fragility functions for a test rain garden site are modeled using EPA-SWMM and calibrated using data from a USGS site in Madison, WI. By perturbing these fragility functions, the study evaluates how the rain garden interacts with different stochastic forcing events over time. Firstly, the long-term effects of clogging on the rain garden are studied. Clogging and other maintenance issues are a major challenge for the long-term performance of green infrastructure. By using an SLCA framework with shock deterioration and no recovery, it was determined that maintenance should be undertaken during a 3-year window in a temperate, humid climate.

The second study modeled back-to-back rainfall events using an SLCA framework, with storms modeled as shock deterioration and interstorm periods modeled as gradual recovery.

Due to the over-designed nature of this particular rain garden, antecedent moisture does not affect rain garden performance unless the garden experiences two large magnitude storms within a very short interstorm period. As a result of the distribution of interstorm duration and rainfall magnitude, this occurrence is statistically unlikely.

The study also modeled spatial variability in green infrastructure. Urban soils are uniquely challenging in this regard due to the high level of variability in soil type and anthropomorphic interference that they typically present. Soil classes across the Calumet River Corridor in Northern Illinois were studied to analyze the effect of native soil types and loading ratios on green infrastructure performance. After categorizing the different soil types into three different textural and hydraulic conductivity classes, these three classes were then used to develop fragility curve 'families' for different loading ratios and planting media thicknesses. Importantly, these fragility curves indicate that well-designed green infrastructure can be effective even in fine-textured native soils.

2. Simulate GSI network performance at the catchment scale

While understanding how green infrastructure performs under uncertainty at a modular level is important in its own right, it is also a crucial first step to understanding how green infrastructure will perform at a systems level. The fragility curves developed in Objective 1 were used to provide a stochastic lens on the importance of scale and location on green infrastructure performance. A case study was developed using a separated sewer within the Gwynn's Run subwatershed in west Baltimore, MD. Random and clustered assignments of green infrastructure were assessed at both small and large network scales.

The results highlighted the importance of location on green infrastructure performance, both with relation to other infrastructure and with regards to placement within the watershed. While green infrastructure was fairly successful for limited coverage options in the smaller catchments, its efficacy was greatly diminished in the larger catchment, as the impacts of green infrastructure placement were diluted across multiple subwatersheds. To avoid this effect, a subwatershed-level consortium is suggested to allow green infrastructure to be clustered by watershed, rather than using a neighbor-based social diffusion approach.

3. Evaluate the policy implications of GSI implementation

To effectively integrate green infrastructure within urban communities, an understanding of what policies help — and hinder — green infrastructure implementation is needed. A collaborative game theory approach was used to evaluate three strategies commonly used by municipalities to incentivize green infrastructure implementation: direct subsidies, municipal regulation, and stormwater fees. Interestingly, stormwater fees led to no decrease in pollutant discharges, despite increased costs to all agents in the game. The results from this analysis also showcased the importance of network location on game outcome, a result with potential environmental justice implications for downstream agents.

Although game theory affords a useful first step in gauging agents' behaviors and outcomes, it does not reflect real human interactions and emergent social behaviors. The Self-Determination Theory (SDT) environmental psychology framework was used to characterize the factors that influence human drive. Practical strategies for green infrastructure implementation, including the recruitment of HOAs and the development green infrastructure skillsets, were suggested that align with the SDT framework.

Finally, green infrastructure is examined within the context of the U.S. Clean Water Act. A case law study and literature review was used to explore the nuances of MS4 NPDES permitting structures, as well as how green infrastructure is currently incorporated into Clean Water Act regulation. This study revealed that green infrastructure is currently treated as a point source solution to a non-point source problem, leading to legal challenges in terms of pollutant attribution as well as monitoring and maintenance burdens. Moreover, because green infrastructure is often used in MS4 NPDES permits as a substitute for numeric effluent standards, the implications of green infrastructure performance uncertainty are currently not incorporated into permitting structures. Although uncertainty is a major component of how TMDLs and their associated WLAs are crafted, it is thus not incorporated into understanding the solutions to the challenges facing impaired watersheds.

By tying together the performance of green infrastructure at modular, systemic, and policy levels through a reliability-based framework, this work offers a unique perspective on the role that GSI can play in the modern urban environment. In doing so, this dissertation offers tools and insights that are vital to the integration of sustainable stormwater technology into urban communities and landscapes.

REFERENCES

[1] United Nations. World's population increasingly urban with more than half living in urban areas, 2014. URL http://www.un.org/en/development/desa/news/population/world-urbanization-prospects-2014.html.

[2] E. Strassler, J. Pritts, and K. Strellec. Preliminary data summary of urban stormwater best management practices, 1999. URL https://www3.epa.gov/npdes/pubs/usw_b.pdf.

[3] Chespeake Bay Foundation. Polluted Runoff, 2016. URL http://www.cbf.org/about-the-bay/issues/polluted-runoff.

[4] M Benedict and E McMahon. *Green infrastructure: Linking landscapes and communities*. Island Press, Washington, DC, 2006.

[5] Aaron A. Jennings. Residential Rain Garden Performance in the Climate Zones of the Contiguous United States. *Journal of Environmental Engineering*, 04016066-1, 2016. ISSN 0733-9372. doi: 10.1061/(ASCE)EE.1943-7870.0001143.

[6] Jennifer K Holman-Dodds, Allen Bradley, and Kenneth W Potter. Evaluation of Hydrologic Benefits of Infiltration Based Urban Storm Water Managment. *Journal of the American Water Resources Association*, 53706:205–215, 2003. ISSN 1093-474X. doi: 10.1111/j.1752-1688.2003.tb01572.x.

[7] Allen P. Davis. Field Performance of Bioretention: Hydrology Impacts. *Journal of Hydrologic Engineering*, 13(2):90–95, 2008. ISSN 1084-0699. doi: 10.1061/(ASCE)1084-0699(2008)13:2(90).

[8] Timothy L. Carter and Todd C Rasmussen. Hydrologic behavior of vegetated roofs. *Journal of the American Waters Research Association*, 42:1261–1274, 2006. ISSN 1093-474X. doi: 10.1111/j.1752-1688.2006.tb05611.x.

[9] Hua Peng Qin, Zhuo Xi Li, and Guangtao Fu. The effects of low impact development on urban flooding under different rainfall characteristics. *Journal of Environmental Management*, 129:577–585, 2013. ISSN 03014797. doi: 10.1016/j.jenvman.2013.08.026.

[10] Jinsong Tao, Zijian Li, Xinlai Peng, and Gaoxiang Ying. Quantitative analysis of impact of green stormwater infrastructures on combined sewer overflow control and urban flooding control. *Frontiers of Environmental Science and Engineering*, 11(4): 11–23, 2017. doi: 10.1007/s11783-017-0952-4.

[11] Nicholaus D. VanWoert, D. Bradley Rowe, Jeffrey A. Andresen, Clayton L. Rugh, R. Thomas Fernandez, and Lan Xiao. Green Roof Stormwater Retention. *Journal of Environment Quality*, 34(3):1036, 2005. ISSN 1537-2537. doi: 10.2134/jeq2004.0364.

[12] Eline Vanuytrecht, Carmen Van Mechelen, Koenraad Van Meerbeek, Patrick Willems, Martin Hermy, and Dirk Raes. Runoff and vegetation stress of green roofs under different climate change scenarios. *Landscape and Urban Planning*, 122:68–77, 2014. ISSN 01692046. doi: 10.1016/j.landurbplan.2013.11.001.

[13] P Natarajan and A Davis. Hydrologic performance of a transitioned infiltration basin managing highway runoff. *Journal of Sustainable Water in the Built Environment*, 1 (3), 2015.

[14] N Dunnett and A Nolan. The effects of substrate depth and supplementary watering on the growth of nine herbaceous perennials in a semi-extensive green roof. *Acta Horticulturae*, 643:305–309, 2004.

[15] Reshmina William and Ashlynn S. Stillwell. Use of fragility curves to evaluate the performance of green roofs. *Journal of Sustainable Water in the Built Environment*, 3(4), 2017. doi: https://doi.org/10.1061/JSWBAY.0000831.

[16] Christopher Chini, James Canning, Kelsey Schreiber, Joshua Peschel, and Ashlynn Stillwell. The Green Experiment: Cities, Green Stormwater Infrastructure, and Sustainability. *Sustainability*, 9(1):105, 2017. ISSN 2071-1050. doi: 10.3390/su9010105.

[17] Daniele Masseroni and Alessio Cislaghi. Green roof benefits for reducing flood risk at the catchment scale. *Environmental Earth Sciences*, 75(7), 2016. ISSN 18666299. doi: 10.1007/s12665-016-5377-z.

[18] Thomas C. Walsh, Christine A. Pomeroy, and Steven J. Burian. Hydrologic modeling analysis of a passive, residential rainwater harvesting program in an urbanized semiarid watershed. *Journal of Hydrology*, 508:204–253, 2014. ISSN 00221694. doi: 10.1016/j.jhydrol.2013.10.038.

[19] L. L. Willard, T. Wynn-Thompson, L. H. Krometis, T. P. Neher, and B. D. Badgley. Does It Pay to be Mature? Evaluation of Bioretention Cell Performance Seven Years Postconstruction. *Journal of Environmental Engineering*, 143(2013):04017041, 2017. ISSN 0733-9372. doi: 10.1061/(ASCE)EE.1943-7870.0001232.

[20] G Lindsey, L Roberts, and W Page. Inspection and maintenance of infiltration facilities. *Journal of Soil and Water Conservation*, 47(6):481–486, 1992.

[21] Yanling Li and Roger W. Babcock. Green roof hydrologic performance and modeling: a review. *Water Science and Technology*, 69(4):727–739, 2014. doi: 10.2166/wst.2013.770.

[22] J Mentens, D Raes, and M Hermy. Green roofs as a tool for solving the rainwater runoff prolem in the urbanized 21st century? *Landscape and Urban Planning*, 77: 221–226, 2005.

[23] Heather E. Golden and Nahal Hoghooghi. Green infrastructure and its catchment-scale effects: An emerging science. *Wiley Interdisciplinary Reviews: Water*, page e1254, 2017. ISSN 20491948. doi: 10.1002/wat2.1254.

[24] A R Martin, L M Ahiablame, and B A Engel. Modeling low impact development in two Chicago communities. *Environmental Science - Water Research & Technology*, 1 (6):855–864, 2015. ISSN 2053-1400. doi: 10.1039/c5ew00110b.

[25] William C. Lucas and David J. Sample. Reducing combined sewer overflows by using outlet controls for Green Stormwater Infrastructure: Case study in Richmond, Virginia. *Journal of Hydrology*, 520:473–488, 2015. ISSN 00221694. doi: 10.1016/j.jhydrol.2014.10.029.

[26] H Tavakol-Davani, S Burian, J Devkota, and D Apul. Performance and cost-based comparison of green and gray infrastructure to control combine sewer overflows. *Journal of Sustainable Water in the Built Environment*, 2(2), 2016.

[27] Hyunju Jeong, Osvaldo A. Broesicke, Bob Drew, Duo Li, and John C. Crittenden. Life cycle assessment of low impact development technologies combined with conventional centralized water systems for the City of Atlanta, Georgia. *Frontiers of Environmental Science and Engineering*, 10(6):1–13, 2016. ISSN 2095221X. doi: 10.1007/s11783-016-0851-0.

[28] Colin D. Bell, Sara K. McMillan, Sandra M. Clinton, and Anne J. Jefferson. Hydrologic response to stormwater control measures in urban watersheds. *Journal of Hydrology*, 541:1488–1500, 2016. ISSN 00221694. doi: 10.1016/j.jhydrol.2016.08.049.

[29] R A Brown, D Line, and W Hunt. Case Study LID Treatment Train : Pervious Concrete with Subsurface Storage in Series with Bioretention and Care with Seasonal High Water Tables. *Journal of Environmental Engineering*, 138(6):689–698, 2012. doi: 10.1061/(ASCE)EE.1943-7870.0000506.

[30] Robert A. Brown and Michael Borst. Nutrient infiltrate concentrations from three permeable pavement types. *Journal of Environmental Management*, 164:74–85, 2015. ISSN 10958630. doi: 10.1016/j.jenvman.2015.08.038.

[31] Jennifer Drake, Andrea Bradford, and Tim Van Seters. Stormwater quality of spring-summer-fall effluent from three partial-infiltration permeable pavement systems and conventional asphalt pavement. *Journal of Environmental Management*, 139:69–79, 2014. ISSN 10958630. doi: 10.1016/j.jenvman.2013.11.056.

[32] Chi-Hsu Hsieh, Allen P Davis, and Brian A Needelman. Bioretention Column Studies of Phosphorus Removal from Urban Stormwater Runoff. *Water Environment Research*, 79(2):177–184, 2007. ISSN 10614303. doi: 10.2175/106143006X111745.

[33] William F. Hunt, Allen P. Davis, and Robert G. Traver. Meeting Hydrologic and Water Quality Goals through Targeted Bioretention Design. *Journal of Environmental Engineering*, 138(6):698–707, 2012. ISSN 0733-9372. doi: 10.1061/(ASCE)EE.1943-7870.0000504.

[34] Marie Charlotte Leroy, Florence Portet-Koltalo, Marc Legras, Franck Lederf, Vincent Moncond'huy, Isabelle Polaert, and Stephane Marcotte. Performance of vegetated swales for improving road runoff quality in a moderate traffic urban area. *Science of the Total Environment*, 566-567:113–121, 2016. ISSN 18791026. doi: 10.1016/j.scitotenv.2016.05.027.

[35] A Roy-Poirier, P Champagne, and Y Filion. Bioretention processes for phosphorus pollution control. *Environmental Reviews*, 18:159–173, 2010. ISSN 1208-6053. doi: 10.1139/A10-006.

[36] J Baik, K Kwak, S Park, and Y Ryu. Effects of building roof greening on air quality in street canyons. *Atmospheric Environment*, 61:48–55, 2012.

[37] Corrie Clark, Peter Adriaens, and F Brian Talbot. Green roof valuation: a probabilistic economic analysis of environmental benefits. *Environmental science & technology*, 42(6):2155–61, 2008. ISSN 0013-936X. doi: 10.1021/es0706652.

[38] G Virk, A Jansz, A Mavrogianni, A Mylona, J Stocker, and M Davies. Microclimatic effects of green and cool roofs in London and their impacts on energy use for a typical office building. *Energy and Buildings*, 88:214–228, 2015.

[39] Reshmina William, Allison Goodwell, Meredith Richardson, Phong V V Le, Praveen Kumar, and Ashlynn S Stillwell. An environmental cost-benefit analysis of alternative green roofing strategies. *Ecological Engineering*, 95:1–9, 2016. ISSN 0925-8574. doi: 10.1016/j.ecoleng.2016.06.091.

[40] Fanhua Kong, Changfeng Sun, Fengfeng Liu, Haiwei Yin, Fei Jiang, Yingxia Pu, Gina Cavan, Cynthia Skelhorn, Ariane Middel, and Iryna Dronova. Energy saving potential of fragmented green spaces due to their temperature regulating ecosystem services in the summer. *Applied Energy*, 183:1428–1440, 2016. ISSN 03062619. doi: 10.1016/j.apenergy.2016.09.070.

[41] Erdem Cuce. Thermal regulation impact of green walls: An experimental and numerical investigation. *Applied Energy*, 2016. ISSN 03062619. doi: 10.1016/j.apenergy.2016.09.079.

[42] Ming Kuo. How might contact with nature promote human health? Promising mechanisms and a possible central pathway. *Frontiers in Psychology*, 6, 2015. doi: 10.3389/fpsyg.2015.01093.

[43] Andrea Taylor and Ming Kuo. Children with attention deficits concentrate better after walk in the park. *Journal of Attention Disorders*, 12(5):402–409, 2009.

[44] Ming Kuo. Parks and other green environments: Essential components of a healthy human habitat. Technical report, National Recreation and Park Association, 2010.

[45] Michelle C. Kondo, Sarah C. Low, Jason Henning, and Charles C. Branas. The Impact of Green Stormwater Infrastructure Installation on Surrounding Health and Safety. *American Journal of Public Health*, 105(3):e114–e121, 2015. ISSN 0090-0036. doi: 10.2105/AJPH.2014.302314.

[46] Mathieu Carrier, Philippe Apparicio, Yan Kestens, Anne-Marie Séguin, Hien Pham, Dan Crouse, Jack Siemiatycki, and Anne-Marie S Eguin. Application of a global environmental equity index in Montreal: Diagnostic and further implications. *Annals of the American Association of Geographers*, 1066(February 2017):1268–1285, 2016. ISSN 2469-4452. doi: 10.1080/24694452.2016.1197766.

[47] Brian C Chaffin, William D Shuster, Ahjond S Garmestani, Brooke Furio, Sandra L Albro, Mary Gardiner, Malisa Spring, and Olivia Green. A tale of two rain gardens: Barriers and bridges to adaptive management of urban stormwater in Cleveland, Ohio. *Journal of Environmental Management*, pages 1–11, 2016. doi: 10.1016/j.jenvman.2016.06.025.

[48] N Nylen and M Kiparsky. Accelerating cost-effective green stormwater infrastructure: learning from local implementation. *Center for Law, Energy, and the Environment*, 48, 2015.

[49] Frauke Hoss, Jordan Fischbach, and Edmundo Molina-Perez. Effectiveness of Best Management Practices for Stormwater Treatment as a Function of Runoff Volume. *Journal of Water Resources Planning and Management*, 142(11):05016009, 2016. ISSN 0733-9496. doi: 10.1061/(ASCE)WR.1943-5452.0000684.

[50] Kyle Eckart, Zach McPhee, and Tirupati Bolisetti. Performance and implementation of low impact development – A review. *Science of the Total Environment*, 607-608: 413–432, 2017. ISSN 18791026. doi: 10.1016/j.scitotenv.2017.06.254.

[51] Theodore C Lim and Claire Welty. Effects of spatial configuration of imperviousness and green infrastructure networks on hydrologic response in a residential sewershed. *Water Resources Research*, 53:1–21, 2017. ISSN 00431397. doi: 10.1002/2017WR020631.

[52] Xiaoling Zhang and Huan Li. Urban resilience and urban sustainability: What we know and what do not know? *Cities*, 72(July 2017):141–148, 2018. ISSN 02642751. doi: 10.1016/j.cities.2017.08.009. URL `https://doi.org/10.1016/j.cities.2017.08.009`.

[53] James D Miller and Michael Hutchins. The impacts of urbanisation and climate change on urban flooding and urban water quality: A review of the evidence concerning the United Kingdom. *Journal of Hydrology: Regional Studies*, 12:345–362, 2017. ISSN 2214-5818. doi: 10.1016/j.ejrh.2017.06.006.

[54] Joseph H.A. Guillaume, Casey Helgeson, Sondoss Elsawah, Anthony J. Jakeman, and Matti Kummu. Toward best practice framing of uncertainty in scientific publications: A review of Water Resources Research abstracts. *Water Resources Research*, 2017. ISSN 00431397. doi: 10.1002/2017WR020609.

[55] J. Mullen, K Calhoun, and G Colson. Preferences for policy attributed and willingness to pay for water quality improvement under uncertainty. *Water Resources Research*, 53:2627–2642, 2017. ISSN 00431397. doi: 10.1002/2013WR014979.Reply.

[56] James DeLisle, Terry Grissom, and Lovisa Hogberg. Sustainable real estate: An empirical study of the behavioral response of developers and investors to the LEED rating system. *Journal of Property Investment and Finance*, 31(1):10–40, 2013. doi: http://dx.doi.org/10.1108/17506200710779521.

[57] S. J. Livesley, G. M. McPherson, and C. Calfapietra. The Urban Forest and Ecosystem Services: Impacts on Urban Water, Heat, and Pollution Cycles at the Tree, Street, and City Scale. *Journal of Environment Quality*, 45(1):119, 2016. ISSN 0047-2425. doi: 10.2134/jeq2015.11.0567.

[58] G Jia, A Tabandeh, and P Gardoni. Life cycle analysis of engineering systems: Modeling deterioration, instantaneous reliability, and resilience. In P Gardoni, editor, *Risk and reliability analysis: Theory and applications*, chapter 6.1, pages 465–494. Springer International Publishing, 2017. doi: 10.1007/978-3-319-52425-2.

[59] Paolo Gardoni, Armen Der Kiureghian, and Khalid M. Mosalam. Probabilistic Capacity Models and Fragility Estimates for Reinforced Concrete Columns based on Experimental Observations. *Journal of Engineering Mechanics*, 128(10):1024–1038, 2002. ISSN 0733-9399. doi: 10.1061/(ASCE)0733-9399(2002)128:10(1024).

[60] Paolo Gardoni, Khalid M. Mosalam, and Armen Der Kiureghian. Probabilistic seismic demand models and fragility estimates for RC bridges. *Journal of Earthquake Engineering*, 7(1):79–106, 2003.

[61] P Gardoni, editor. *Risk and reliability analysis: Theory and applications*. Springer, 2017.

[62] Paolo Gardoni and J LaFave, editors. *Multi-hazard approaches to civil infrastructure engineering*. Springer, 2016. ISBN 978-3-319-29713-2.

[63] D Stewart. Urban drainage systems. In P Sayers, editor, *Flood risk: Planning, design and managment of flood defense infrastructure*, chapter 7, pages 139–171. ICE Publishing, London, 2012.

[64] P Sayers, J Flickweert, and A Kortenhaus. Supporting flood risk management through better infrastructure design and management. In P Sayers, editor, *Flood risk: Planning, design and managment of flood defense infrastructure*, chapter 4, pages 73–101. ICE Publishing, London, 2012.

[65] O Ditlevsen and H Madsen. *Structural reliability methods*. Wiley, 2.3 edition, 1996. ISBN 0-471-96086-1.

[66] T Haukaas and Armen Der Kiureghian. Finite Element Reliability Using MATLAB (FERUM), 1999. URL `http://projects.ce.berkeley.edu/ferum/`.

[67] R. Kumar, D. Cline, and Paolo Gardoni. A stochastic framework to model deterioration in engineering systems. *Structural Safety*, 53:36–43, 2015.

[68] R Kumar and P Gardoni. Modeling structual degradation of RC bridge columns subjected to earthquakes and their fragility estimates. *Journal of Structural Engineering*, 138(1):42–51, 2012.

[69] M Pandey and J. van der Weide. Stochastic renewal process models for estimation of damage cost over the life-cycle of a structure. *Structural Safety*, 67:27–38, 2017.

[70] K. Canter, D Kennedy, D Montgomery, J Keats, and W Carlyle. Screening stochastic Life Cycle assessment inventory models. *International Journal of Life Cycle Assessment*, 7(18), 2000.

[71] M Naizi, C Nietch, and M Maghrebi. Stormwater management model: Performance review and gap analysis. *Journal of Sustainable Water in the Built Environment*, 3 (2), 2017.

[72] Franco Montalto, Christopher Behr, Katherine Alfredo, Max Wolf, Matvey Arye, and Mary Walsh. Rapid assessment of the cost-effectiveness of low impact development for CSO control. *Landscape and Urban Planning*, 82(3):117–131, 2007. ISSN 01692046. doi: 10.1016/j.landurbplan.2007.02.004.

[73] D.N. Moriasi, J.G. Arnold, M.W. Van Liew, R.L. Binger, R.D. Harmel, and T.L. Veith. Model evaluation guidelines for systematic quantification of accuracy in watershed simulations. In *Transactions of the ASABE*, volume 50, pages 885–900, 2007. ISBN 0001-2351. doi: 10.13031/2013.23153.

[74] International Institute for Land Reclamation and Improvement (ILRI). Drainage research in farmers' fields: analysis of data. Technical report, 2002. URL `www.waterlog.info/pdf/analysis.pdf`.

[75] NRCS. Web Soil Survey, 2017. URL `https://websoilsurvey.sc.egov.usda.gov/App/WebSoilSurvey.aspx`.

[76] B Das. *Advanced Soil Mechanics*. Taylor and Francis, New York, NY, 2008.

[77] Z Yang. *Study of minimum void ratio for soils with a range of grain-size distributions*. PhD thesis, University of Massachusetts at Amhurst, 2013.

[78] Stevens Water Monitoring System. Hydro Probe Soil Sensor: User manual. Technical report, 2015. URL `http://stevenswater.com/resources/documentation/hydraprobe/HydraProbe_Manual_92915_Jan_2015.pdf`.

[79] Sébastien Le Coustumer, Tim D. Fletcher, Ana Deletic, Sylvie Barraud, and Justin F. Lewis. Hydraulic performance of biofilter systems for stormwater management: Influences of design and operation. *Journal of Hydrology*, 376(1-2): 16–23, 2009. ISSN 00221694. doi: 10.1016/j.jhydrol.2009.07.012.

[80] Sébastien Le Coustumer, Tim D. Fletcher, Ana Deletic, Sylvie Barraud, and Peter Poelsma. The influence of design parameters on clogging of stormwater biofilters: A large-scale column study. *Water Research*, 46(20):6743–6752, 2012. ISSN 00431354. doi: 10.1016/j.watres.2012.01.026.

[81] B Hatt, T Fletcher, and A Deletic. Hydrologic and pollutant removal performance of stormwater bioinfiltration systems at the field scale. *Journal of Hydrology*, 365(3): 310–321, 2009.

[82] G Viviani and M Iovino. Wastewater reuse effects on soil hydraulic conductivity. *Journal of Irrigation and Drainage Engineering*, 130(6):476–484, 2004. ISSN 07339437. doi: 10.1061/(ASCE)0733-9437(2004)130:6(476).

[83] H Li and A Davis. Urban Particle Capture in Bioretention Media. II: Theory and Model Development. *Journal of Environmental Engineering*, 134(6):419–432, 2008. ISSN 0733-9372. doi: 10.1061/(ASCE)0733-9372(2008)134:6(419).

[84] M Fuerhacker, T Haile, B Monai, and A Mentler. Performance of a filtration system with filter media for parking lot runoff treatment. *Desalination*, 275:118–125, 2011.

[85] Wright Water Engineers and Geosyntec Consultants. International Stormwater Best Management Practices (BMP) Database: User's Guide for BMP Data Entry Spreadsheets. Technical Report November, International Stormwater BMP Database, Denver, CO, 2016.

[86] Minnesota Pollution Control Agency. Pre-treatment considerations for stormwater infiltration, 2015. URL `https://stormwater.pca.state.mn.us/index.php?title=Pre-treatment_considerations_for_stormwater_infiltration`.

[87] University of New Hampshire Stormwater Center. Regular inspection and maintenance guides for bioretention system/tree filters, 2011. URL `https://www.unh.edu/unhsc/sites/unh.edu.unhsc/files/UNHSCBiofilterMaintenanceGuidanceandChecklist1-11_0.pdf`.

[88] Andrew S. Mehring and Lisa A. Levin. Potential roles of soil fauna in improving the efficiency of rain gardens used as natural stormwater treatment systems. *Journal of Applied Ecology*, 52(6):1445–1454, 2015. ISSN 13652664. doi: 10.1111/1365-2664.12525.

[89] Brad J. Wardynski and William F. Hunt. Are Bioretention Cells Being Installed Per Design Standards in North Carolina? A Field Study. *Journal of Environmental Engineering*, 138(12):1210–1217, 2012. ISSN 0733-9372. doi: 10.1061/(ASCE)EE.1943-7870.0000575.

[90] J Lee, K Bang, L Ketchum, J Choe, and M Yu. First flush analysis of urban storm runoff. *Science of The Total Environment*, 293:163–175, 2002.

[91] Seattle Public Utilites. Green stormwater operations and maintenance manual. Technical report, Seattle Public Utilities, Seattle, WA, 2009. URL `http://www.seattle.gov/util/cs/groups/public/@spu/@usm/documents/webcontent/spu02_020023.pdf`.

[92] University of Rhode Island. Professional rain garden maintenance, 2018. URL `https://web.uri.edu/riss/files/Professional_Maintenance.pdf`.

[93] J Houle. A Comparison of Maintenance Cost, Labor Demands, and System Performance for LID and Conventional Stormwater Management. In *Proceedings of the EWRI conference on Operations and Maintenance of Stormwater Control Measures*, Denver, CO, 2017. ASCE.

[94] William Lord and S Waickowski. Tasks and Costs Associated With SCM Inspection and Maintenance in North Carolina. In *Proceedings of the EWRI conference on Operations and Maintenance of Stormwater Control Measures*, Denver,CO, 2017. ASCE.

[95] Blue Water Baltimore. Routine maintenance for rain gardens, 2018. URL `https://www.bluewaterbaltimore.org/wp-content/uploads/RainGardenRoutineMaintenance1.pdf`.

[96] Rutgers. Rain garden inspection and maintenance, 2018. URL `http://water.rutgers.edu/Rain_Gardens/RGWebsite/CertificationProgram/RGS_RGST_RGInspMaintenance.pdf`.

[97] Luca Locatelli, Ole Mark, Peter Steen, Karsten Arnbjerg-Nielsen, Marina Bergen, and Philip John. Modelling of green roof hydrological performance for urban drainage applications. *Journal of Hydrology*, 519:3237–3248, 2014. ISSN 0022-1694. doi: 10.1016/j.jhydrol.2014.10.030.

[98] D Schlea, J Martin, A Ward, L Brown, and S Suter. Performance and water table responses of retrofit rain gardens. *Journal of Hydrologic Engineering*, 19(8), 2014. ISSN 1084-0699. doi: 10.1061/(ASCE)HE.1943-5584.0000797.

[99] K. Brander, K Owen, and K Potter. Modeled impacts of development type on runoff volumet and infiltration performance. *Journal of the American Water Resources Association*, 40(4):961–969, 2004.

[100] Jennifer A P Drake, A Bradford, and T Seters. Stormwater quality of spring-summer-fall effluent from three partial-infiltration permeable pavement systems and conventional asphalt pavement. *Journal of Environmental Management*, 139:69–79, 2014.

[101] Brian J Pearson, Richard C Beeson Jr, Amy Shober, Carrie Reinhart-adams, Gary Knox, and Michael Olexa. Influence of soil , precipitation , and antecedent moisture on stormwater runoff and leachate from runoff boxes containing simulated urban landscape soils. *Florida Scientist*, 77(3):109–125, 2014.

[102] Bridget M Wadzuk, Conor Lewellyn, Ryan Lee, and Robert G Traver. Green Infrastructure Recovery : Analysis of the Influence of Back-to-Back Rainfall Events. *Journal of Sustainable Water in the Built Environment*, 3(1):1–7, 2017. doi: 10.1061/JSWBAY.0000819.

[103] W. Selbig and N Balster. Evaluation of turf-grass and prairie-vegetated rain gardens in a clay and sand soil, Madison, Wisconsion, Water Years 2004-2008. Technical report, U.S. Geological Survey, Reston, VA, 2010.

[104] University of Connecticut. Rain Gardens: Siting and Sizing, 2018. URL `http://nemo.uconn.edu/raingardens/sizing.htm`.

[105] A Dietrich, R Yarlagadda, and C Grudu. Estimating the potential benefits of green stormwater infrastructure on developed sites using hydrological model simulation. *Environmental Progress and Sustainable Engineering*, 2016.

[106] S Pathiraja, S Westra, and A Sharma. Why continuous simulation? The role of antecedent moisture in design flood estimation. *Water Resources Research*, 48(9): W06534, 2012. doi: https://doi.org/10.1029/2011WR010997.

[107] Bridget M. Wadzuk, Conor Lewellyn, Ryan S Lee, and Robert G. Traver. Closure to "Green infrastructure recovery: Analysis of the influence of back-to-back rainfall events" by Bridget M. Wadzuk, Conor Lewellyn, Ryan Lee, and Robert G. Traver. *Journal of Sustainable Water in the Built Environment*, 4(3):07018002–1, 2018. doi: https://doi.org/10.1061/JSWBAY.0000819.

[108] M Valdelfener, E Sibeaud, L Bacot, G Besnard, Y Rozier, S Barraud, and P Marmonier. Development of mosquitoes (Diptera, Culicidae) in sustainable urban drainage systems: Example of the metropole of Lyon. *Techniques-Sciences-Methodes*, 4:55–70, 2018.

[109] Gwendolyn Wong and C Jim. Abundance of urban male mosquitoes by green infrastructure types: implications for landscape design and vector management. *Landscape Ecology*, 33(3):475–489, 2018.

[110] G Wong and C Jim. Do vegetated rooftops attract more mosquitoes? Monitoring disease vecto abundance on urban green roofs. *Science of the Total Environment*, 573:222–232, 2016. doi: 10.1016/j.scitotenv.2016.08.102.

[111] P Avellaneda, A Jefferson, J Grieser, and S Bush. Simulation of the cumulative hydrological response to green infrastructure. *Water Resources Research*, 53: 3087–3101, 2017. ISSN 00431397. doi: 10.1002/2016WR019836.

[112] Rui Guo and Yiping Guo. Discussion of "Green infrastructure recovery: Analysis of the influence of back-to-back rainfall events" by Bridget M. Wadzuk, Conor Lewellyn, Ryan Less, and Robet G. Traver. *Journal of Sustainable Water in the Built Environment*, 4(3):07018001, 2018. doi: 10.1061/JSWBAY.0000819.

[113] Cory Gallo, Austin Moore, and Joe Wywrot. Comparing the adaptability of infiltration based BMPs to various U.S. regions. *Landscape and Urban Planning*, 106 (4):326–335, 2012. ISSN 01692046. doi: 10.1016/j.landurbplan.2012.04.004.

[114] Dustin L. Herrmann, William D. Shuster, and Ahjond S Garmestani. Vacant urban lot soils and their potential to support ecosystem services. *Plant & Soil*, 413(1/2): 45–57, 2017.

[115] Qizheng Mao, Ganlin Huang, Alexander Buyantuev, Jianguo Wu, Shanghuang Luo, and Keming Ma. Spatial heterogeneity of urban soils: the case of the Beijing metropolitan region, China. *Ecological Processes*, 3(23), 2014. doi: 10.1186/s13717-014-0023-8.

[116] A Greinart. The heterogeneity of urban soils in the light of their properties. *Journal of Soils and Sediments*, 15(8):1725–1737, 2015.

[117] M McGuire, A Phillips, and D Grimley. Illinois-Indiana Sea Grant (IISG) Research Project Annual Report fo 2018 #NA18OAR4170082. Technical report, University of Illinois at Urbana-Champaign, Urbana, IL, 2019.

[118] Maria Garcia-Serrana, John S. Gulliver, and John L. Nieber. Calculator to estimate annual infiltration performance of roadside swales. *Journal of Hydrologic Engineering*, 23(6):1–10, 2018. ISSN 1084-0699. doi: 10.1061/(asce)he.1943-5584.0001650.

[119] Dustin L. Herrmann, Laura A. Schifman, and William D. Shuster. Widespread loss of intermediate soil horizons in urban landscapes. *Proceedings of the National Academy of Sciences*, 115(26):6751–6755, 2018. ISSN 0027-8424. doi: 10.1073/pnas.1800305115.

[120] R Brown and W Hunt. Impacts of Construction Activity on Bioretention Performance. *Journal of Hydrologic Engineering*, 15(6):386–394, 2010. ISSN 1084-0699. doi: 10.1061/(ASCE)HE.1943-5584.0000165.

[121] City of Madison Engineering. 1,000 rain gardens, 2018. URL `https://www.cityofmadison.com/engineering/stormwater/raingardens/1000raingardens.cfm`.

[122] Philadelphia Water Department. Green City, Clean Waters, 2018.

[123] City of Chicago. City of Chicago Green stormwater infrastructure strategy. Technical report, Chicago, IL, 2006. URL http://www.cityofchicago.org/dam/city/depts/dps/ContractAdministration/StandardFormsAgreements/CDOT_FederallyFundedNonFTA_04202005.pdf.

[124] Kun Zhang and Ting Fong May Chui. Linking hydrological and bioecological benefits of green infrastructures across spatial scales – A literature review. *Science of the Total Environment*, 646:1219–1231, 2019. ISSN 18791026. doi: 10.1016/j.scitotenv.2018.07.355.

[125] Moira Zellner, Dean Massey, Emily Minor, and Miquel Gonzalez-Meler. Exploring the effects of green infrastructure placement on neighborhood-level flooding via spatially explicit simulations. *Computers, Environment and Urban Systems*, 59: 116–128, 2016. ISSN 01989715. doi: 10.1016/j.compenvurbsys.2016.04.008.

[126] Laurent M Ahiablame, Bernard A Engel, and Indrajeet Chaubey. Effectiveness of low impact development practices in two urbanized watersheds : Retro fitting with rain barrel / cistern and porous pavement. *Journal of Environmental Management*, 119:151–161, 2013.

[127] Jessica A. Hekl and Randel L. Dymond. Runoff Impacts and LID Techniques for Mansionization-Based Stormwater Effects in Fairfax County, Virginia. *Journal of Sustainable Water in the Built Environment*, 2(4):05016001, 2016. ISSN 2379-6111. doi: 10.1061/JSWBAY.0000815.

[128] Isam Alyaseri, Jianpeng Zhou, Susan M. Morgan, and Andrew Bartlett. Initial impacts of rain gardens' application on water quality and quantity in combined sewer: field-scale experiment. *Frontiers of Environmental Science & Engineering*, 11 (4):19, 2017. ISSN 2095-2201. doi: 10.1007/s11783-017-0988-5.

[129] Maria Matos Silva and João Pedro Costa. Urban Flood Adaptation through Public Space Retrofits: The Case of Lisbon (Portugal). *Sustainability*, 9(5):816, 2017. ISSN 2071-1050. doi: 10.3390/su9050816.

[130] Laurene Autixier, Alain Mailhot, Samuel Bolduc, Anne Sophie Madoux-Humery, Martine Galarneau, Miche'le Prevost, and Sarah Dorner. Evaluating rain gardens as a method to reduce the impact of sewer overflows in sources of drinking water. *Science of the Total Environment*, 499:238–247, 2014. ISSN 18791026. doi: 10.1016/j.scitotenv.2014.08.030.

[131] Chunlu Liu, Yan Li, and Jun Li. Geographic information system-based assessment of mitigating flash-flood disaster from green roof systems. *Computers, Environment and Urban Systems*, 64:321–331, 2017. ISSN 01989715. doi: 10.1016/j.compenvurbsys.2017.04.008.

[132] Arturo Casal-Campos, Guangtao Fu, David Butler, and Andrew Moore. An Integrated Environmental Assessment of Green and Gray Infrastructure Strategies for Robust Decision Making. *Environmental Science and Technology*, 49(14): 8307–8314, 2015. ISSN 15205851. doi: 10.1021/es506144f.

[133] Congying Li, Tim D Fletcher, Hugh P Duncan, and Matthew J Burns. Can stormwater control measures restore altered urban flow regimes at the catchment scale? *Journal of Hydrology*, pages –, 2017. ISSN 0022-1694. doi: 10.1016/j.jhydrol.2017.03.037.

[134] Baltimore Ecosystem Study. The Baltimore Ecosystem Study Virtual Tour: Gwynn's Run above Gwynn's Fall, 2009. URL `https://beslter.org/virtual_tour/GFuGR.html`.

[135] S Dance. Halfway to cleanup deadline, Chesapeake Bay hits goals for phosphorus, sediment, but misses nitrogen target, July 2018.

[136] Mathew Fitzsimmons. *Rediscovering Nature - Daylighting an Urban Stream (Gwynns Run, Baltimore, MD)*. PhD thesis, 2005.

[137] Baltimore City Public Health. 2011 Neighborhood Health Profile: Southwest Baltimore. Technical report, Baltimore, 2011.

[138] Pravara Thanapura, Dennis L Helder, Suzette Burckhard, Eric Warmath, Mary O Neill, and Dwight Galster. Mapping Urban Land Cover Using QuickBird NDVI and GIS Spatial Modeling for Runoff Coefficient Determination. *Photogrammetric Engineering and Remote Sensing*, 73(1):57–65, 2007.

[139] Illinois Department of Natural Resources. Rain Garden Requirements and Plant Lists, 2018. URL `https://www.dnr.illinois.gov/education/pages/plantlistraingarden.aspx`.

[140] Laura Garcia-Cuerva, Emily Zechman Berglund, and Louie Rivers. An integrated approach to place Green Infrastructure strategies in marginalized communities and evaluate stormwater mitigation. *Journal of Hydrology*, 559:648–660, 2018. ISSN 00221694. doi: 10.1016/j.jhydrol.2018.02.066.

[141] Sean A. Woznicki, Kelly L. Hondula, and S. Taylor Jarnagin. Effectiveness of landscape-based green infrastructure for stormwater management in suburban catchments. *Hydrological Processes*, 32(15):2346–2361, 2018. ISSN 10991085. doi: 10.1002/hyp.13144.

[142] Yang Yang and Ting Fong May Chui. Integrated hydro-environmental impact assessment and alternative selection of low impact development practices in small urban catchments. *Journal of Environmental Management*, 223:324–337, 2018. ISSN 10958630. doi: 10.1016/j.jenvman.2018.06.021. URL `https://doi.org/10.1016/j.jenvman.2018.06.021`.

[143] Wen Liu, Weiping Chen, and Chi Peng. Assessing the effectiveness of green infrastructures on urban flooding reduction: A community scale study. *Ecological Modelling*, 291:6–14, 2014. ISSN 03043800. doi: 10.1016/j.ecolmodel.2014.07.012.

[144] David A. Newburn and Anna Alberini. Household response to environmental incentives for rain garden adoption. *Water Resources Research*, 52(2):1345–1357, 2016. ISSN 19447973. doi: 10.1002/2015WR018063.

[145] Joshua F. Cerra. Emerging strategies for voluntary urban ecological stewardship on private property. *Landscape and Urban Planning*, 157:586–597, 2017. ISSN 01692046. doi: 10.1016/j.landurbplan.2016.06.016. URL `http://dx.doi.org/10.1016/j.landurbplan.2016.06.016`.

[146] Sébastien Foudi, Joseph V. Spadaro, Aline Chiabai, Josué M. Polanco-Martínez, and Marc B. Neumann. The climatic dependencies of urban ecosystem services from green roofs: Threshold effects and non-linearity. *Ecosystem Services*, 24:223–233, 2017. ISSN 22120416. doi: 10.1016/j.ecoser.2017.03.004.

[147] C Malina. Up on the roof: Implementing local government policies to promote and achieve the environmental, social and economic benefits of green roof technology. *Geogretown International Law Review*, 23(3):437–463, 2011. ISSN 0717-6163. doi: 10.1007/s13398-014-0173-7.2.

[148] USDE. Green roof improvement fund (Chicago, IL 2006), 2012. URL `https://www.energycodes.gov/resource-center/policy/green-roof-improvement-fund-chicago-il-2006`.

[149] B Sonne. Managing stormwater by sustianable measures: Preventing neighborhood flooding and green infrastructure in New Orleans. *Tulane Environmental Law Journal*, 27:323–350, 2014.

[150] Roger Myerson. *Game theory: Analysis of conflict*. Harvard University Press, Cambridge, MA, 1st edition, 1991. ISBN 0-674-3411-3.

[151] Joaquin Sanchez-Soriano. An overview on game theory applications to enginering. *International Game Theory Review*, 15(3):1–19, 2013. doi: 10.1142/S0219198913400197.

[152] K. Madani. Game theory and water resources. *Journal of Hydrology*, 381:225–238, 2010.

[153] M. Sivapalan, M. Konar, V. Srinivasan, A. Chhatre, A. Wutich, C. Scott, J. Wescoat, and I. Rodriguez-Iturbe. Socio-hydrology: Use-inspired water sustainability sceince for the Antrhopocene. *Earth's Future*, 2(4):225–230, 2014. doi: 10.1002/2013EF000164.

[154] E Eleftheriadou and Y Mylopoulous. Game theorectical approach to conflict resolution in transboundary water resources management. *Journal of Water Resources Planning and Management*, 134(5):466, 2009.

[155] S. Schreider, P. Zeephongsekal, and M. Fernandes. A game theoretic approach to water quality management. In L. Oxley and D. Kulasiri, editors, *MODSIM 2007 International Congress on Modelling and Simulation*, pages 2312–2318. Modelling and Simulation Society of Australia and New Zealand, 2007.

[156] K Yeo and Y Jung. Cost allocation of river water quality management based on the seperable cost remaining method (SCRB) method. *Journal of Environmental Planning and Management*, 59(6):1040–1053, 2016.

[157] A Bhaduri and J Liebe. Cooperation in transboundary water sharing with issue linkage: Game-theoretical case study in the Volta Basin. *Journal of Water Resources Planning and Management*, 139(3):235–245, 2013.

[158] M Homayounfar, M Zomorodian, C Martinez, and S Lai. Two month continous dynamic model based on Nash Bargaining Theory for conflict resolution in reservoir system. *PLoS ONE*, 10(12):e0143198, 2015.

[159] G. Hardin. The tragedy of the commons. *Science*, 162:1243–1248, 1968.

[160] R. Teasley and D. McKinney. Calculating the benefits of transboundary river basin cooperation: Syr Darya Basin. *Journal of Water Resources Planning and Management*, 137(6):481–490, 2011.

[161] Georg B Frisvold and Margriet F Caswell. Transboundary Water Management: Game Theoretic Lessons for Projects on the US-Mexico Border. *Agricultural Economics*, 24:101–111, 2000. ISSN 0169-5150.

[162] L. Fernandez. Wastewater pollution abatement across an international border. *Environment and Development Economics*, 14(1):67–88, 2008.

[163] Guang Ming Shi, Jin Nan Wang, Bing Zhang, Zhe Zhang, and Yong Liang Zhang. Pollution control costs of a transboundary river basin: Empirical tests of the fairness and stability of cost allocation mechanisms using game theory. *Journal of Environmental Management*, 177:145–152, 2016. ISSN 10958630. doi: 10.1016/j.jenvman.2016.04.015.

[164] T Schueler. Controlling urban runoff: a practical manual for planning and designing urban BMPs. Technical report, Metropolitan Washington Council of Governments, Washington, DC, 1987.

[165] M Leisenring, J. Clary, and P. Hobson. International stormwater best management practices (BMP) database pollutant category statistical summary report. Technical report, International Stormwater BMP Database, 2014. URL `http://www.bmpdatabase.org/Docs/2014WaterQualityAnalysisAddendum/BMPDatabaseCategorical_StatisticalSummaryReport_December2014.pdf`.

[166] T Schueler and H Holland. Irreducible Pollutant Concentrations Discharged From Stormwater Practices. *Watershed Protection Techniques*, 2(2):377–380, 2000.

[167] CASQA. California stormwater BMP handook: Bioretention (TC-32). Technical report, 2003. URL https://www.casqa.org/sites/default/files/BMPHandbooks/tc-32_from_newdevelopmentredevelopment_handbook.pdf.

[168] A Narayanan and R Pitt. *Costs of urban stormwater control practices*. PhD thesis, University of Alabama, Tuscaloosa, AL, 2006.

[169] City of Austin Urban Design Divison. EnVision Tomorrow Green Infrastructure App. Technical report, City of Austin, 2014.

[170] City of Baltimore. City of Baltimore Geographic Information System data, 2017.

[171] L. Shapley. Cores of convex games. *International Journal of Game Theory*, 1(1): 11–26, 1971.

[172] Casey Furlong, Kein Gan, and Saman De Silva. Governance of Integrated Urban Water Management in Melbourne, Australia. *Utilities Policy*, 2002:1–11, 2016. ISSN 0957-1787. doi: http://dx.doi.org/10.1016/j.jup.2016.04.008.

[173] J. Gabe, S. Trowsdale, and R. Vale. Achieving integrated urban water management: Planning top-down or bottom-up? *Water Science and Technology*, 59(10):1999–2008, 2009. ISSN 02731223. doi: 10.2166/wst.2009.196.

[174] USEPA. Green infrastructure case studies: Municipal policies for managing stormwater with green infrastructure. Technical report, 2010. URL http://www.sustainablecitiesinstitute.org/Documents/SCI/Report_Guide/Guide_EPA_GICaseStudiesReduced4.pdf.

[175] By John Whitler and Jennifer Warner. Integrated Urban Water Management for Planners. *PAS memo*, (October):13, 2014.

[176] Heather E Wright Wendel, Joni A. Downs, and James R. Mihelcic. Assessing equitable access to urban green space: The role of engineered water infrastructure. *Environmental Science and Technology*, 45(16):6728–6734, 2011. ISSN 0013936X. doi: 10.1021/es103949f.

[177] John Nash. Non-cooperative games. *Annals of Mathematics*, 54(2):286–295, 1951.

[178] Texas A&M. Groundwater conservation districts, 2014. URL http://texaswater.tamu.edu/groundwater/groundwater-conservation-districts.html.

[179] V Kelly Turner and Dorothy C Ibes. The Impact of Homeowners Associations on Residential Water Demand Management in Phoenix , Arizona. *Urban Geography*, 32 (8):1167–1188, 2011. doi: 10.2747/0272-3638.32.8.1167.

[180] Cory Rayburn. Implementating green infrastructure: Atlanta's post-development stormwater management ordinance. Technical report, City of Atlanta, Office of Watershed Protection, Atlanta, GA, 2013. URL `http://www.atlantawatershed.org/greeninfrastructure/post-development-handout-03-13-13/`.

[181] D McKenzie-Mohr. *Fostering Sustainable Behavior: Community-based social marketing*. McKenzie-Mohr & Associates, Inc, 2010. URL `http://www.cbsm.com/pages/guide/preface/`.

[182] R Katzev and A Pardini. The comparative effectiveness of reward and commitment approaches in motivating community recycling. *Journal of Environmental Systems*, 17(2):93–114, 1987.

[183] D Allen, D Sprenkel, and P. Vitale. Reactance theory and alcohol consumption laws: Further confirmation among collegiate alcohol consumers. *Journal of Studies on Alcohol*, 50(1):34–40, 1994.

[184] R Gordon and S Minor. Attitudes towards a change in legal drinking age: Reactance versus compliance. *Journal of College Student Development*, 33(2):171–176, 1992.

[185] A Wit and H Wilke. The presentation of rewards and punishments in a simulated social dilemma. *Social Behaviour*, 5(4):231–245, 1990.

[186] Dan Pink. *Drive: The surprising truth about what motivates us*. Riverhead Books, New York, NY, 2011. ISBN 1594484805.

[187] R Ryan and E Deci. Self-determination theory and the facilitation of intrinsic motivation, social development, and well-being. *American Psychologist*, 55:68–78, 2000.

[188] S Greybar, D Antonuccio, L Boutilier, and D Varble. Pscyhological reactance as a factor affecting patient compliance to physician advice. *Scandinavian Journal of Behaviour Theory*, 18(1):43–51, 1989.

[189] D Nowlis, E Wortz, and H Watters. Tektite II Habitability Research Program. 1972.

[190] A Stukas, M Snyder, and E Clary. The effects of mandatory volunteerism on intentions to volunteer. *Psychological Science*, 10(1):59–63, 1999.

[191] N Schwarz, M Kumpf, and W Bussman. Resistance to persuasion as a consequence of influence attempts in advertising and non-advertising communications. *Psychology: A Quaterly Journal of Human Behavior*, 22(2):72–76, 1986.

[192] R Cialdini and M Trost. Social Influence: Social Norms, Conformity and Compliance. In D Gilbert, S Fiske, and G Lindzey, editors, *The Handbook of Social Psychology*, pages 151–192. McGraw-Hill, 4th edition, 1998.

[193] Tom Chatfield. 7 ways games reward the brain. URL https://www.ted.com/talks/tom_chatfield_7_ways_games_reward_the_brain.

[194] M Ro, M Brauer, K Kuntz, R Shukla, and I Bensch. Making Cool Choices for sustainability: Testing the effectiveness of a game-based approach to promoting pro-environmental behaviors. *Journal of Environmental Psychology*, 53:20–30, 2017.

[195] Jonathan van't Riet, J. Sijtsema Siet, Hans Dagevos, and Gert-Jan De Bruijn. The importance of habits in eating behaviour. An overview and recommendations for future research. *Appetite*, 57:585–596, 2011.

[196] Icek Ajzen. A Comparison of the Theory of Planned Behavior and the Theory of Reasoned Action. *Personality and Social Psychology Bulletin*, 18:3–9, 1992.

[197] Lee Breckenridge. Green infrastructure in cities: Expanding mandates under federal law, 2016. URL https://www.americanbar.org/groups/environment_energy_resources/publications/trends/2013-14/july-august-2014/green_infrastructure_cities_expanding_mandates_under_federal_law/g.

[198] Les Robinson. A summary of diffusion of innovation. In *Changeology: How to Enable Groups, Communities and Societies to Do Things They've Never Done Before*. UIT Cambridge, Ltd, 2009.

[199] A Reese. Developing Technical Policy with Non-Technical People. In *International Low Impact Development Conference*, Nashville, TN, 2018. ASCE.

[200] Andy Szatko and Steve Rodie. Have a Thick Skin, it Pays Off: The Acceptance of Green Infrastructure by the Community. In *International Low Impact Development Conference*, Nashville, TN, 2018. ASCE.

[201] E Wentz, S Rode, X Li, E Tellman, and B Turner II. Impact of homeowner association (HOA) landscaping guidelines on residential water use. *Water Resources Research*, 52:3373–3386, 2016. doi: 10.1002/2015WR018238.Received.

[202] S Cuff. What drought? Blackhawk orders homeowners to green up, April 2016.

[203] WEF. Five types of green infrastructure incentive programs, 2013. URL http://stormwater.wef.org/2013/01/five-types-of-green-infrastructure-incentive-programs/.

[204] J Nassauer. Care and stewardship: From home to planet. *Landscape and Urban Planning*, 100:321–333, 2011.

[205] A Trinkaus. If LID is so easy to implement, how come we keep getting it wrong? In *International Low Impact Development Conference*, Nashville, TN, 2018. ASCE.

[206] R Percival, C Schroeder, A Miller, and J Leape. *Environmental Regulation: Law, Science, and Policy*. Wolters Kluwer Law & Business, Frederick, MD, 7th edition, 2013. ISBN 9781454822288.

[207] E Witte. Nonpoint source pollution control. In M Ryan, editor, *The Clean Water Act Handbook*, chapter 10. ABA Publishing, 4th edition, 2018. ISBN 9781634258586.

[208] R Hill and S Horowitz. Wet Weather Regulations: Control of Stormwater and Discharges from Concentrated Animal Feeding Operations and Other Facilities. In M Ryan, editor, *The Clean Water Act Handbook*, chapter 9. ABA Publishing, 4th edition, 2018.

[209] USEPA. National Nonpoint Source Program: A catalyste for water quality improvements. 2016.

[210] B Grumbles. Establishing TMDL "Daily" Loads in Light of the Decision by the U.S . Court of Appeals for the D. C. Circuit in Friends of the Earth, Inc. v. EPA, et al., No.05-5015, (April 25, 2006) and Implications for NPDES Permits, 2006.

[211] Committee on reducing stormwater to water pollution. *Urban Stormwater Management in the United States*. National Academies Press, Washington, DC, 2006. URL `https://www.nap.edu/read/12465/chapter/1`.

[212] Des Moines Water Works. Federal District Court Rules Against Des Moinses Water Works, 2017. URL `http://www.dmww.com/about-us/news-releases/federal-district-court-rules-against-des-moines-water-works-state-legislature-should-address-drainag.aspx`.

[213] California State Water Resources Control Board. Storm Water Program, 2004. URL `https://www.waterboards.ca.gov/water_issues/programs/stormwater/smallms4faq.shtml`.

[214] B Fagan. Is the Maximum Extent Practicable?, 2014. URL `http://stormwatertools.com/2014/04/05/is-the-maximum-extent-practicable/`.

[215] A Sapp. When is 'maximum extent' practicable?, 2012. URL `https://www.estormwater.com/when-maximum-extent-practicable`.

APPENDIX A

BEST FIT REGRESSIONS

Multi-variable linear and logistic regression models were used to determine the relationship between runoff, precipitation, and a variety of soil and environmental independent variables that impact green infrastructure performance. These regressions were used to formulate a loosely-coupled relationship between the SWMM test model and the Monte Carlo reliability analysis conducted in FERUM. A loose coupling was used in order to improve computational efficiency. The regression equations are presented in the main text of the document; the following plots present the best-fit regressions calculated for each of the types of curve. Each of the regression models were created using ordinary least-squares (OLS) error minimization coupled with appropriate Box Cox transformations to remove heteroscedasticity of residuals.

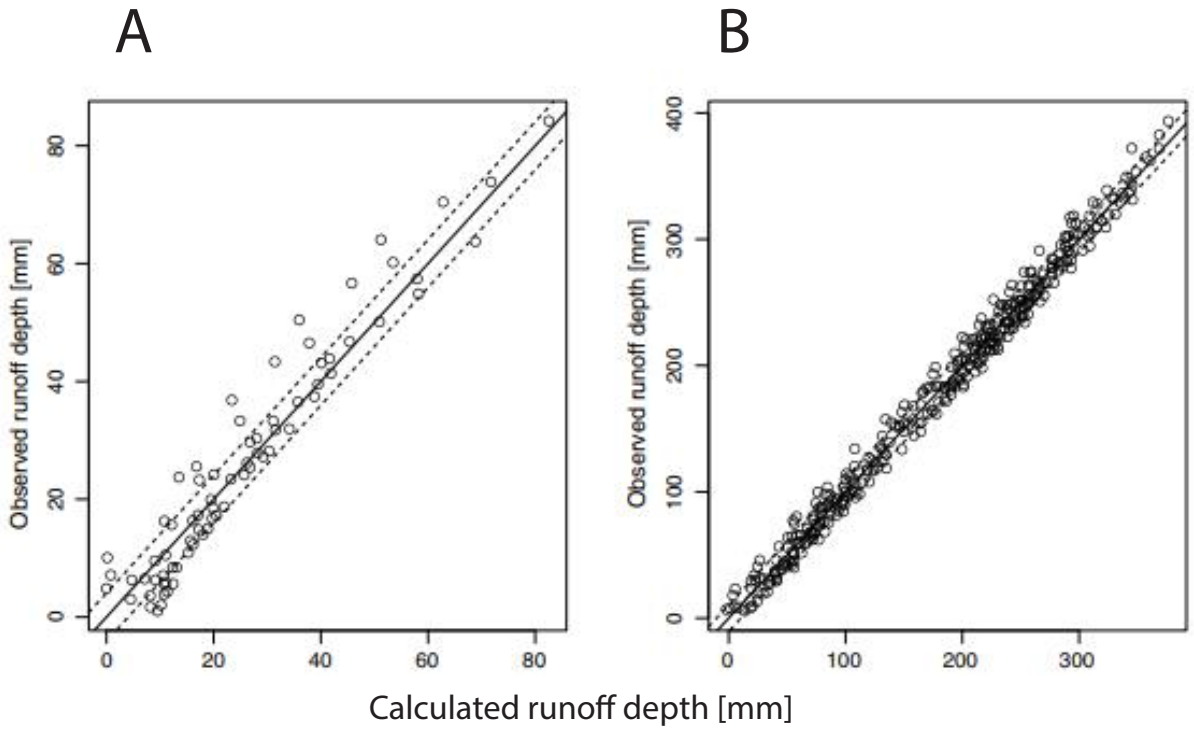

Figure A.1: Best-fit curves of observed versus calculated runoff for (A) Section 1 and (B) Section 2 for a 2-hour duration storm. These regressions were used in calculating the impact of clogging on the green infrastructure system.

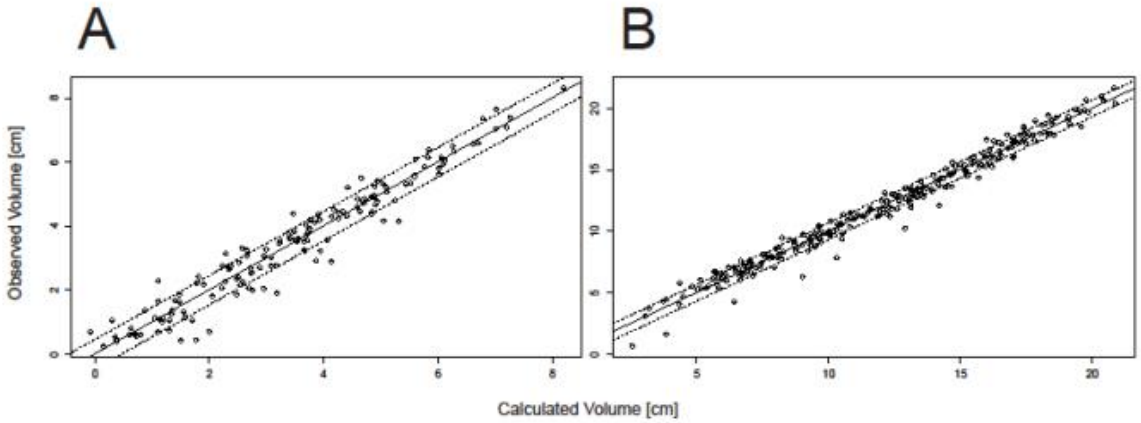

Figure A.2: Best-fit curves of observed versus calculated runoff for (A) Section 1 and (B) Section 2 for a 24-hour duration storm. These regressions were used in calculating the impact of back-to-back rainfall on the green infrastructure system.

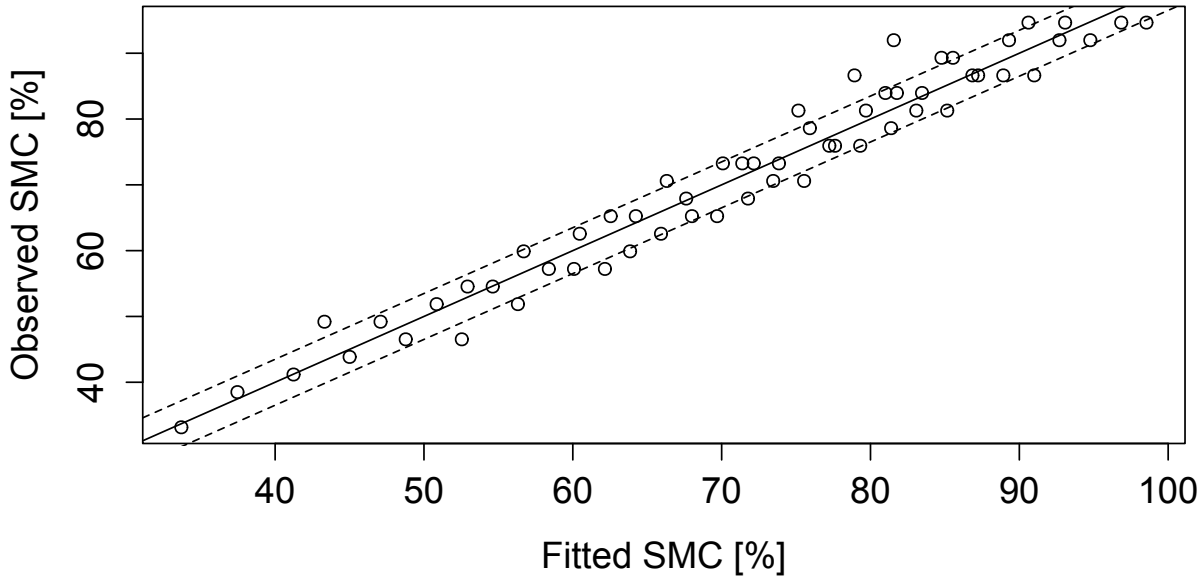

Figure A.3: Soil moisture content is a function of precipitation and initial saturation.

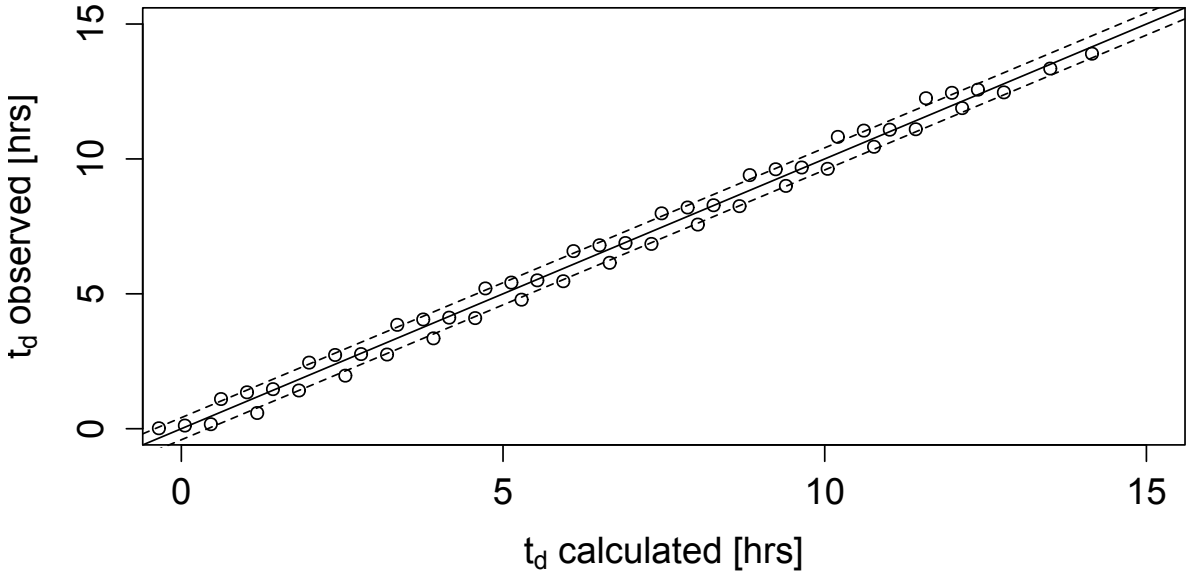

Figure A.4: The time to drain (t_d) can be defined as a function of precipitation and initial saturation.

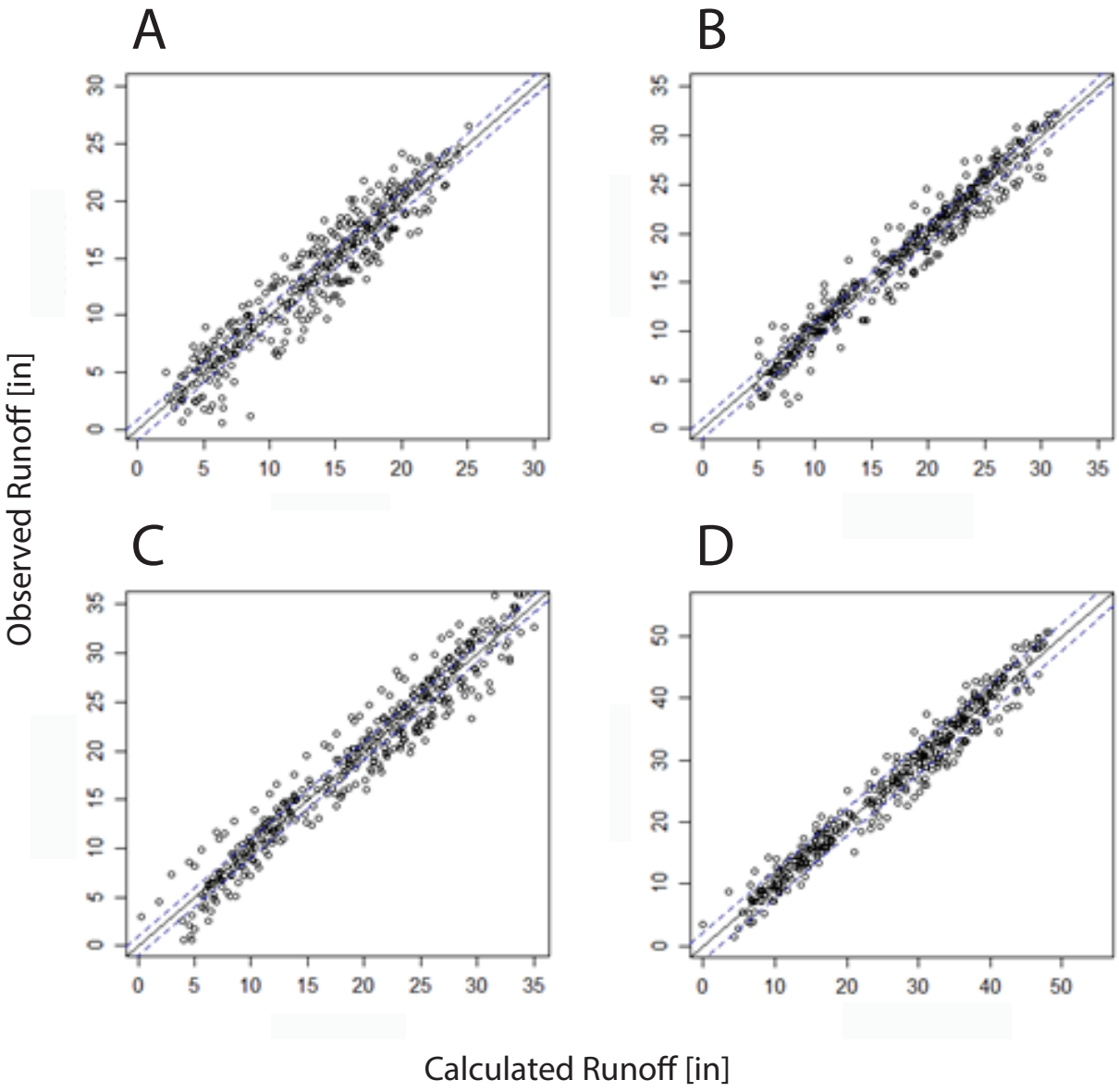

Figure A.5: Best-fit curves of observed versus calculated runoff for (A) sandy loam, (B) loam, (C) legore, and (D) sandy clay soils. These four regressions formed the basis of the analysis for Objective 2. The sandy loam and loam regressions were also used to generate the "coarse" and "fine/mixed" fragility curves for Objective 1.

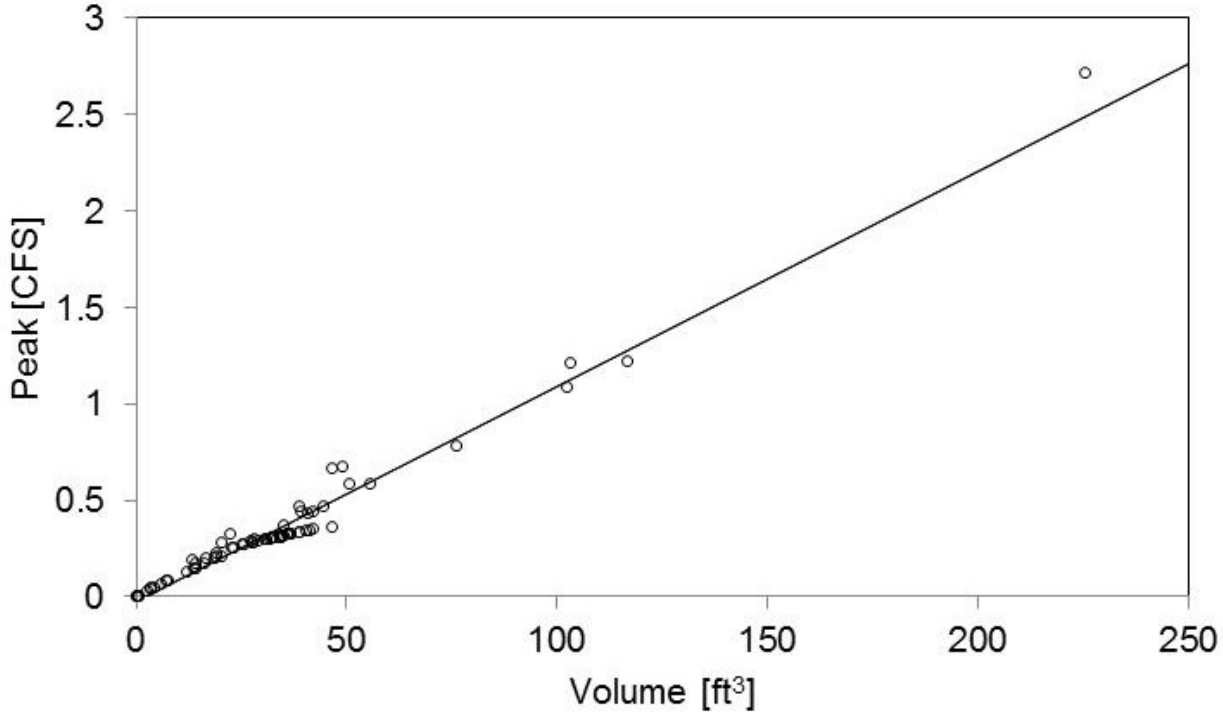

Figure A.6: The relationship between volume and peak runoff is linear.

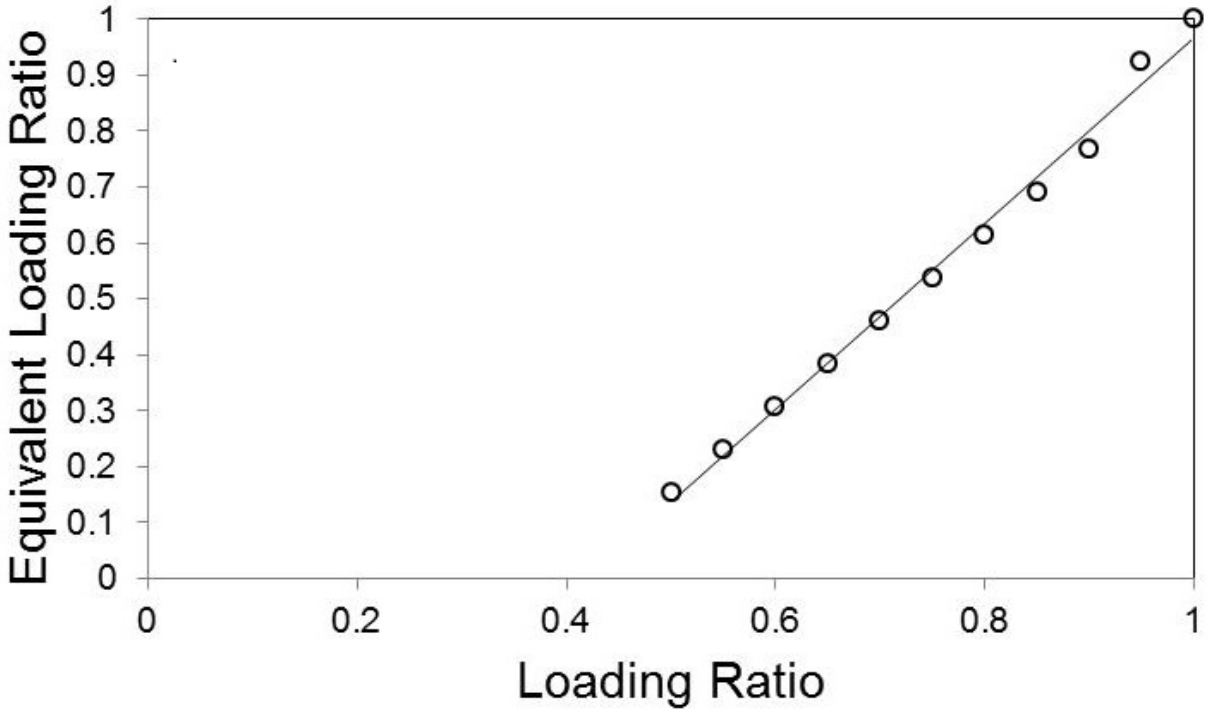

Figure A.7: The ratio between the loading ratio and the equivalent loading ratio is linear.